ASSESSMENT OF THE ATOKA GROUP OF SOUTHWEST KANSAS AS A POTENTIAL PETROLEUM SYSTEM

By

TIMOTHY M. SAMSON

Bachelor of Science in Geology

Dickinson College

Carlisle, PA

2005

Submitted to the Faculty of the
Graduate College of the
Oklahoma State University
in partial fulfillment of
the requirements for
the Degree of
MASTER OF SCIENCE
May, 2007

ASSESSMENT OF THE ATOKA GROUP OF

SOUTHWEST KANSAS AS A POTENTIAL

PETROLEUM SYSTEM

Thesis Approved:

Dr. Anna Curse

Thesis Adviser

Dr. Jim Puckette

Dr. Jay Gregg

Dr. A. Gordon Emslie

Dean of the Graduate College

Acknowledgements

Mom and Dad: For their support over the past six years of school both financially and emotionally.

Andrew: For his brotherly advice and for not forgetting to check in on me in Oklahoma.

Anna Cruse: For being my advisor and making sure I finished. She also made Oklahoma feel more like home.

John McLeod: For being my mentor at EOG Resources and acting as a valuable advisory committee member.

Gail Meyer: For supporting my ideas and giving me the chance to work with EOG.

My Friends: For all the good times.

EOG Resources: For allowing me turn my work into a thesis project and providing me with a job before and after graduation.

Oklahoma State University: For a quality education and a chance to succeed.

TABLE OF CONTENTS

Chapter Page

I. Introduction 1

Hypothesis....1
The Problem....3
Geologic Setting....5
Hugoton Embayment 6
Anadarko Basin....8
Las Animas Arch....11
Pratt Anticline 12
Central Kansas Uplift....12
Cambridge Arch 12
Stratigraphy....13
Petroleum System 13
Molecular Composition and Stable Isotopes 15

II. Review of Literature....20

Quantity of Organic Matter: Total Organic Carbon (TOC) 21
Quality of Organic Matter: Kerogen Type 24
Richness of Organic Matter: Evaluation of Maturity 28
Vitrinite Reflectance 28
Carbon Isotopes 29

III. METHODOLOGY 33

IV. RESULTS AND DISCUSSION....39

Petrographic Analysis 39
Vitrinite Reflectance 40
Rock-Eval Pyrolysis....41
Total Organic Carbon....42
Isotopic Data 44

V. Discussion....74

VI. Conclusion 76

References....78

LIST OF TABLES

Table Page

1. Measured vitrinite reflectance values……..…… 42
2. Rock-Eval and TOC data…….…… 43
3. Collected isotope data Apsley 1 #1, Joyce 14 #1, and Sullins 34 #1……..….49
4. Collected isotope data Elkhart Forest 14 #1 and Hamilton 15 #1……..…. 50
5. Collected isotope data Norman 22 #1, Toto 15 #3 and Debra 32 #1……..…. 51
6. Gas composition data Apsley 1 #1, Joyce 14 #1, and Sullins 34 #1……52
7. Gas composition data Elkhart Forest 14 #1 and Hamilton 15 #1……..……..... 53
8. Gas composition data Norman 22 #1, Toto 15 #3 and Debra 32 #1…… 54
9. Average isotopic data collected from the Atoka Group…….……..… 55

LIST OF FIGURES

Figure Page

1. Well log of Atoka Group…… 2
2. Hugoton Embayment Production Charts……. 4
3. Map of the Hugoton Embayment and Associated Structural Features…… 6
4. Well Log Showing Mud log and Gamma Ray Log (API units)……...…… 7
5. Regional Gamma Ray thickness map……..…… 8
6. Structural Feature Map of the Anadarko Basin…… 10
7. Map of the Southern Oklahoman Aulacogen……... 11
8. Stratigraphic Column of Hugoton Embayment of Kansas..……. 14
9. Plot of $C_1/(C_2+C_3)$ vs. Methane (Modified from Bernard, 1977)……..…… 17
10. Natural Gas as produced from Sapropelic and Humic Kerogen……...…18
11. Carbon 12 and Carbon 13 Isotopes Schematic……..… 19
12. Van Krevelen Diagram……. 25
13. Modified Van Krevelen Diagram……. 27
14. Schematic showing phases of thermal maturation……28
15. Schoell's Chart to classify gas phase using isotopes…… 31
16. Diagram showing relationship between gas and temperature…….. 32
17. Sampling locations……... 34
18. Isotube sampling manifold……... 36
19. Gas collection schematic…….. 36
20. Rock-Eval peak schematic……....38
21. Thin sections from Sullins 34 #1…….…….. 40

22. Total Depth vs. measure vitrinite reflectance……... 41

23. Modified Van Krevelen Diagram with collected data……. 44

24. Well log profile of Debra 32 #1 with TOC values....…… 45

25. Well log profile of Hamilton 15 #1 with TOC values.…….... 46

26. Well log profile of Norman 22 #1 with TOC values……...…… 47

27. Well log profile of Sullins 34 #1 with TOC values.……...…….. 48

28. Map of study area with isotopic methane compositional data..…… 55

29. Total Depth vs. Isotopic Methane…… 57

30. Total Depth vs. Isotopic Methane by well…… 57

31. Isotopic Methane vs. Gas Wetness (Bernard)……... 58

32. Isotopic Methane vs. Gas Wetness (Schoell)……... 60

33. Estimated vitrinite reflectance values for all wells……...… 61

34. Estimated vitrinite reflectance values for Atoka samples……. 62

35. Map of study area with isotopic ethane compositional data..……...… 62

36. Map of study area with isotopic propane compositional data..…… 63

37. Debra 32 #1 sub sea-level vs. $\delta^{13}C$……... 66

38. Toto 15 #3 sub sea-level vs. $\delta^{13}C$……..… 67

39. Hamilton 15 #1 sub sea-level vs. $\delta^{13}C$……...… 68

40. Norman 22 #1 sub sea-level vs. $\delta^{13}C$…… 69

41. Elkhart Forest 14 #1 sub sea-level vs. $\delta^{13}C$……...… 70

42. Sullins 34 #1 sub sea-level vs. $\delta^{13}C$……..…… 71

43. Joyce 14 #1 sub sea-level vs. $\delta^{13}C$……....72

44. Apsley 1 #1 sub sea-level vs. $\delta^{13}C$……... 73

Chapter I

Introduction

1.1 Hypothesis

The purpose of this study is to test the hypothesis that the Atoka Stage of Southwest Kansas represents a traditional petroleum system (Magoon and Dow, 1994), with the organic rich Atoka Marls as the source, the base of the Cherokee Formation as the seal and the Novi carbonate as the reservoir (Figure 1). Analysis of thermal maturity, organic richness and abundance of Atoka rocks using stable carbon isotope, molecular composition, Rock Eval, and total organic carbon (TOC) data will help to determine if Atoka source rocks have charged the Atoka/Novi beds above. This information will be used to constrain the geologic history of the Hugoton Embayment and to determine the extent of a possible Atoka/Novi hydrocarbon play.

Correlation of hydrocarbon accumulations to source rocks is an essential part in identifying a Petroleum System. This study uses isotope compositions of methane, ethane, and propane from eight wells within Hugoton Embayment to identify variations in gas type (e.g. thermogenic and biogenic) and maturity. Gas isotopes are useful analytical tools for evaluating vertical communication in wells and in defining potential, effective, and spent petroleum in source rocks (Ellis et al., 2003). Other possible applications for carbon isotopes include verifying mud gas shows, evaluating the quality

of a seal and identifying the level of mixing and migration of petroleum in a reservoir volume, and determining quality of organic matter helps to estimate the amount of petroleum Ellis et al., 2003; Ellis et al., 1999). Rock Eval and TOC data can be used to establish type and quality of kerogen within source rocks, and will be combined with the gas isotope data to provide a more rigorous test of the development of a petroleum system.

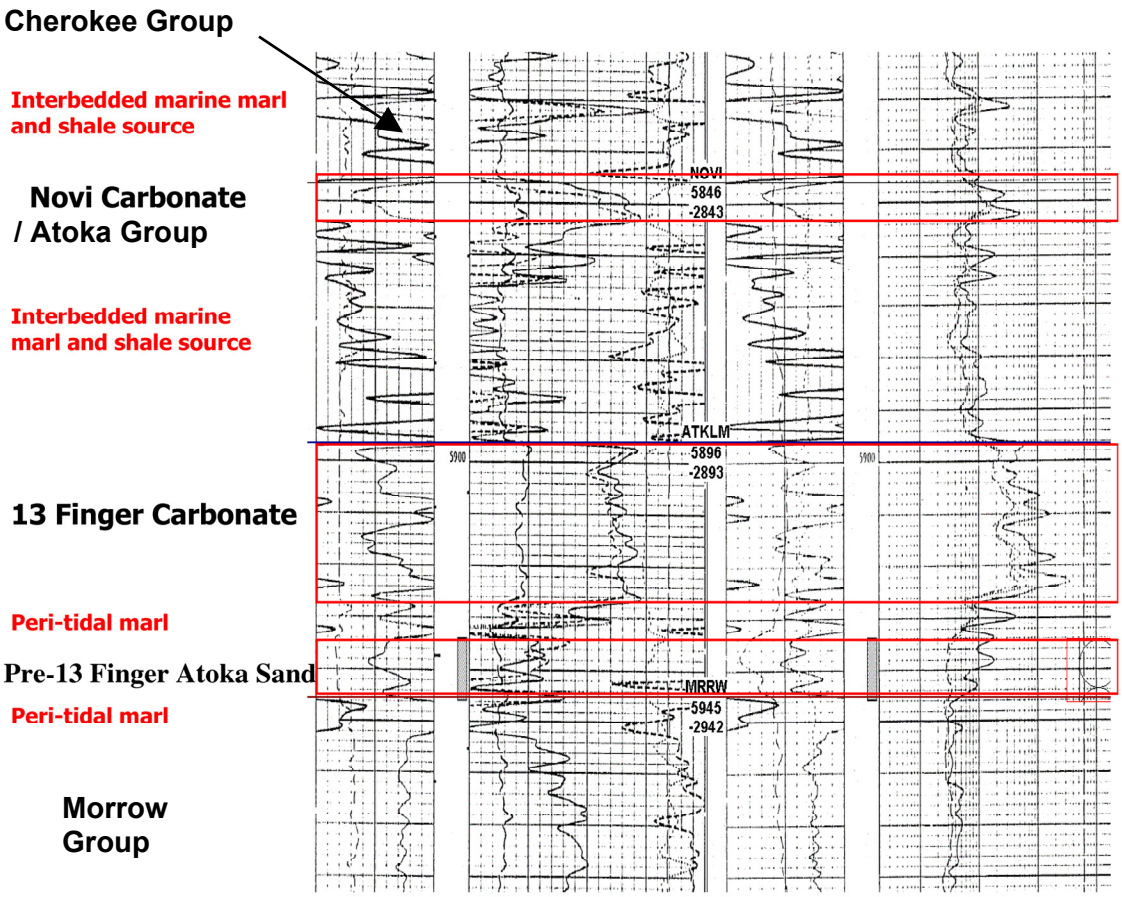

Figure 1. A portion of a well log of the Atoka Group. Columns from left to right include a gamma-ray log, density/neutron porosity log, gamma-ray log, and a resistivity log. In this cross section the top of the Atoka interval is picked at the same elevation as the top of the Novi, which sits below the Cherokee Group.

1.2 The Problem

In the petroleum industry the purpose for the collection of organic geochemical data from a sedimentary basin is to better understand the character of the source rocks. A major application of this type of work is to identify potential drillable prospects. Organic geochemical data such as thermal maturity, kerogen type, volume, and quality of organic matter help to estimate the amount of petroleum available to accumulate in traps (Magoon and Dow, 1994; Hunt, 1996). A petroleum trap must have a reservoir component and a seal component in order to hold hydrocarbon accumulations (Biddle and Wielchowsky, 1994). The reservoir must have sufficient porosity so that accumulations have storage space and permeability so fluids can be exchanged (e.g. water and oil) (Biddle and Wielchowsky, 1994). The seal must be impervious enough so that hydrocarbons cannot migrate out of the reservoir. This study will determine the extent of the organic rich Atoka marls (source rock) relative to the trap components.

As indicated by the Kansas Geological Survey (KGS) (Figure 2) relatively less hydrocarbon exploration interest has been paid to the Atoka Group of southwestern Kansas as compared to the Chase Group, Council Grove Group, and Morrowan Stage. The primary reason for this discrepancy is oil and gas production to date (Figure 2). The production numbers in this study indicate the percentage of cumulative oil or gas produced from a stratigraphic group in Kansas. Between 1987 and 1998 the Chase and Morrowan Stage produced 64.5 % and 17.4 % of the cumulative gas production in Kansas, respectively (Gerlach, 1999). However, the success of unconventional plays such as the Barnett Shale in Texas and Woodford shale of Oklahoma has sparked an interest in zones once deemed non-productive. An unconventional resource play is

neither easily nor unanimously defined. However, in a basic sense it can be described as a combination between a nontraditional prospect and an economic petroleum accumulation. Data collection, drilling strategies and costs vary with unconventional resource plays because the objective is to gather either new data or examine data that was over looked. The Atoka Group of Kansas as treated as a conventional play has had little economic success but could become a feasible unconventional target. Therefore, further analyses are required to determine whether the Atoka Group contains an unconventional shale resource play or a more conventional source, reservoir, seal and trap play.

A. B.

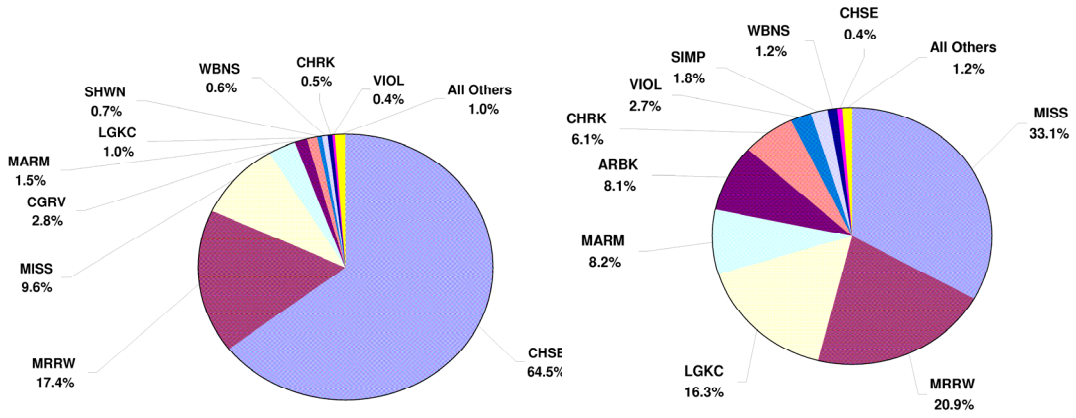

Figure 2. State of Kansas oil and gas production percentages by formation (KGS, 1987 to 1998). A. Gas production. B. Oil Production.
ARBK = Arbuckle Group, CGRV = Council Grove Group, CHRK = Cherokee Group, CHSE = Chase Group, LGKC = Lansing and Kansas City Groups, MARM = Marmaton Group, MISS = Mississippian System, MRRW = Morrow Group, SHWN = Shawnee Group, SIMP = Simpson Group, VIOL = Viola Formation, WBNS = Wabaunsee Group.

It is unknown if the Atoka Group contains a regional repeater play in southwest Kansas and the Oklahoma Panhandle. A repeater play is an economic petroleum accumulation that can be drilled along a pattern because it is productive over a

predictable area. It is important to identify repeatitional plays because they can typically improve total costs. The Atoka Group includes streaks of 'hot' intervals in terms of elevated gamma ray log radioactivity (>150 API) throughout most of the Hugoton Embayment. Information recorded on mud logs indicate the presence of gas based on data from gas chromatography during drilling (Whittaker, 1992). Above these zones lies a carbonate interval with observed porosity ranging between four to ten percent. However, the maturity level, gas type, and trap location remains unclear.

The Atoka group of the Hugoton Embayment has an approximate average burial depth between of 5,000 to 6,000 ft. Thus, establishing the maximum amount of overburden that has covered Atoka rocks in the past is critical to understanding its thermal history. This information will aid in solving the problem of whether or not these intervals have sourced nearby reservoirs.

1.3 Geologic Setting

The structural history of the Mid-Continent is a result of multiple deformation events since the Precambrian, the majority of which occurred during the Late Paleozoic (Jewett and Merriam, 1959). A large depression known as the Hugoton Embayment located in southwestern Kansas and the Oklahoma and Texas panhandles is surrounded by several of these tectonic features (Figure 3; Merriam, 1963).

The Atoka Group in southwest Kansas and the panhandle of Oklahoma/Texas includes intervals containing 'hot' streaks (Gamma Ray > 150 API) along with mud log reported increases observed on gas chromatograph logs during drilling (Figure 4). These kicks represent the presence of gas in the Atoka as the drill bit grinds the volume of rock

equivalent to bit diameter. An increase in net thickness of Atoka 'hot' gamma ray (>150 API) streaks from Kansas southward into the Oklahoma panhandle suggests a shelf to basin trend from Kansas to the Oklahoma panhandle (Figure 5). An increase in gamma ray response is likely the result of a thicker section of organic-rich rocks.

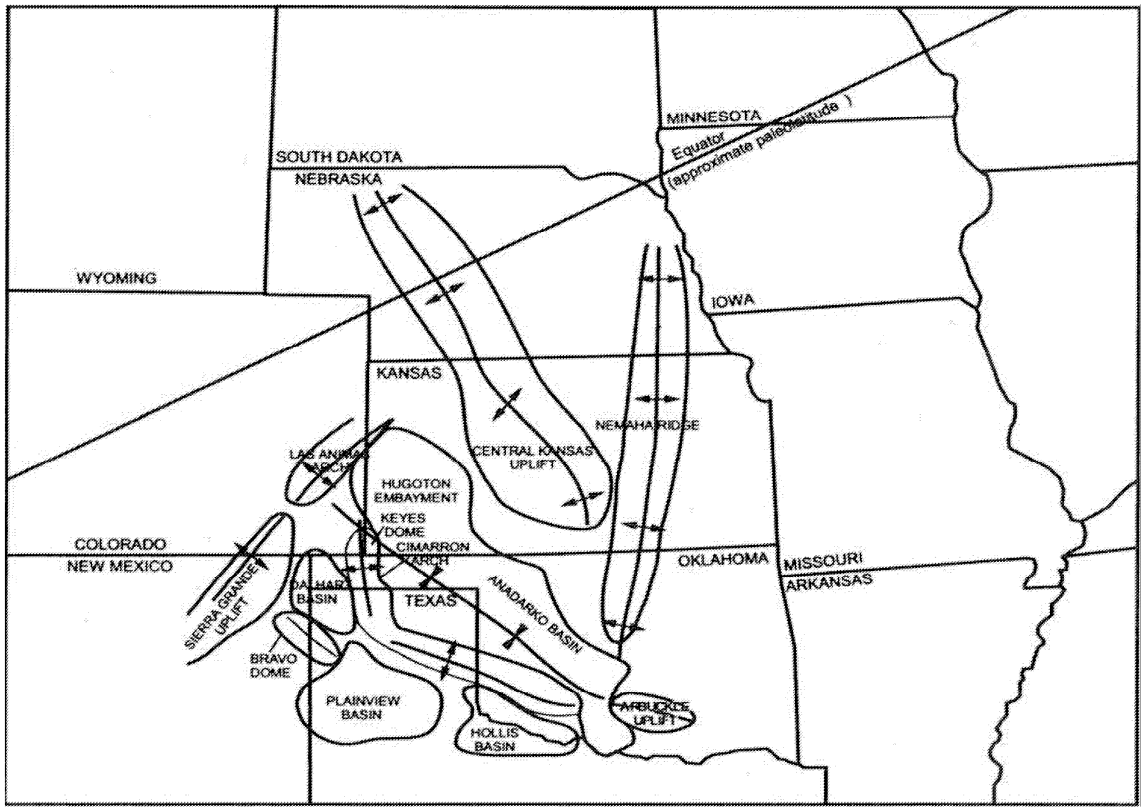

Figure 3. Tectonic features of the Mid-continent. (From Jorgenson, 1989).

1.3.1 Hugoton *Embayment*

The Hugoton embayment has an area of approximately 28,600 square miles (Merriam, 1963). Sediments thickened toward the center of the embayment and southward into the Anadarko Basin (Merriam, 1963), reaching approximately 9,000 ft near the Kansas – Oklahoma border.

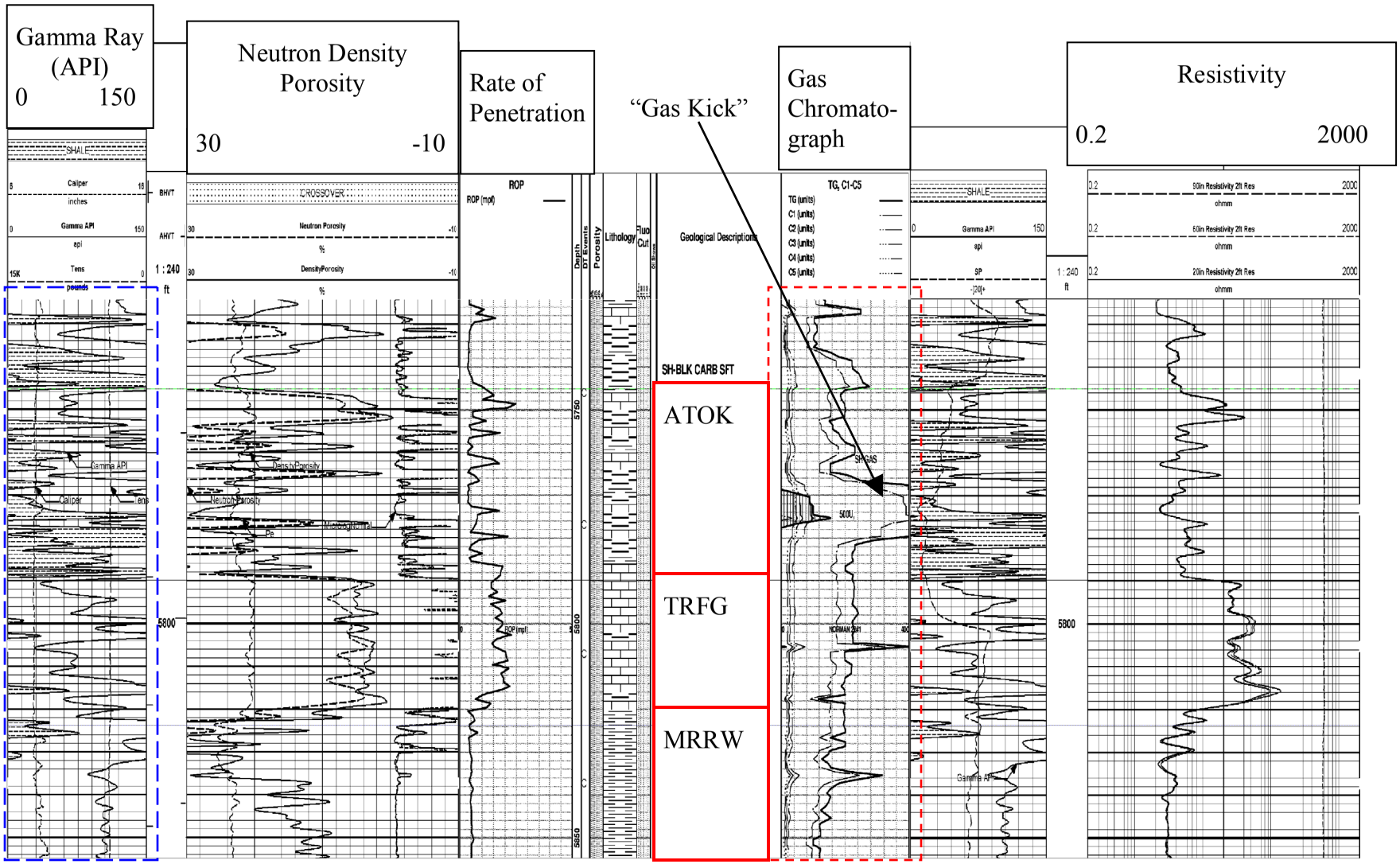

Figure 4. Copies of a portion of wireline well logs of the Atoka Group including Atoka (ATOK) and Thirteen Finger (TRFG), and Morrow Series (MRRW) tops along with sub sea-level depth and total depth indicated below formation names, respectively. Logs from left column include gamma ray (large blue dashes) and caliper, neutron – density, photoelectric log (PE) and microlog, rate of penetration (ROP), mud logger interpretation of lithology during drilling, gas chromatography (red dashes), repeat of gamma ray and caliper logs, and high resolution resistivity log on far right.

To the east, the Hugoton Embayment is bordered by the Pratt Anticline and Central Kansas Uplift, to the west, it is bordered by the Cimarron Arch and the Las Animas Arch of Colorado, to the north, it is bordered by the Cambridge Arch, and to the south, the Hugoton Embayment merges with the Anadarko Basin (Figure 3).

Every Paleozoic system in the Hugoton Embayment has produced hydrocarbons and the USGS recognizes 25 petroleum plays with in the Embayment and Anadarko Basin combined (USGS, 1995).

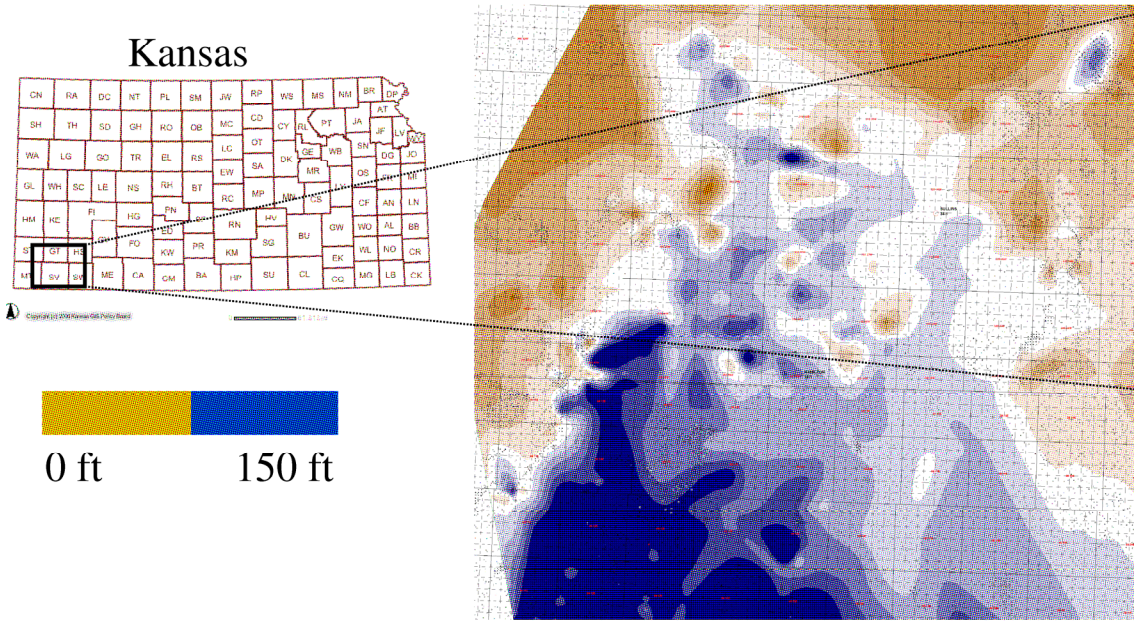

Figure 5. Map illustrating the thickness distribution of rock with a gamma ray value cutoff of > 150 API.

1.3.2 Anadarko Basin

The Anadarko Basin is a Paleozoic northwest-trending asymmetric foreland basin located in Oklahoma and the Texas panhandle (Figure 5; Evans, 1979). It is surrounded by the Amarillo – Wichita uplift and Marietta Basin to the south, Ardmore Basin and

Arbuckle uplift to the southeast, the Nemaha Ridge to the east, the Northern Shelf area to the north and extends into the Hugoton Embayment to the northwest (Figure 5).

During the late Proterozoic and Paleozoic, the southern margin of North America underwent a complete cycle of continental rifting, ocean opening and closing, and collision that influenced the structural features of Oklahoma and Texas. The Southern Oklahoma aulacogen occurred as a result of post-Cambrian rifting during the opening of the proto-Atlantic Ocean (Iapetus Ocean). Burke and Dewey (1973) described this event as a failed arm of a triple junction and Hoffman (1974) labeled the event as a Lower Paleozoic aulacogen (Figure 6). An overall increase in density and thickness of the Southern Oklahoman lithosphere followed in association with the extrusion of the Carlton Rhyolite Group / Timbered Hills Group along with the Wichita Granite Group (Denison, 1982; Gilbert, 1983).

Subsidence followed collision, occurring between the Late Cambrian and the Early Mississippian. Relative to the surrounding craton, this subsidence resulted in increased carbonate sedimentation in what would become the modern day Anadarko Basin. By the Silurian, continental thinning slowed (Feinstein, 1981) and an isostatic imbalance remained until the Pennsylvanian (Dickinson and Yarborough, 1977).

The southern Oklahoma aulacogen is superimposed on the Anadarko Basin (Hoffman et al., 1974; Hoffman, 1989). The Amarillo – Wichita uplift formed syndepositionally with the Anadarko Basin during the Late Mississippian – Early Pennsylvanian (Chesterian to Morrowan) due to the collision of the North and South American plates. This event is related to the Ouachita – Marathon orogeny (Ham and

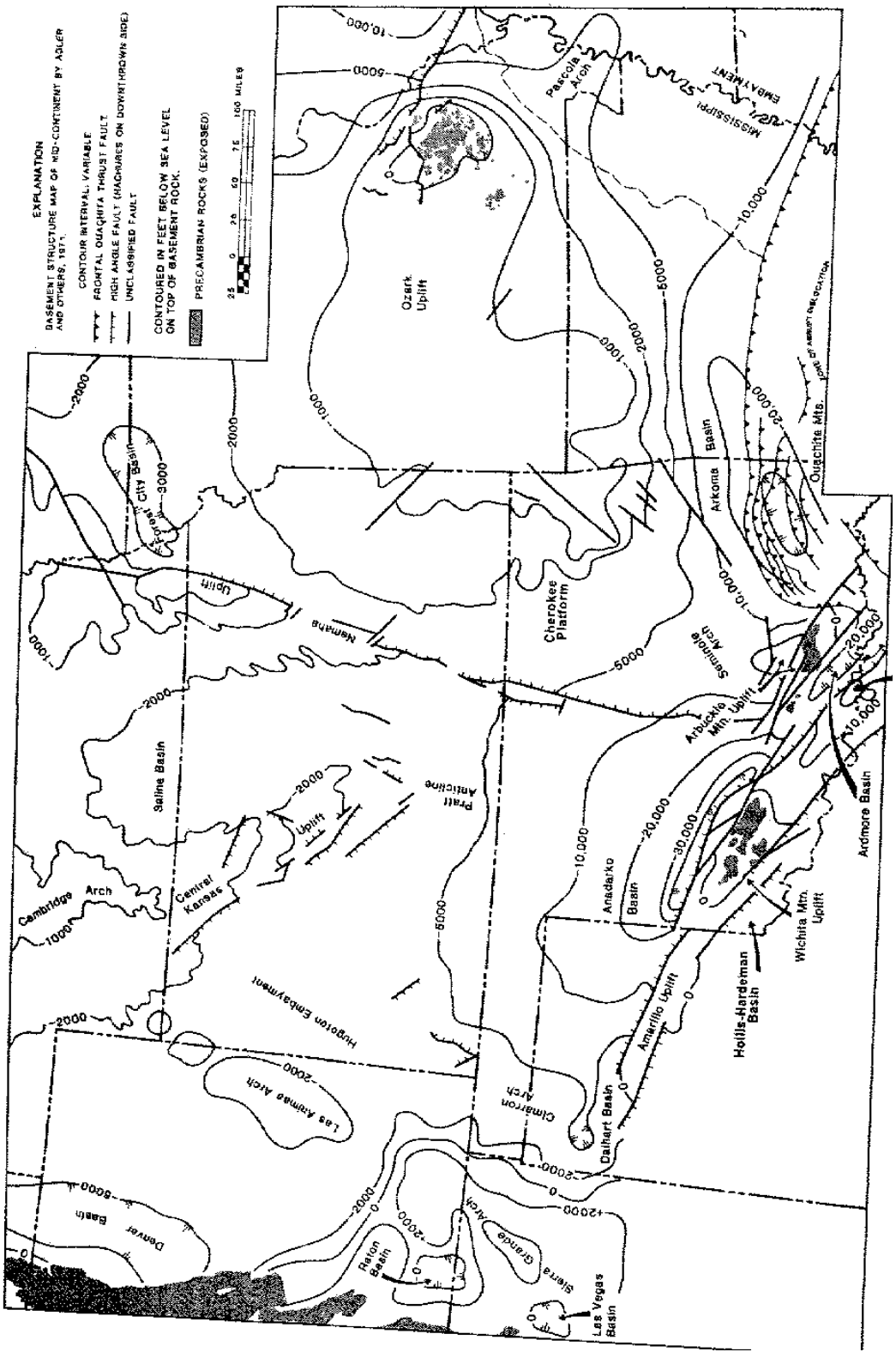

Figure 6. Structure of basement features of the Mid Continent showing the Anadarko Basin and Hugoton Embayment. (Modified from Adler and others, 1988).

Wilson, 1967; Burgess, 1976). There is little evidence of extensional faulting and it is believed that the formation of the Amarillo – Wichita uplift is a result of basement thrusting along ancestral planes of weakness (Ham et al., 1964). Approximately 15 ± 5 km of crustal shortening occurred as a result (Brewer, 1983). The remnant Southern Oklahoma aulocogen was divided between the northeast trending Amarillo – Wichita uplift and the Anadarko Basin. During the Early Permian (Wolfcampian) red beds and evaporites filled the basin and structurally the southern Oklahoma has been quiescent since (Johnson et al., 1988).

1.3.3 Las Animas Arch

The Las Animas Arch is located primarily in eastern Colorado but a small portion extends into western Kansas. It is a northeastward plunging anticline of post-Cretaceous age that separates the Hugoton Embayment from the Denver Basin (Figure 3).

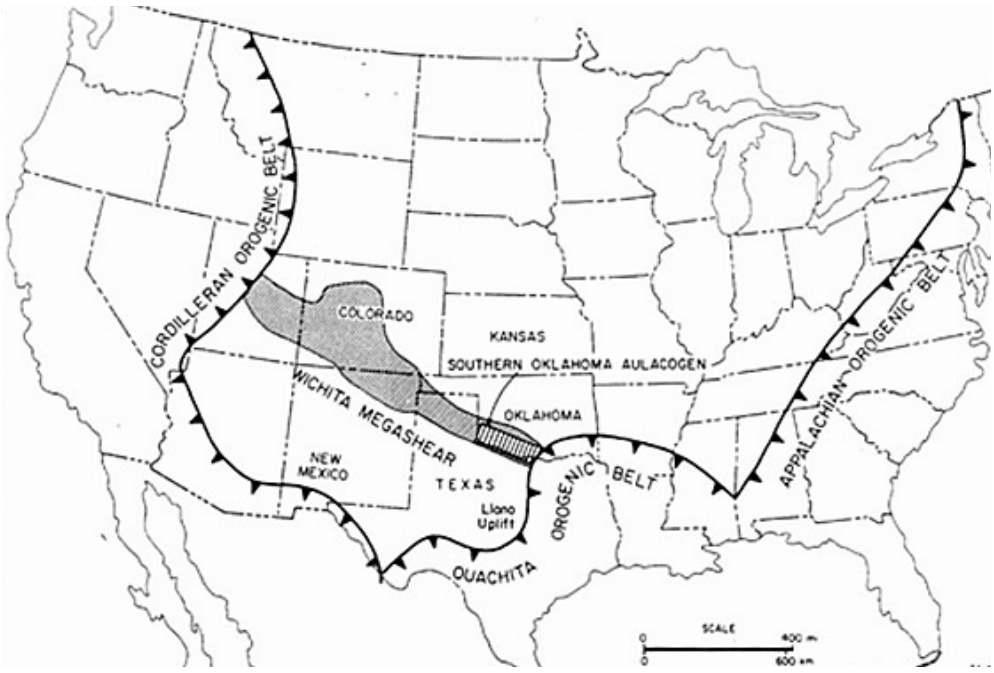

Figure 7. Map of the United States showing location of Southern Oklahoma Aulacogen (SOA). From Budnik (1986).

1.3.4 Pratt Anticline

The Pratt Anticline resulted from deformation in the Early Paleozoic and later deformation in Morrowan – Atoka time (Merriam, 1963). It is considered to be the smallest structural feature in Kansas with an area of 1,000 sq ft (Figure 3). This broad southward plunging anticline separates the Hugoton Embayment to its west from the Sedgwick Basin on its east. To the south, the Pratt Anticline merges with the Hugoton Embayment.

1.3.5 Central Kansas Uplift

The Central Kansas Uplift is a large (5,700 sq mi) northwest trending positive feature that separates the Hugoton Embayment from the Salina and Sedgwick Basins (Merriam, 1963). This uplift occurred between Pre – Desmoinesian and Post – Mississippian time (Merriam, 1963).

1.3.6 Cambridge Arch

The Cambridge Arch is a relatively small (1,000 sq. ft.) northwest aniticlinal feature of western Kansas (Merriam, 1963). Movement occurred multiple times during its formation including Pre – Desmoinesian, Pre – Desmoinesian and Post – Mississippian, and during the Mesozoic (Merriam, 1963). The Cambridge Arch borders the northern limit of the Hugoton Embayment (Figure 3).

1.4 Stratigraphy

The stratigraphy of the Hugoton Embayment is shown schematically in (Figure 7; Bebout and others, 1993). The Atoka Group (Middle Pennsylvanian System) includes rocks below the Cherokee Group (Middle Pennsylvanian) and above the Morrowan Stage (Lower Pennsylvanian) (Figure 7). The Morrowan Series is also known as the Kearny Formation in Kansas (Jewett, 1968). Atoka carbonates are separated from Morrow siliclastics by a third order sequence boundary (Bowen and Weimer, 2003). In this study, the Atoka Group is broken into three lithostratigraphic units: the Atoka sandstone, the Thirteen Finger limestone (Jewett, 1968), the Atoka limestone / marl, and the Novi carbonate (Figure 1).

1.5 Petroleum System

A petroleum system, as described by Magoon and Dow (1994), is identified by the association between an active pod of source rock and the accumulation of oil or gas. A total petroleum system model consists of a charge factor, migration drainage style, and entrapment style (Demaison and Huizinga, 1994). It takes into account all the fundamental elements and process that are necessary for a hydrocarbon accumulation to exist. Complete analysis of a petroleum system will assess the source rock, reservoir rock, seal rock, overburden rock, and the timing of generation, migration and accumulation of hydrocarbons within a reservoir (Magoon and Dow, 1994). The potential for a trap also plays an essential role in identifying a system. Understanding the petroleum system is necessary to reduce the risk associated in identifying plays and developing drillable prospects.

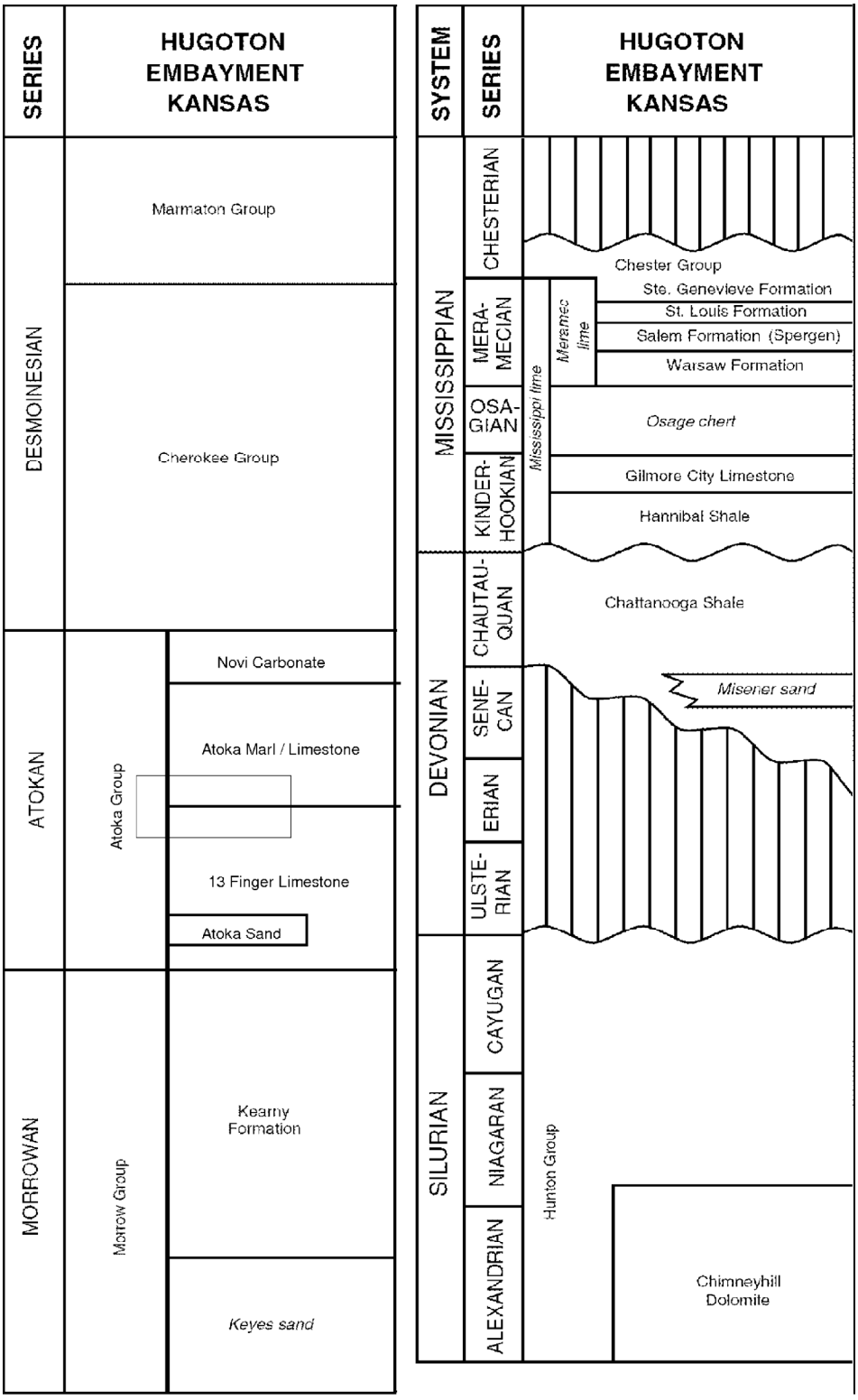

Figure 8. Stratigraphic nomenclature of Hugoton Embayment portion of southwest Kansas. Modified from Bebout and others (1993).

1.6 Molecular Composition and Stable Isotope Interpretation of Carbon

In general, geochemical analysis of molecular composition, which is used in natural gas studies, is constrained to five aliphatic compounds: methane (C_1), ethane (C_2), propane (C_3), iso-butane (i-C_4), and n-butane (n-C_4). Samples with higher carbon number (C_{5+}) alkanes can often times be heavily fractionated (compositionally) relative to the initial gas composition due to a condensation effect caused by shifts in pressure and temperature as the sample reaches the surface (Whiticar, 1994). Molecular composition data can be useful in identifying gas type (i.e. thermogenic vs. bacterial; Bernard 1977; Figure 8). These data are also useful in estimating wetness values (Equation 1; Schoell, 1978; Faber, 1987). Wetness values are calculated as follows:

$$\text{Bernard Parameter (vol. \%): } \frac{C_1}{C_2 + C_3} = \text{Wetness} \quad (1)$$

Where C is reported in ppm concentration, and the subscript refers to the number of carbons in the n-alkane molecules. Wetness ratios indicate rocks with elevated amounts of higher hydrocarbons, which are important for identifying the phase of hydrocarbon generation (Whiticar, 1994). The Berner parameter is used to estimate wetness in drill cuttings and mud gas logs where there is a greater chance of dynamic compositions (Whiticar, 1994). Wetness (C_{2+}) values will initially increase as a rock enters the oil window, but with an increase in temperature the relative amount of wetness will peak and eventually decrease (Figure 9). While molecular composition can provide broad characterizations of gas it does not provide a level of detail equivalent to stable isotope ratios. For example, isotope ratios can help to discern information from natural gas such

as estimating kerogen types, levels of thermal maturation, and identifying migrated or mixed gases. Typically molecular composition data will be used in conjunction with isotope data to characterize a source rock.

Stable isotope ratios allow for a more detailed analysis of natural gas than molecular composition alone (Smith et al., 1971; Waples and Tornheim, 1978; James, 1983; Chung et al., 1988; Whiticar, 1994). Carbon isotopes can be used to identify various kerogen types (i.e. sapropelic or humic; Bernard et al., 1977; Schoell 1983), estimate the thermal maturity of a source rock (Evans et al, 1971; Tissot et al., 1974; Hood et al., 1975; James, 1983, 1990), verify mud gas shows (Ellis et al., 2003), evaluate the quality of a seal, identify the level of mixing and migration (Silverman, 1965) of petroleum in a reservoir, and to correlate source rock to oil/gas accumulations (Stahl, 1977).

Carbon has two stable isotopes, C^{12} (6 neutrons) and C^{13} (7 neutrons), which are often referred to as: "light" and "heavy", respectively (Figure 10). C^{12} and C^{13} make up 98.9% and 1.1 % of the total carbon pool on earth, respectively (NNDC, 2005). The stable carbon isotopic composition is typically reported as the C^{12}/C^{13} ratio of a sample relative to a Vienna Pee Dee Belemnite (V-PDB) standard, as follows:

$$\delta^{13}\mathrm{C}\,(‰, \mathrm{V\text{-}PDB}) = \left[\frac{{}^{13}\mathrm{C}/{}^{12}\mathrm{C}_{\mathrm{Sample}} - {}^{13}\mathrm{C}/{}^{12}\mathrm{C}_{\mathrm{Standard}}}{{}^{13}\mathrm{C}/{}^{12}\mathrm{C}_{\mathrm{Standard}}} \right] * 1000 \qquad (2)$$

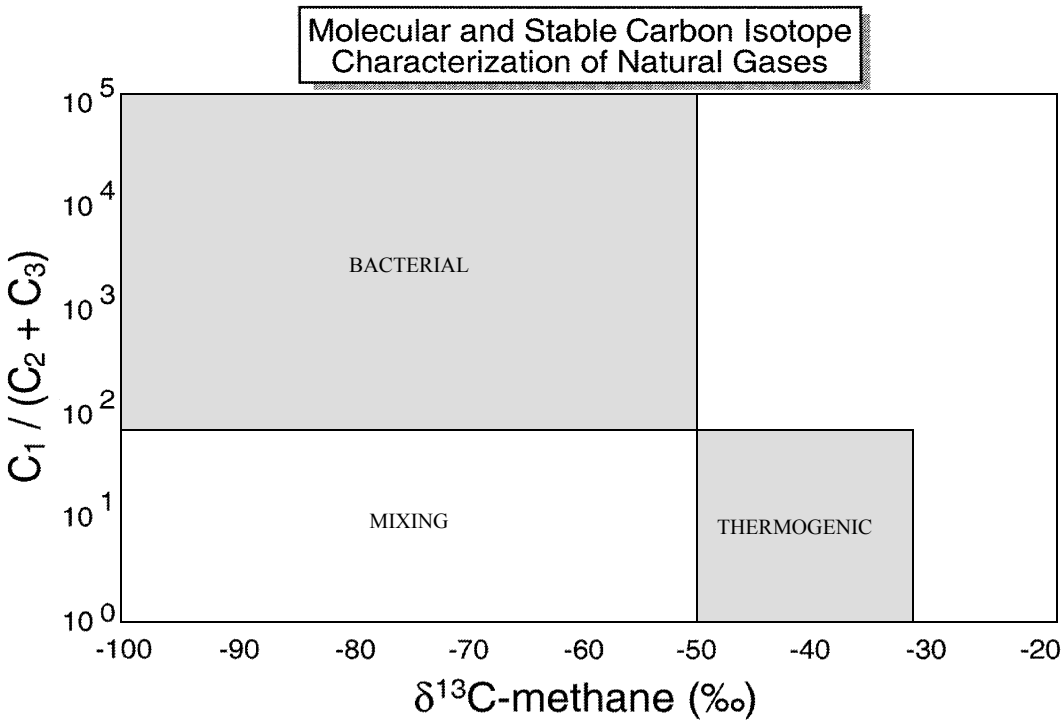

Figure 9. Chart used to identify thermogenic vs. bacterial gas. Y-axis and X-axis plot gas wetness ($C_1/ (C_2+C_3)$) vs. isotopic methane, respectively. Modified from Bernard (1977).

The carbon isotopic composition of hydrocarbons varies with thermal maturity (James, 1983; Sundberg and Bennett; Schütze and Mühle, 1986; Faber, 1987; Galimov, 1988; Berner; 1989; Zhang and Feng, 1990; Clayton, 1991; Berner et al., 1995). This relationship is due to kinetic isotopic effects. Isotope effects are influenced by differences in reaction rates caused by variations in the atomic mass of an element (Sackett, 1968). Kinetic isotope effects occur in carbon when C^{12} is replaced by C^{13} causing a decrease in vibrational frequency of a carbon chemical bond. Therefore, a greater amount of energy is required to break the carbon bond, which results in a higher activation energy. Isotope effects are manifest as differences in the isotopic abundances between products and reactants.

Isotopic fractionation is the separation of isotopes during physical or chemical processes and is a function of molecular vibrational energies (Anderson and Arthur, 1983). Vibrational frequency is inversely proportional to the mass of a molecule, therefore, larger molecules (lower vibrational energy) allows for easier bonding. Hence, molecules that contain light isotopes are more reactive than molecules formed from heavy isotopes.

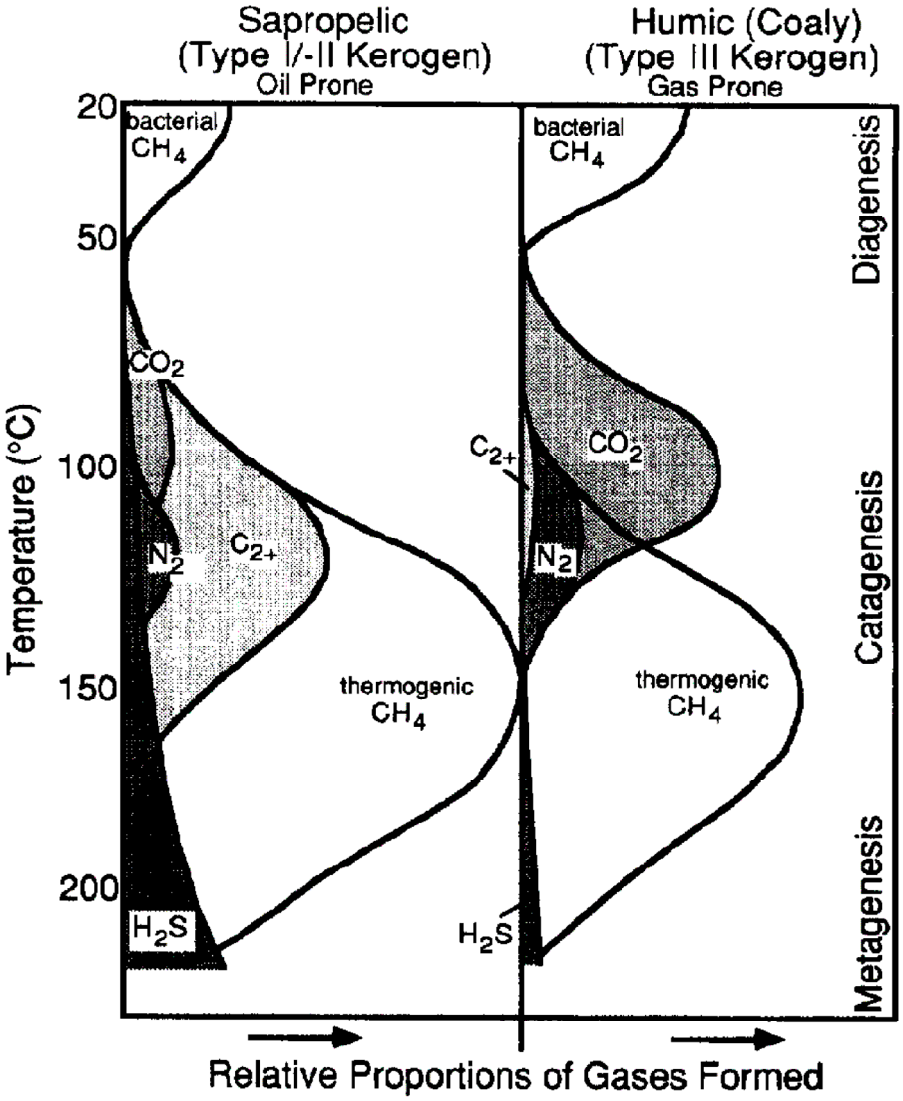

Figure 10. Relative proportions of natural gas produced from Sapropelic and Humic kerogen with increasing thermal maturity. C_{2+} initially increase and eventually decreases with increased thermal maturation. From Hunt (1979) and Whiticar (1994).

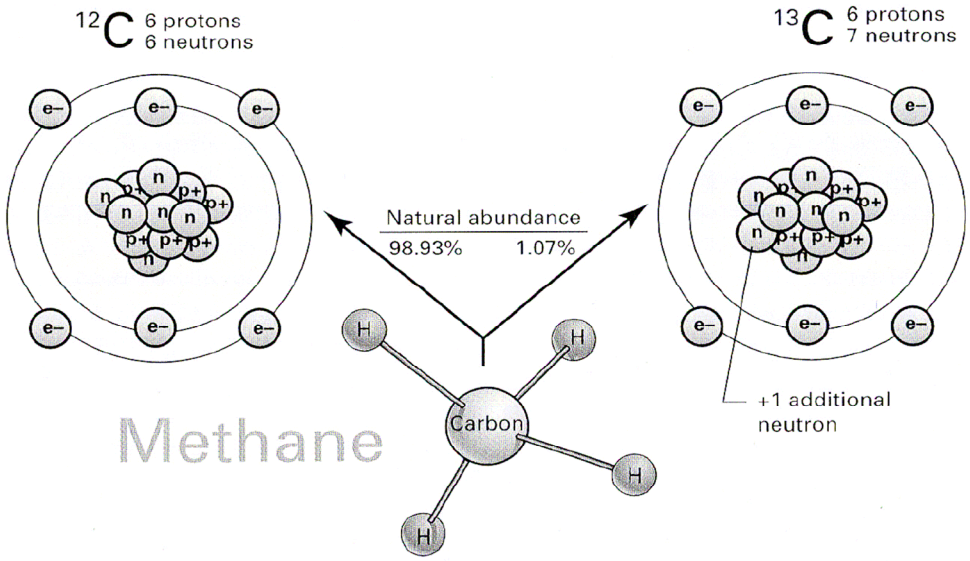

Figure 11. Carbon 12 and Carbon 13 isotopes. Modified from Ellis et al. (2003).

Chapter II

Review of Literature

When evaluating a petroleum system it is essential to understand the character of the source rock. Since source rock volumes and richness are not limited to a function of tectonic style (Ulmishek, 1986; Grunau, 1987) it is necessary to assess a source rock according to a geochemical framework. Geochemical sampling techniques including carbon isotope ratios, TOC, and Rock Eval have been used as prospecting tools in hydrocarbon exploration (Magoon and Dow, 1994). The primary purpose of such data is to evaluate the potential of a source rock to produce petroleum in economic quantities. To do so it is necessary to measure and assess the quality, quantity, and maturity of source rocks.

Paleolatitudinal and paleoclimatic factors are more important to source rock distribution than tectonic style (Bois et al., 1982; Klemme, 1990). The tectonic style provides a setting for geochemical processes to occur and does necessarily ensure that they will. Thus, it is critical to use geochemistry to identify the charge of a petroleum system. Where charge is the richness and the volume of a source rock (Magoon and Dow, 1994).

The relative amount of charge is dependent upon temporal geochemical conditions allowing for a biogeochemical and abiotic transformation of once-living organic matter into kerogen (Demaison, 1984) and the thermodynamic processes that transform kerogen into hydrocarbons (Tissot et al., 1987). The total amount of hydrocarbons that accumulate in a reservoir or play cannot accurately be estimated from a source alone due to the uncertainty of expulsion efficiency and primary and secondary migration losses (Peters and Cassa, 1994). Expulsion efficiency is affected by factors such as source rock volumes, sediment fabric, mineralogy, kerogen type, maturity, and pressure (Demaison and Huizinga, 1994). Migration losses are influenced by the angle of dip, interfacial tension, wettability, and rock heterogeneity, and the oil and water density (Schowalter, 1989).

The interpretation that organic matter is primarily buried in argillaceous muds and in smaller amounts in calcareous/sandy muds and marls were initially recognized by numerous geologists including Snider (1934). Hunton and Jamieson (1956) were the first to show an association between crude-oil extracts in source rocks and reservoir oil from the Powder River Basin, Wyoming. Baker (1962) evaluated source rocks data from the Cherokee Formation of Oklahoma and showed a similar relationship. These early studies depicted a link between hydrocarbons and a source rock, however, more recent studies use quantity, quality, and maturity to assess a source rock (Hunt, 2002).

2.1 Quantity of Organic Matter: Total Organic Carbon (TOC)

TOC, preserved in sediments does not correlate directly with modern primary biological activity (Demaison and Moore, 1980). However, this is not especially

significant because it is the preserved organic matter that is of interest in petroleum exploration. In other words, TOC is a measurement of the amount of biological matter preserved rather than the amount present at any given time. Only about 0.6 % of organic carbon produced in marine basins is actually buried (Hunt, 1979). Preserved organic matter can be linked to various depositional environments with relative amounts of TOC (Bralower and Thierstein, 1984). For example, Bralower and Thierstein (1984) demonstrated that nearshore sediments have greater bulk TOC preservation than either hemipelagic or pelagic sediments in terms of spatial distribution. However, nearshore TOC preservation quality is not necessarily as great. Quality is analogous to kerogen type, where relatively improved quality is associated with Type I and II kerogens. Therefore, using TOC as single paleoenvironmental interpretive tool may be misleading because OM can be preserved in both deep anoxic basins and in highly productive shelf settings (Demaison and Moore, 1980; Pedersen and Calvert, 1990). This can be important in oil and gas exploration when modeling the thickness of a source rock relative to expected gas production.

Potonie (1908) identified two major types of OM (sapropelic and humic) used in current studies. The terms sapropelic and humic are operational definitions because they can be identified by their chemical structure. The chemical structure of sapropelic oil generating kerogens have long chains and individual ring structures (Hunt, 1996). The chemical structure of humic kerogens consist of a large number of condensed rings with a relatively small number of short side chains and single methyl groups (Hunt, 1996). It is important to note that humic structures can evolve from once sapropelic oil generating kerogen that has since matured from the oil-generating phase into the gas generation

phase. Thus, humic kerogen is used in identifying gas producing source rocks and sapropelic kerogen is used in identifying the oil generating source rocks.

Phytoplankton (plants) and zooplankton (animals) contribute the majority of sapropelic OM. Sapropelic OM is chemically distinct from humic OM by higher hydrogen content relative to carbon content (Hydrogen/Carbon; H/C). Sapropelic OM is typically characterized by H/C ratios of 0.8 to 1.9 while humic OM H/C ratios generally range from 0.1 to 1.0. (Hunt, 1996). Sapropelic OM is believed to form in oxygen-restricted areas and be deposited in marine or lacustrine muds. Identification of OM type is important in establishing a relationship between reservoir hydrocarbons and a source rock.

Terrestrial organic matter such as land plant material, wind blown spores, pollen, organic debris, and recycled organic matter contribute to humic OM. This OM has a lower H/C ration than sapropelic OM and typically forms in oxygenated environments and is typically deposited in swamps (Hunt, 1996).

TOC values required for commercially productive source rocks vary between potentially gaseous source rocks and oil source rocks. This difference is a result of primary expulsion mechanisms for each hydrocarbon system (Leythaeuser and Poelchau, 1991). Oil source rocks requires a hydrocarbon saturated pore space, while gas only needs a concentration gradient (Katz et al., 1999). A gaseous source rock is considered commercially viable when it contains TOC greater than 0.5 wt % (Rice and Claypool, 1981). An oil prone source rock is considered commercially viable when it contains TOC equal to or greater than 1 wt % (Bissada, 1982).

2.2 Quality of Organic Matter: Kerogen Type

Kerogen is the remnant fraction of organic matter from a sedimentary rock after it has been extracted using organic solvents (Durand, 1980; Tissot and Welte, 1984). In other words kerogen is not deposited, it forms from deposited organic matter during diagenesis. This realization that organic matter first transformed into kerogen before becoming petroleum was purposed by Forsman and Hunt (1958). Later the relationship between kerogen and petroleum formation was firmly established by Ableson (1963), which recognized that kerogen formed from organic matter. Bitumen is defined as the remnant fraction of organic matter that is soluble in organic solvents. Bitumen can form from lipids but the majority is formed from the cracking of kerogen (Peters and Cassa, 1994).

Van Krevelen (1961) plotted H/C vs. O/C ratios to analyze processes that occur during coalification (Figure 11). Later Tissot et al (1974) used the Van Krevelen diagram to plot various sedimentary rocks and in doing so classified three types of kerogen that could be identified using the plot (a fourth type was added later). Since the Van Krevelen diagram requires time consuming extraction of kerogen form each sample Espitalie et al (1974) developed a quicker analytical tool that utilized rock eval pyrolysis. Espitalie et al (1974) plotted the Hydrogen Index (mg HC / g TOC) vs. the Oxygen Index (mg CO2 / g TOC). This innovative step drastically reduced the time required to gather information to plot on the Van Krevelen diagram.

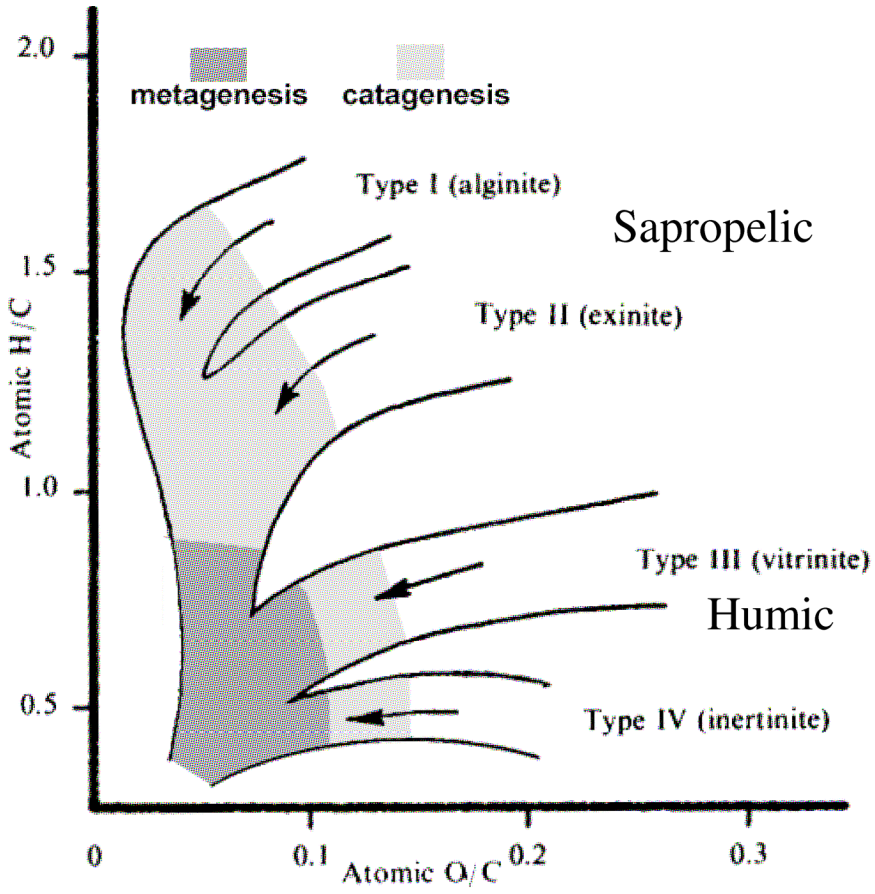

Figure 12. Van Krevelen diagram illustrating relationship between hydrogen / carbon and oxygen / carbon ratios. Modified from Waples (1985).

Type I kerogen is characterized as hydrogen rich, oxygen poor (high H/C ratio) with a high potential for oil and is derived from algal OM (Wignall, 1994). Type II kerogen is characterized a by moderate H/C ratio and is typical of most marine petroleum source rocks. Type II kerogen results from 'bacterially derived' OM (i.e. phytoplankton) and minor amounts of terrigenous organic matter (TOM) (Wignall, 1994). Type I and II kerogens are preserved under anoxic conditions (Wignall, 1994). Type III kerogen is characterized by low H/C ratios and high O/C ratios. This type consists mostly of TOM and unlike types I and II it can be preserved under oxic/suboxic conditions (Wignall,

1994). Rock-Eval pyrolysis is used to obtain the data necessary to create a pseudo-Van Krevelen plot (Figure 13).

Organic facies can be related to depositional environments through the interpretation of pyrolysis data (Jones, 1987). Jones (1987) classified organic facies into A, AB, B, BC, C, CD, and D based on a modified Van Krevelen plot (Figure 12). Organic Facies A consists of the highest H/C ratio while organic facies D consists of the lowest H/C ratio. Organic facies A consists of mostly algal matter and is extremely rare because it lacks any amount of TOM (Wignall, 1994). Organic facies AB consists of algal and bacterial OM and minor amounts of TOM. Organic facies B consists of algal and bacterial OM and TOM. Organic facies AB and B are characteristic of transgressive black shales and black shales respectively.

There is an exponential relationship between hydrocarbon formation from kerogen (from shales) and increasing depth (temperature) (Larskaya and Zhabrev, 1964). During diagenesis, the initial phase of heating, hydrocarbons are generated from organic matter (at low temperatures relative to the oil generation process). At approximately 50^{o}C diagenesis is replaced by catagenesis (Hunt, 1996). During the initial stages of catagenesis temperatures are high enough to cause hydrocarbon fragments to break away from kerogen. In other words bitumen is formed from kerogen and petroleum is generated from bitumen (Lewan et al., 1979). Around 200^{o}C the catagenesis stage ends and the metagenesis stage begins.

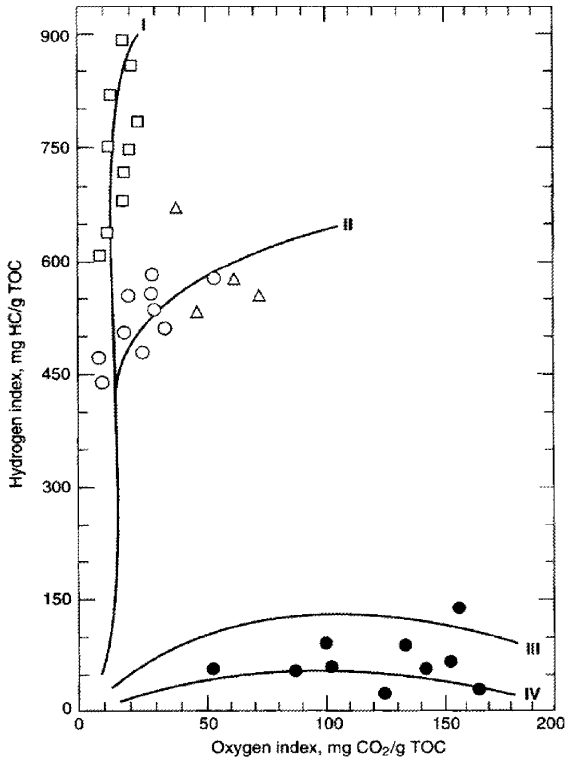

Figure 13. Modified Van Krevelen diagram. From (Hunt, 1996).

There is an inverse relationship between maturity and the size of hydrocarbons evolved which accounts for a zone of oil formation ('oil window') and a wet gas zone. The first hydrocarbons produced during the 'oil window', ranges in temperature between 100°C and 150°C, are relatively heavy, average composition $C_{34}H_{54}$, but gradually reduce in weight as temperature increases. Eventually the wet gas zone is reached (around 150°C) and a mixture of gaseous and liquid hydrocarbons is present. With increasing temperature the relative amounts of gaseous hydrocarbons increase while the relative amount of liquid hydrocarbons decrease. Eventually the dry gas zone or cracking zone is reached during the end of catagenesis where only gas is formed, mostly methane (CH_4) and CO_2. It is believed that labile kerogen produces oils, refractory kerogen produces gas and inert kerogen produces non-hydrocarbons. These non-hydrocarbons eventually

metamorphose to graphite under extremely high temperature and pressure conditions. Graphite is the most stable form of carbon under surface conditions.

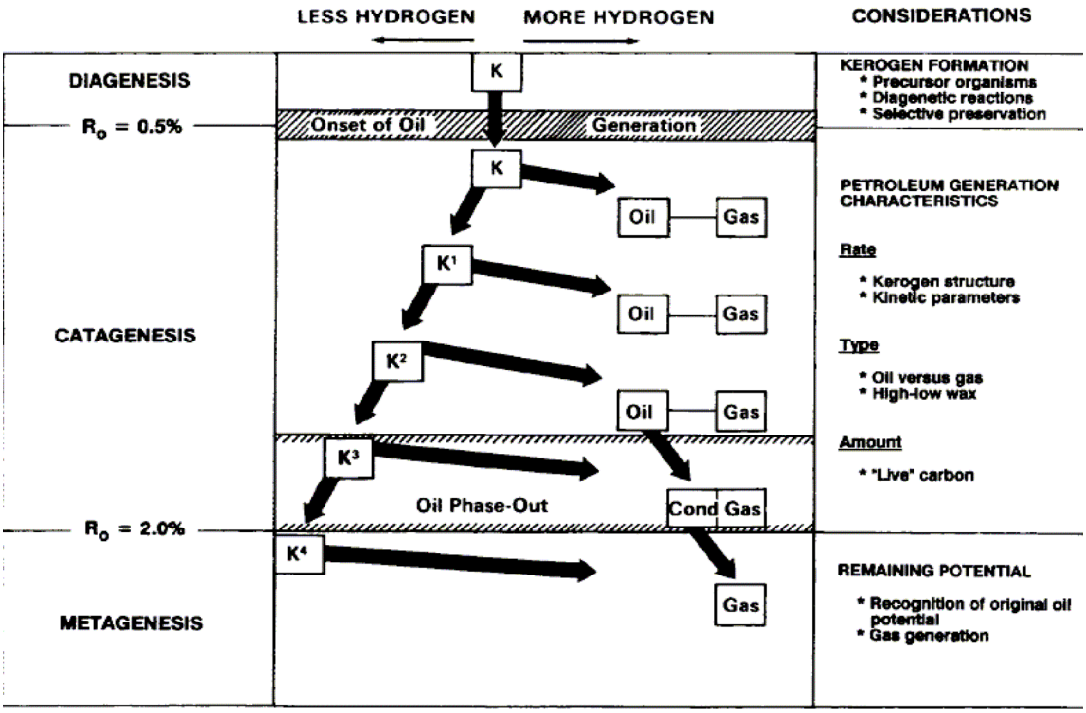

Figure 14. Phases of thermal maturation shown in a simplified schematic with diagenesis, catagenesis, and metagenesis zones delineated by thermal maturity. From Horsfield and Rullkötter (1994).

2.3 Richness of Organic Matter: Evaluation of Maturity

2.3.1 Vitrinite Reflectance

Vitrinite Reflectance was originally used by White (1915) to demonstrate a relationship between coal rank and oil. In 1958 Marlies Teichmüller used vitrinite reflectance values to study the maturity of the Wealden Basin, Southern United Kingdom, where the presence of coal was lacking. Teichmüller determined a similar relationship

between coal rank and oil as there was with small vitrinite inclusions that occur in carbonates and sandstones and oil.

Light reflected off of a vitrinite surface will vary depending on maturity. The reflectivity is related to the molecular structure of a vitrinite maceral. Structural changes occur as aromatic rings fuse together and increase in size with greater temperature. It has been noted that %Ro values are not influenced significantly by pressure (Hunt, 1996). Gradually, ordered sheets of aromatic ring-like structures form along planes of preferred orientation, which eventually cause greater reflectivity.

2.3.2 Carbon Isotopes

Early bulk carbon isotope studies performed by Silverman and Epstein (1958) showed that marine oils could be distinguished from non – marine oils in various Tertiary environments. Kvenvolden and Squire (1967) were able to identify differences in oils from West Texas using carbon isotopic compositions. However, not all studies have shown similar results. For example Galimov (1973) preformed a study in the Urals using Carboniferous oils that showed no distinction in isotopic composition.

Welte (1975) and Stahl (1977) suggested that ^{12}C concentration decreases with a rocks age. Silverman (1965) identified variations in isotopic composition such as a depletion of ^{13}C with an increase migration distance of oil. He explained this relationship as a result of a relative increase in isotopically light saturates and a decrease in isotopically heavier components (i.e. aromatics, polars, asphaltenes) during migration. Stahl (1977) applied carbon isotope analyses to methane and noticed a similar

relationship in which methane isotopic compositions become heavier with increasing maturity and biodegradation.

Schoell (1978) plotted $\delta^{13}C$ (‰, V - PDB) methane vs. C_{2+} wetness values as a result of the relationship (Figure 14). This plot can be used to identify petroleum type in terms of hydrocarbon generation phase.

The original explanation proposed to clarify the relationship between thermogenic hydrocarbons and carbon isotopes was the equilibrium isotope effect (Petersil'ye, 1967; Galimov and Ivlev, 1973; Galimov, 1974; and James, 1983). However, the current view by various authors suggest that this relationship is a result of a kinetic isotope effect (Chung et al., 1988; Hoşgörmez et al., 2005). A kinetic isotope effect occurs because ^{12}C – ^{12}C bonds are lighter and more mobile than ^{12}C – ^{13}C bonds, therefore, the former tend to break with less energy. This results in ^{13}C enrichment within the residue of the gaseous source and depletion of ^{13}C in the released gas (Sackett et al., 1968; Sackett, 1978). According to this model the weight of collected gas is isotopically heavier with increased thermal cracking or maturity.

Berner et al., (1995) showed that proportions of methane, ethane, and propane obtained in a laboratory mimic that of isotopic variations in natural gasses. In the majority of worldwide basins an increase in the number of carbon atoms in a gas molecule has a positive correlation with increasing isotopic weight (Smith et al., 1971; Galimov, 1974; Sakett, 1978; Waples and Tornheim, 1978; James, 1983; Sundberg and Bennett; Chung et al., 1988). In other words methane is lighter than ethane, which in turn is lighter than propane and so on.

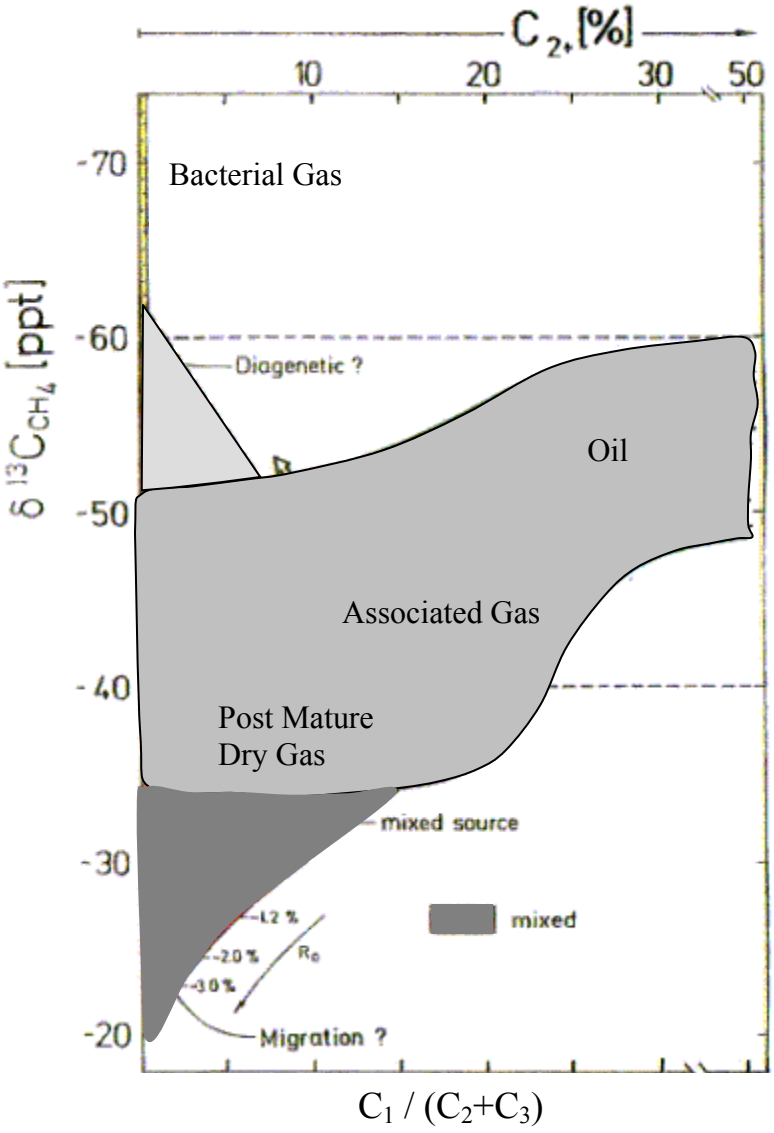

Figure 15. Chart used to determine phase of petroleum from isotopic and compositional data. Ms and Md arrows indicate compositional shifts as a result of shallow and deep migration. Modified from Schoell (1983).

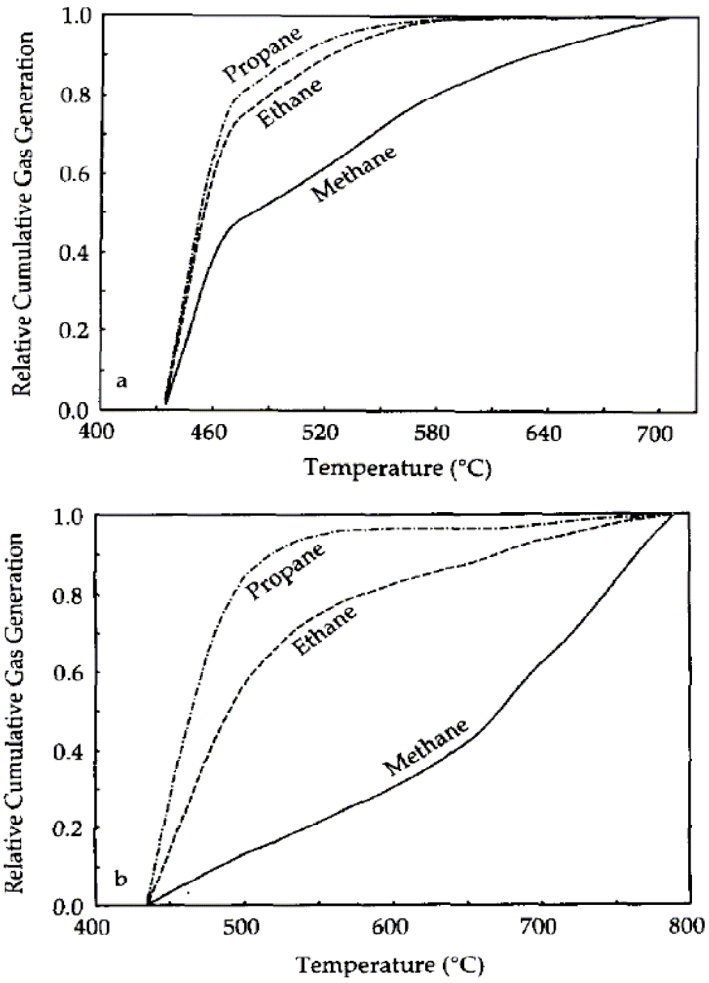

Figure 16. Shows relationship between gas generation and temperature in propane, ethane, and methane. Modified from Berner et al. (1995).

Chapter III

Methods

Sampling for this study incorporated well logs, stable carbon isotopes (Table 1), gas composition (Table 2), Rock Eval Pyrolysis (Table 3), TOC (wt %) (Table 3), Vitrinite Reflectance (%Ro) (Table 4), core, and thin sections. Regionally the greatest control came from well logs. Carbon isotopes, complete gas composition, hydrocarbon gas composition, TOC, and Rock Eval were the second most frequent source. Vitrinite reflectance was measured in two wells as a proxy for inferred isotopic thermal maturity values. Core, thin sections, and XRD data was collected from a single well, which is located in the center of the study area (Figure 16).

Well log distribution is regionally and stratigraphically extensive throughout most of the Hugoton Embayment. Regionally the Hugoton Embayment is a large feature that includes the Oklahoma panhandle and a large portion of SW Kansas. Stratigraphically the Atoka sits above the Morrow Series, which is a primary exploration target for oil and gas reservoirs. Therefore, many well logs are drilled and logged through the Atoka to reach the Morrow.

Well logs used in this study include gamma ray logs, neutron-density logs (including the photoelectric log (PE)), and resistivity logs. Gamma Ray values are

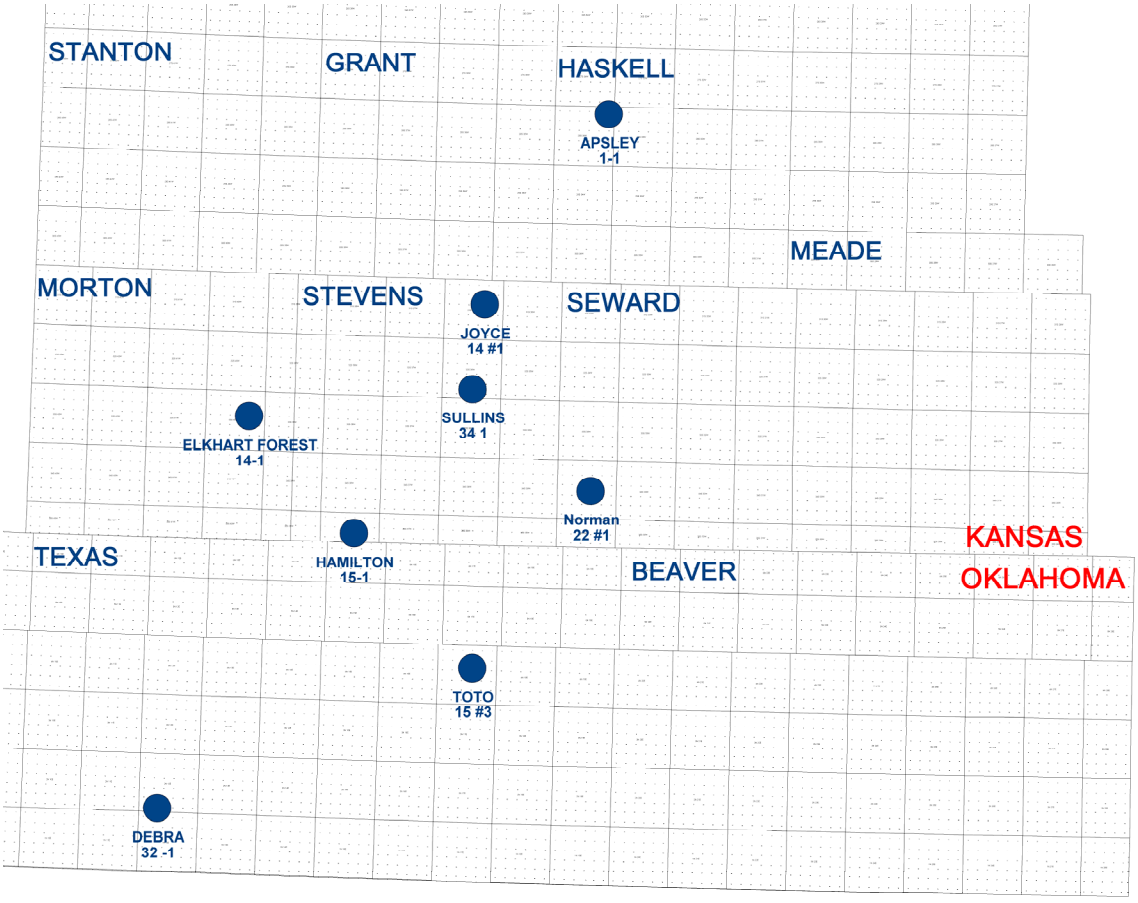

Figure 17. Well sampling locations in Oklahoma and Kansas. County names in blue and state names in red.

measured relative to the API standard (American Petroleum Institute). The gamma ray tool reacts to the radioactive nature of a formation and is used to identify variations in lithology (i.e. shale). Generally 150 API is considered a 'Hot Shale" and is can be used as a general cut off for organic-rich fine-grained rocks. The Neutron-Density combination log is commonly used to identify formation porosity. This log is also a useful lithology indicator especial when used in conjunction with gamma ray and PE curves. The neutron log measures a formations hydrogen concentration, which is associated with a formations fluid filled pore space. The density log tool emits gamma ray particles into a formation and measures the return of gamma ray particles after they

collided with formation electrons. The density tool measures a high-energy range and a low-energy range, which measure the amount of Compton scattering and the photoelectric effect, respectively. The level of Compton scattering is proportional to electron density, which is related to bulk density (Tittman and Wahl, 1965). Bulk density is influenced by formation porosity. Resistivity logs are typically used to identify water bearing versus hydrocarbon bearing formations.

Eight wells were selected based on regional extent and availability of drilling locations for stable isotope sampling. External factors played a role in sampling locations. However, a large enough number of drilling sites were available for a widespread study to be preformed (Figure 16). Two locations are in Oklahoma and six locations are in Kansas (Figure 16). The sampling area covers a large portion of the Hugoton Embayment of the Anadarko Basin. Due to external factors sample locations were not done in a systematic fashion, instead they were performed with respect to a rig schedule. Each well includes approximately 10 to12 mud gas samples. Gas samples come from the same stream as a mud logging gas flow line and are collected into metal cylinders. Sampling was completed based on mud log shows, with the judgment of an onsite mud-logger and using nearby well logs as analogues for predicting intervals of interest.

Gas collection is initiated by placing a metal cylinder (IsoTube® container) into a manifold (Figure 17). As gas is collected into a gas chromatograph tool (while rig is drilling) it is redirected and bypasses through the manifold. When a sampling location is identified (by an increase in gas content on the gas chromatograph and by correlating the drilling depth with the intended sampling interval) the mud logger pulls the manifold

lever, which redirects the intended sample gas into an IsoTube® container. After the mud gas is gathered in an IsoTube container it is analyzed using a gas chromatograph at an off-site laboratory. A second aliquot of samples is also analyzed for their stable isotopic compositions using gas chromatrgraph-irms.

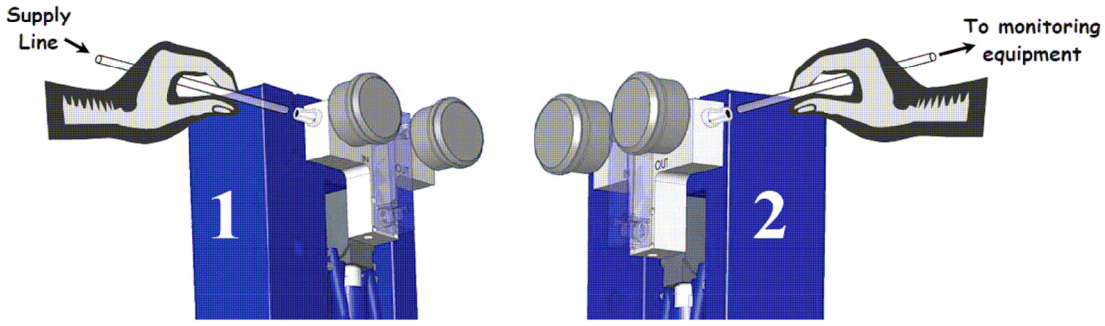

Figure 18. Manifold for Gas IsoTube sampling. Modified from Isotech instruction manual.

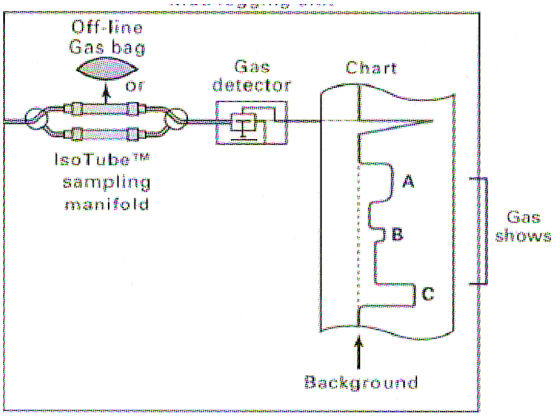

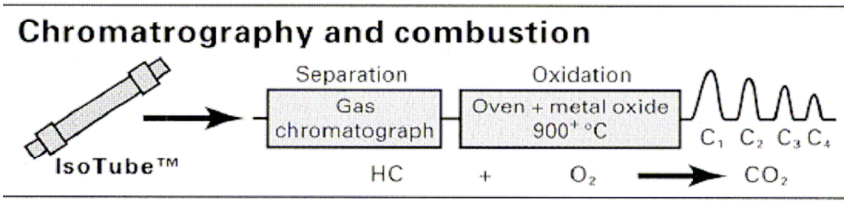

Figure 19. After gas is collected it is analyzed in a gas chromatograph. Modified from Ellis et al. (2003).

Total Organic Carbon (TOC) and Rock Eval Pyrolysis analyses were performed on well cuttings taken while drilling. An exception was the Sullins 34 #1 well, where these analyses were performed on core samples. TOC is the total weight percent of organic carbon in a sample. TOC was obtained for this study using the LECO method (LECO C230 Carbon Determinator, by GeoMark) (Figure 19). The first step of the LECO method is to remove inorganic carbon by soaking a sample in hydrochloric acid (HCL) for approximately 12 – 16 hours or until no effervescence is observed with the addition of acid and stirring (Jarvie, 1991). The sample is then rinsed, dried, and heated in a furnace at 1700^{o}C (oxygen free) while CO_2 is generated and measured.

Rock Eval Pyrolysis data was collected from sample cuttings during drilling. Espitalie (1977) developed the Rock Eval Pyrolysis technique. This process is performed using a flame ionization detector to measure vapors generated by a flow of helium over 100 mg of pulverized rock. Each sample is initially heated to 300^{o}C followed by an incremental increase in temperature of 25^{o}C / minute until the sample reaches 550^{o}C. Peaks P1 (S1), P2 (S2), and P3 (S3) are measured during the heating process (Figure 19). These peaks are used to identify the mg HC/g rock of free hydrocarbons from deposition or generated from kerogen post deposition, the mg HC/g rock value from cracked kerogen between 350^{o}C and 550^{o}C, and the mg CO_2 / g rock value from the carboxyl groups of the sample between 300^{o}C and 390^{o}C, respectively. Rock Eval can also be used to determine TOC values, however, it was not used in this method because values are not generally as accurate as the LECO procedure.

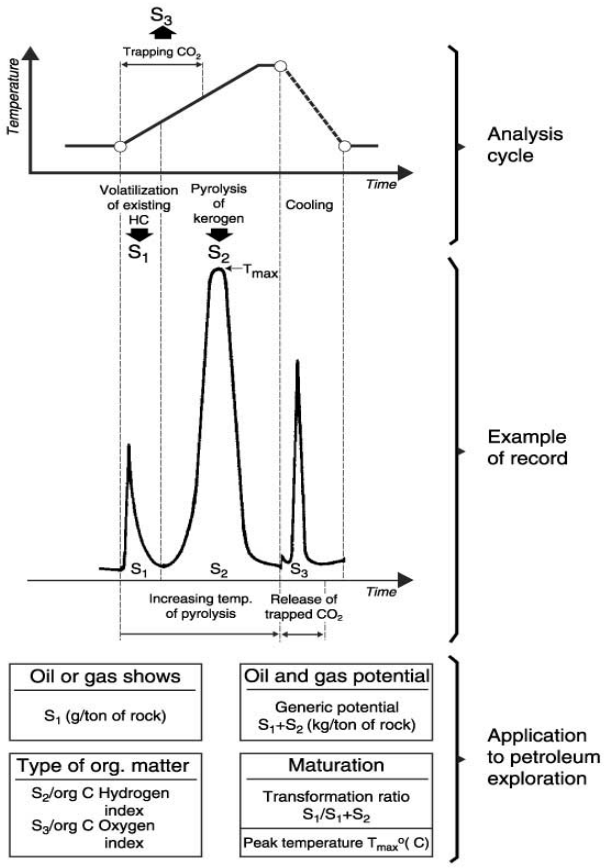

Figure 20. Rock Eval pyrolysis peaks. From Tissot and Welte (1984).

Vitrinite reflectance measurements are made on telocollinite (a coal maceral of vitrinite) using a reflective microscope (Hunt, 1996). The percentage of light reflected back through the microscope is measured as %Ro. The statistical average of the %Ro value is determined using a histogram. %Ro values have been related to oil and gas generation for values between 0.35 %Ro to 3.5 %Ro (Hunt, 1996). Typically %Ro values between 0.5 to 0.6 mark the onset of oil generation, peak oil formation occurs at 0.8 %Ro, the end of oil formation / initiation of gas formation occurs at 1.3 % Ro and dry gas has a %Ro value of 3.5 (Dow, 1977).

Chapter IV

Results

4.1 Petrographic Analysis

Thin section data from five samples within the Sullins 34 #1 well provide primary constraints on the character of Atoka source rocks and provided a geological framework within which to consider geochemical data. Sample one taken at 5620 ft consisted of a dolomite matrix with moderate fossil content including brachiopods, ostracode shell fragments and early stages of pyrite and silica replacement (Figure 20a). Sample two taken at 5631 ft consisted of a calcite matrix with moderate fossil content including burrows and shell fragments with pyrite and silica replacement (Figure 20b). Sample three taken at 5636 ft consisted of a clay rich matrix with numerous dolomite rhombs present. This sample also included a relatively high amount of pyrite, some phosphate, brachiopod and ostracode shell fragments with pyrite and silica replacement (Figure 20c). Sample four taken at 5636.4 included a dolomite matrix with sparse fossil content (Figure 20d). Sample five taken at 5641 ft included a fossilliferous calcite matrix with moderate clay content (Figure 20e). This sample was heavily burrowed with brachiopod and ostracode shell fragments in the early stages of pyrite and silica replacement. Sample six collected from 5641.4 ft included a fossilliferous calcite matrix and was heavily

burrowed (Figure 20f).

Variations in compositions are related to variations in sea level as continental seas periodically inundated the mid-continent during the Pennsylvanian System.

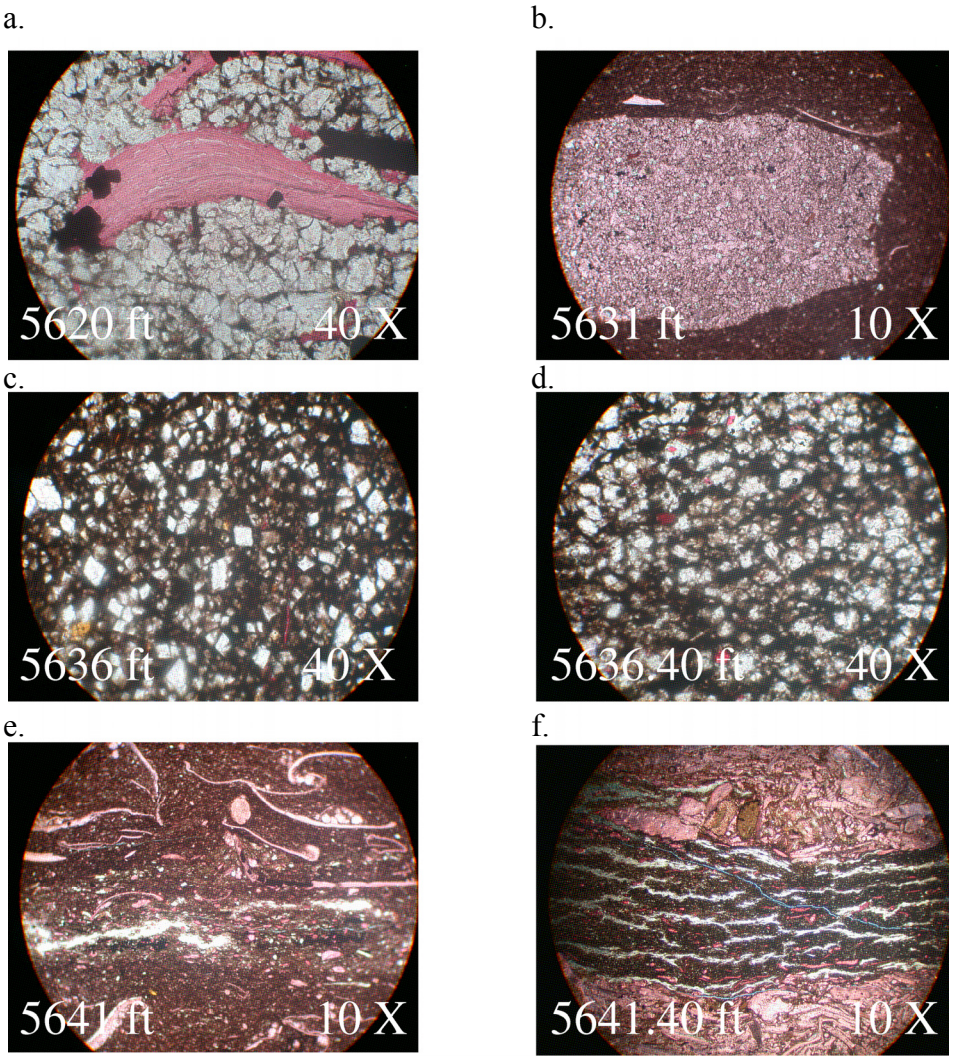

Figure 21. Photomicrographs of thin sections of Atoka rocks collected from the Sullins 34 #1 well.

4.2 Vitrinite Reflectance

Vitrinite reflectance values were collected from the Debra 32 #1, Norman 22 #1, and Sullins 34 #1 wells (Figure 21; Table 1). Vitrinite was determined visually and

values were plotted on a histogram to estimate an accurate average vitrinite value. Vitrinite data analyses were out sourced and completed by Minerals End Inc.

Average values from the Debra 32 #1, Norman 22 #1, and Sullins 34 #1 were 0.83 (% Ro), 1.01 (% Ro), and 1.17 (% Ro), respectively.

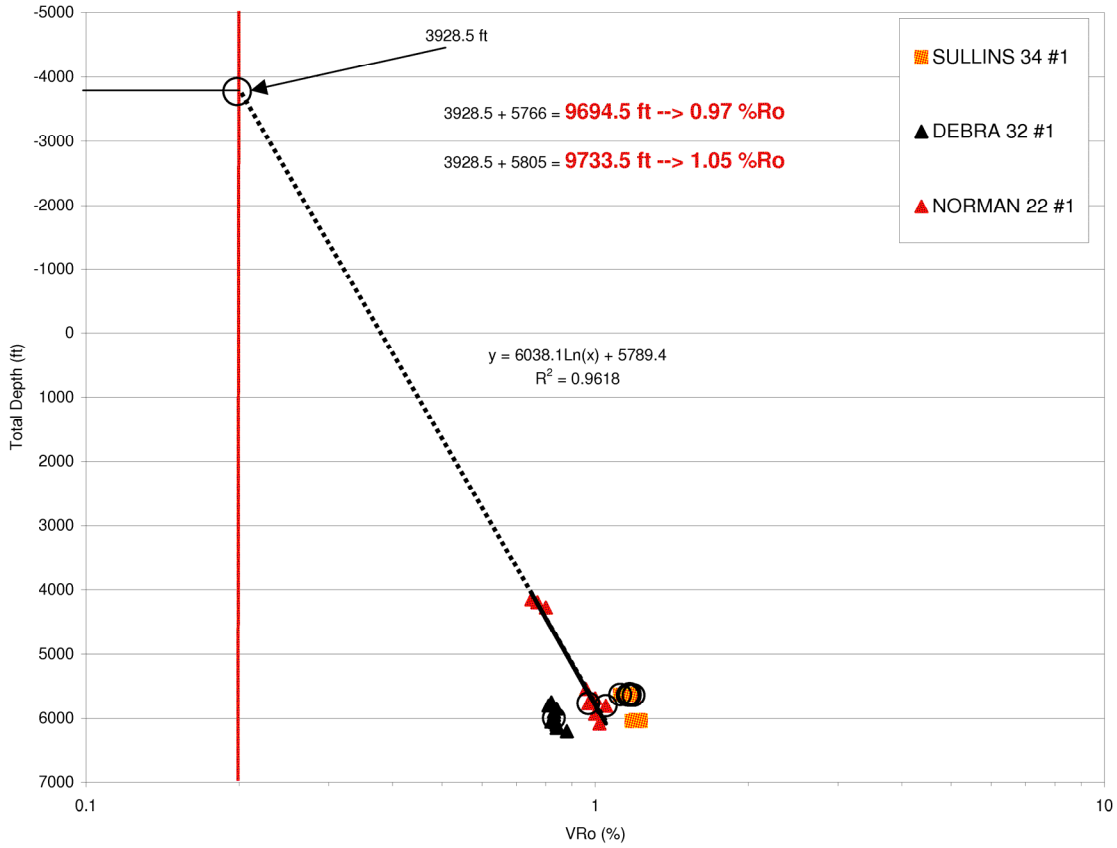

Figure 22. Plot of total depth in feet vs. measure vitrinite reflectance values in log scale from three wells. The Norma 22 #1 well included values from multiple intervals and is used to estimate overburden removal at the intersection of 0.2 (% Ro).

4.3 Rock Eval Pyrolysis

Rock Eval data was collected from four wells along with TOC data (Table 2). These data were used to identify kerogen type by plotting oxygen indices (mg CO_2 / g TOC) versus hydrogen indices (mg HC / g TOC; Van Krevelen, 1961; Espitalie et al., 1974). Kerogen types collected from the Atoka group of southwest Kansas were

predominantly type II and type III (Figure 22). All kerogen types collected from ten samples within the Atoka Group are type II kerogen as plotted on the van Krevelen Diagram (Figure 22).

Well Name	Total Depth (ft)	Subsea Depth	VRo (%)	ATOK
SULLINS 34 #1	5620.15	2572.15	1.17	ATOK
SULLINS 34 #1	5630.7	2582.7	1.12	ATOK
SULLINS 34 #1	5636	2588	1.16	ATOK
SULLINS 34 #1	5636.4	2588.4	1.19	ATOK
SULLINS 34 #1	5640.9	2592.9	1.17	ATOK
SULLINS 34 #1	5641.4	2593.4	1.19	ATOK
SULLINS 34 #1	6025.7	2977.7	1.2	
SULLINS 34 #1	6026.9	2978.9	1.22	
SULLINS 34 #1	6032.5	2984.5	1.23	
SULLINS 34 #1	6043.7	2995.7	1.23	
SULLINS 34 #1	6045	2997	1.18	
DEBRA 32 #1	5750	2443	0.82	
DEBRA 32 #1	5800	2493	0.81	
DEBRA 32 #1	5850	2543	0.84	
DEBRA 32 #1	5900	2593	0.83	
DEBRA 32 #1	5950	2643	0.83	
DEBRA 32 #1	6000	2693	0.83	ATOK
DEBRA 32 #1	6050	2743	0.82	
DEBRA 32 #1	6100	2793	0.84	
DEBRA 32 #1	6150	2843	0.84	
DEBRA 32 #1	6200	2893	0.88	
NORMAN 22 #1	4146	1216	0.75	
NORMAN 22 #1	4194	1264	0.77	
NORMAN 22 #1	4274	1344	0.8	
NORMAN 22 #1	5544	2614	0.96	
NORMAN 22 #1	5684	2754	1	
NORMAN 22 #1	5766	2836	0.97	ATOK
NORMAN 22 #1	5805	2875	1.05	ATOK
NORMAN 22 #1	5929	2999	1	
NORMAN 22 #1	6084	3154	1.02	

Table 1. Measured Vitrinite Reflectance values from the Sullins 34 #1, Debra 32 #1, and Norman 22 #1 wells.

4.4 Total Organic Carbon (TOC)

Samples for TOC analyses were collected from the Debra 32 #1, Hamilton 15 #1, Sullins 34 #1, and the Norman 22 #1 wells (Table 2). Samples were collected as cuttings with the intention of being sampled near gas kicks as recorded on a gas chromatograph while the well was being drilled. The Atoka Group includes various lithologic features including interbedded organic/non-organic rich clays/shale and organic/non-organic rich limestone/marl. The Atoka also sometimes includes thin sand intervals in the basal

Well name	Depth	Subsea Depth	S1	S2	S3	LECO-TOC	Tmax	S2/S3	HI	OI	PI	S1 / TOC
DEBRA 32#1	5750	2443.00	0.18	0.94	0.87	0.73	436	1.08	129	119	0.16	25%
DEBRA 32#1	5800	2493.00	0.20	1.38	0.55	0.93	434	2.51	148	59	0.13	22%
DEBRA 32#1	5850	2543.00	0.12	1.29	0.58	1.00	432	2.22	129	58	0.09	12%
DEBRA 32#1	5900	2593.00	0.61	6.87	0.63	2.52	436	10.9	273	25	0.08	24%
DEBRA 32#1	5950	2643.00	0.23	5.13	2.53	2.65	432	2.03	194	95	0.04	9%
DEBRA 32#1	6000	2693.00	0.22	2.99	1.61	1.41	438	1.86	212	114	0.07	16%
DEBRA 32#1	6050	2743.00	1.29	12.76	1.56	5.35	429	8.18	239	29	0.09	24%
DEBRA 32#1	6100	2793.00	0.11	1.89	1.08	1.72	428	1.75	110	63	0.05	6%
DEBRA 32#1	6149	2842.00	0.11	1.84	1.60	1.56	437	1.15	118	103	0.06	7%
DEBRA 32#1	6200	2893.00	0.02	0.19	0.90	0.49	432	0.21	39	184	0.1	4%
HAMILTON 15 #1	5470	2267.00	0.08	0.37	0.30	0.29	428	1.23	128	103	0.18	27%
HAMILTON 15 #1	5510	2307.00	0.11	0.51	0.46	0.37	429	1.11	138	124	0.18	29%
HAMILTON 15 #1	5645	2442.00	2.76	29.95	0.68	6.38	429	44.04	469	11	0.08	43%
HAMILTON 15 #1	5820	2617.00	0.68	6.66	0.47	2.55	436	14.17	261	18	0.09	27%
HAMILTON 15 #1	5885	2682.00	0.74	10.50	0.64	3.47	433	16.41	303	18	0.07	21%
HAMILTON 15 #1	5915	2712.00	0.58	7.75	0.46	2.64	433	16.85	294	17	0.07	22%
HAMILTON 15 #1	5967	2764.00	1.49	14.79	0.66	4.35	434	22.32	340	15	0.09	34%
HAMILTON 15 #1	5980	2777.00	1.48	13.74	0.47	4.21	436	29.26	326	11	0.10	35%
HAMILTON 15 #1	6040	2837.00	0.39	2.76	0.48	1.54	433	5.73	179	31	0.12	25%
HAMILTON 15 #1	6055	2852.00	0.51	3.83	0.30	1.73	437	12.63	222	18	0.12	29%
HAMILTON 15 #1	6120	2917.00	0.27	2.61	0.35	1.94	433	7.37	135	18	0.09	14%
HAMILTON 15 #1	6095	2892.00	0.26	2.60	0.26	1.61	438	9.92	162	16	0.09	16%
HAMILTON 15 #1	6165	2962.00	0.17	1.10	0.57	1.12	436	1.93	98	51	0.13	15%
SULLINS 34 #1	5410	2362.00	0.17	1.38	0.56	1.00	440	2.46	138	56	0.11	17%
SULLINS 34 #1	5467	2419.00	0.66	6.35	0.57	2.82	440	11.14	225	20	0.09	23%
SULLINS 34 #1	5505	2457.00	0.14	1.48	0.79	1.03	438	1.87	144	77	0.09	14%
SULLINS 34 #1	5529	2481.00	0.42	3.62	0.68	1.79	440	5.32	202	38	0.1	23%
SULLINS 34 #1	5573	2525.00	0.34	2.74	1.86	1.45	437	1.47	189	128	0.11	23%
SULLINS 34 #1	5616	2568.00	0.40	2.96	0.62	2.00	440	4.77	148	31	0.12	20%
SULLINS 34 #1	5640	2592.00	0.70	6.27	0.69	2.81	440	9.09	223	25	0.1	25%
SULLINS 34 #1	5655	2607.00	0.87	7.25	0.72	3.30	440	10.07	220	22	0.11	26%
SULLINS 34 #1	5679	2631.00	0.58	4.79	0.82	2.34	439	5.84	205	35	0.11	25%
SULLINS 34 #1	5690	2642.00	0.56	4.85	1.68	2.24	438	2.89	217	75	0.1	25%
SULLINS 34 #1	5725	2677.00	0.49	4.98	0.94	2.78	439	5.30	179	34	0.09	18%
SULLINS 34 #1	5760	2712.00	0.38	3.40	0.85	2.45	439	4.00	139	35	0.10	16%
NORMAN 22 #1	4146	1204.00	0.30	1.21	0.13	0.75	432	9.31	161	17	0.20	40%
NORMAN 22 #1	4194	1252.00	0.48	3.43	0.18	1.25	434	19.06	274	14	0.12	38%
NORMAN 22 #1	4274	1332.00	0.17	2.30	0.45	1.64	429	5.11	140	27	0.07	10%
NORMAN 22 #1	5544	2602.00	0.42	3.18	0.16	1.13	438	19.88	281	14	0.12	37%
NORMAN 22 #1	5684	2742.00	0.25	2.30	0.15	1.17	439	15.33	197	13	0.10	21%
NORMAN 22 #1	5766	2824.00	0.38	5.54	0.24	2.67	441	23.08	207	9	0.06	14%
NORMAN 22 #1	5805	2863.00	0.15	2.31	0.33	1.93	437	7.00	120	17	0.06	8%
NORMAN 22 #1	5929	2987.00	0.13	1.22	0.20	1.38	439	6.10	88	14	0.10	9%
NORMAN 22 #1	6084	3142.00	0.18	0.81	0.09	0.88	435	9.00	92	10	0.18	20%

Table 2. TOC and Rock-Eval data from the Debra 32 #1, Hamilton 15 #1, Sullins 34 #1 and the Norman 22 #1 wells. HI = Hydrogen Index (mg HC / g TOC).
OI = Oxygen Index (mg CO_2 / g TOC). T_{MAX}= S2 peak temperature. S2 / S3 = Hydrocarbon Index Type.

portion of the group. Due to this variability TOC was sampled from different lithologies making a regional comparison by well difficult. However, the amount of TOC collected is significant enough to indicate the presence of a source rock. TOC values measured on samples from four wells range between 0.29 and 6.38 (Table 2).

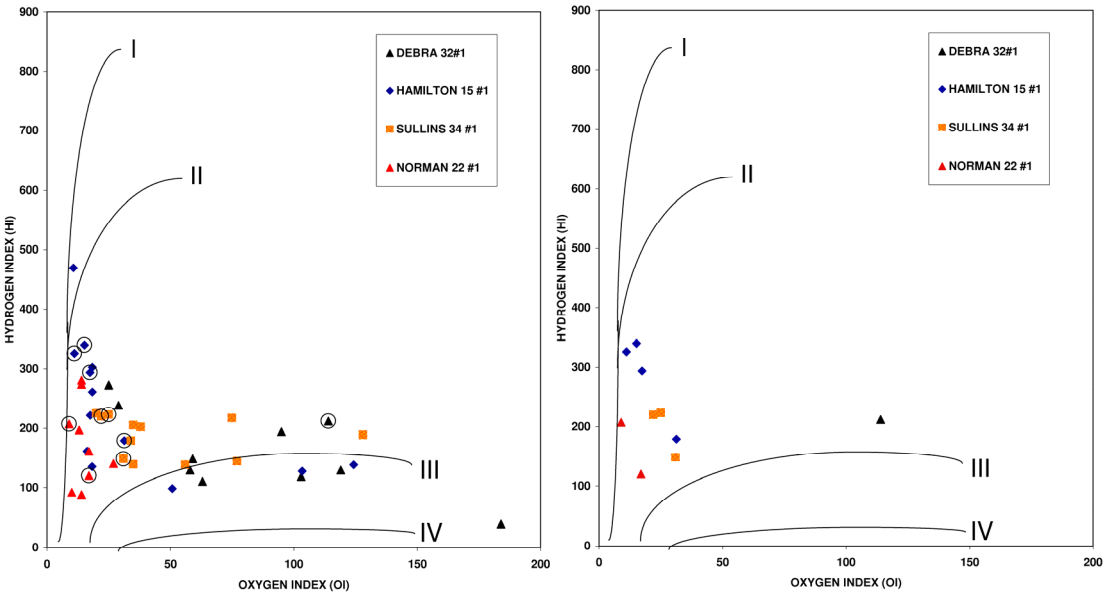

Figure 23. Modified Van Krevelen Diagram. Kerogen type estimated from TOC and Rock-Eval Pyrolysis data. Black circles indicated samples collected from the Atoka Group. Values from Atoka Group are plotted on right.

4.5 Isotopic Data

Isotopic composition and gas composition data is reported in Tables 3 to 8. Methane values from the Apsley 1 #1 well have an average value of -46.03 ‰, which is the highest average methane isotopic composition observed in the study area. The lowest methane isotopic values were observed in the Toto 15 #3 well, which had a average value of –51.26 ‰. The Hamilton 15 #1, Norman 22 #1, Debra 32 #1, Sullins 34 #1, and Joyce 14 #1 wells have average methane isotopic compositions of -50.44 ‰, -48.99 ‰, -48.23 ‰, -46.86 ‰, and –46.82 ‰, respectively (Figure 27).

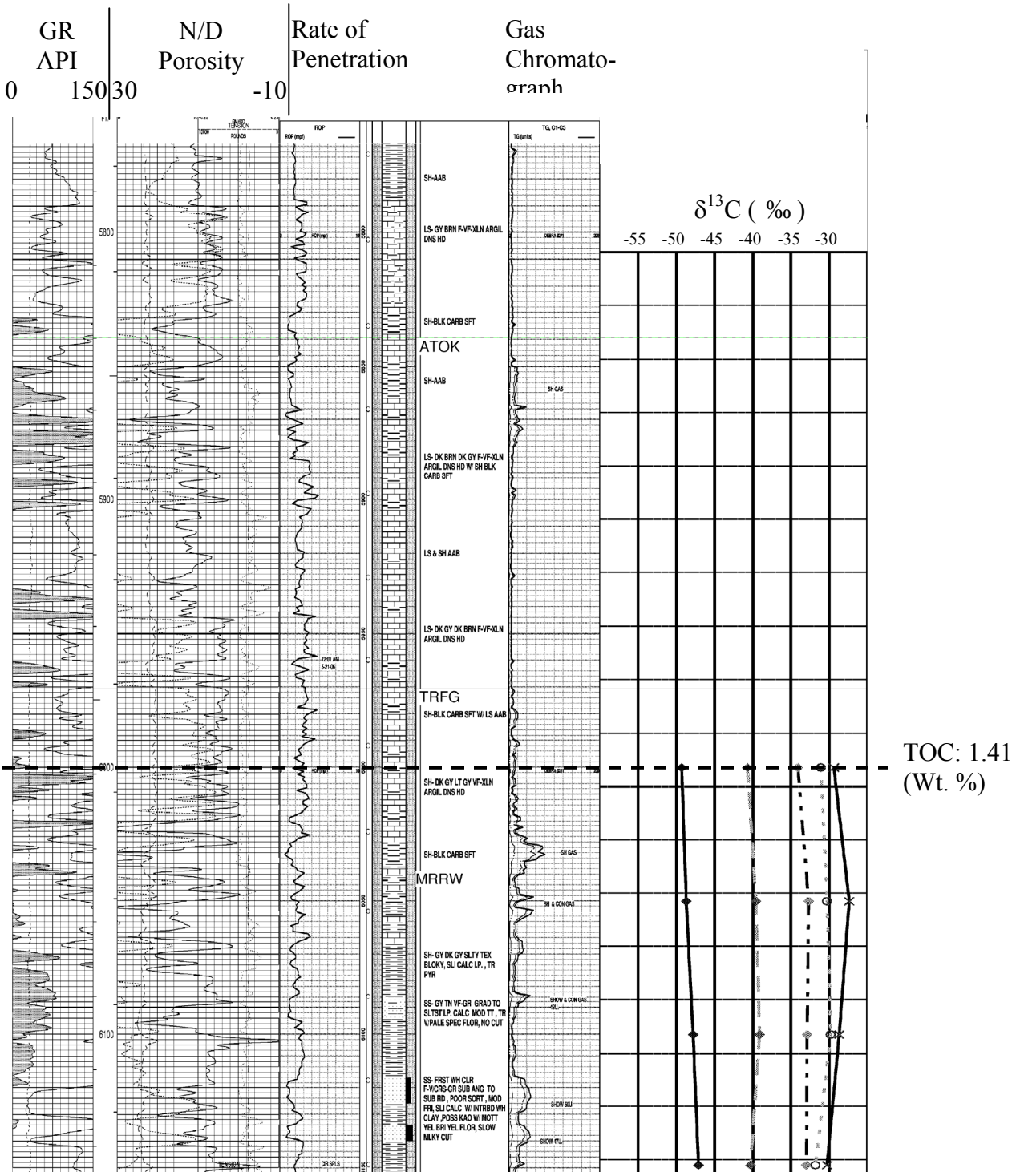

Figure 24. Well log of the Debra 32 #1 well with neutron density log on left, mud log center and isotopic compositions on right. Atoka TOC sampling intervals indicated by horizontal dashed line.

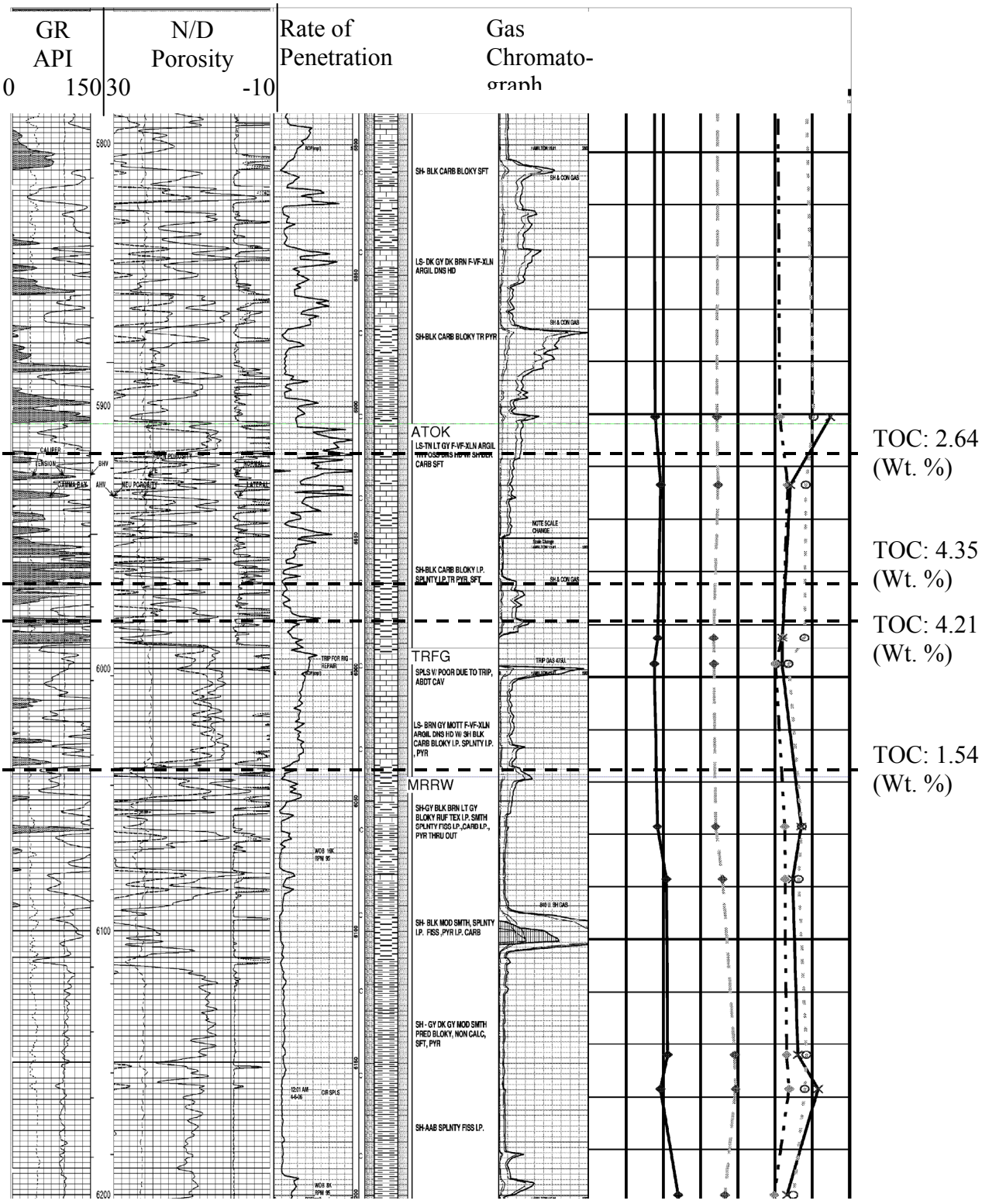

Figure 25. Well log of the Hamilton 15 #1 well with neutron density log on left, mud log center and isotopic compositions on right. Atoka TOC sampling intervals indicated by horizontal dashed line.

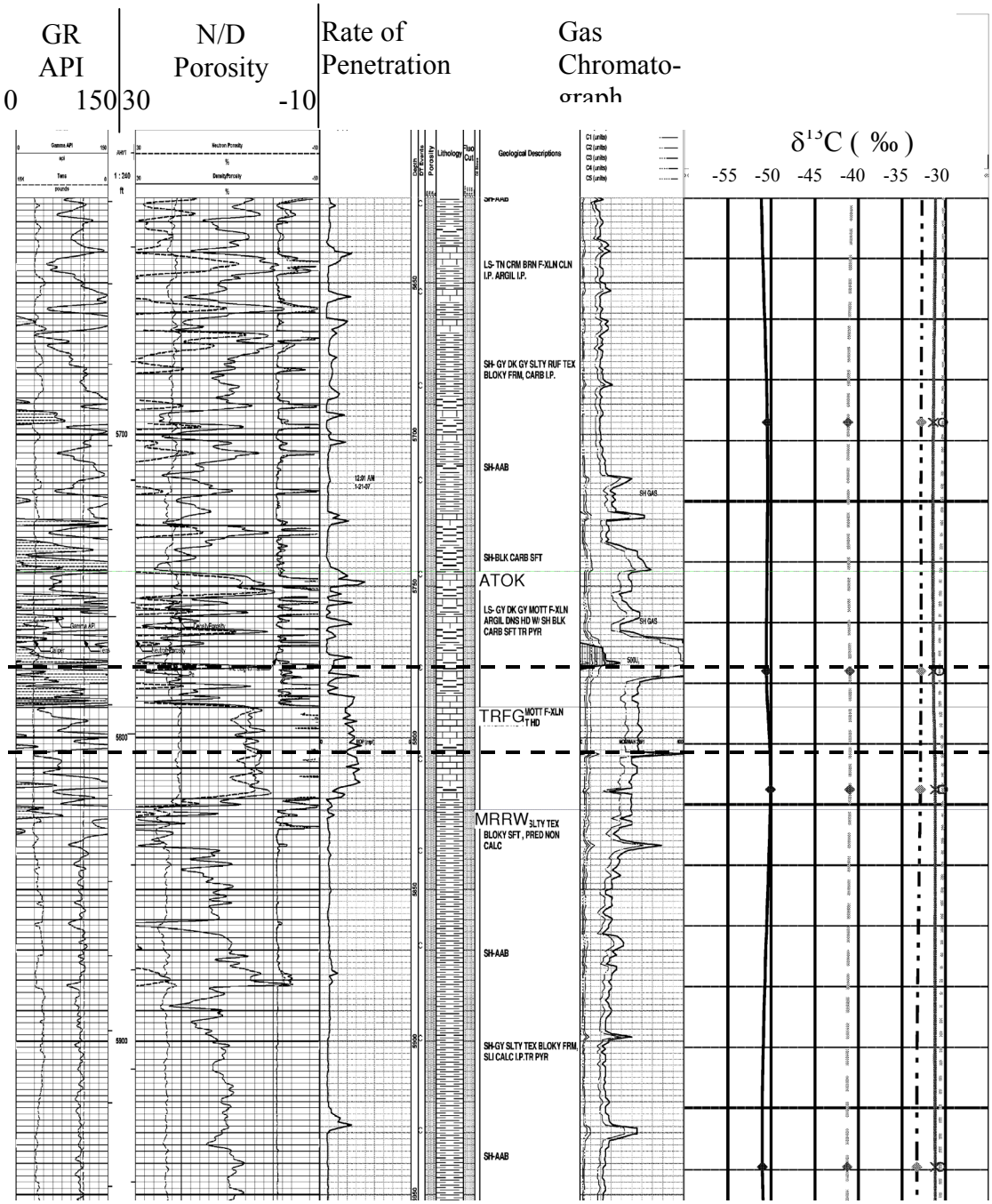

Figure 26. Well log of the Norman 22 #1 well with neutron density log on left, mud log center and isotopic compositions on right. Atoka TOC sampling intervals indicated by horizontal dashed line.

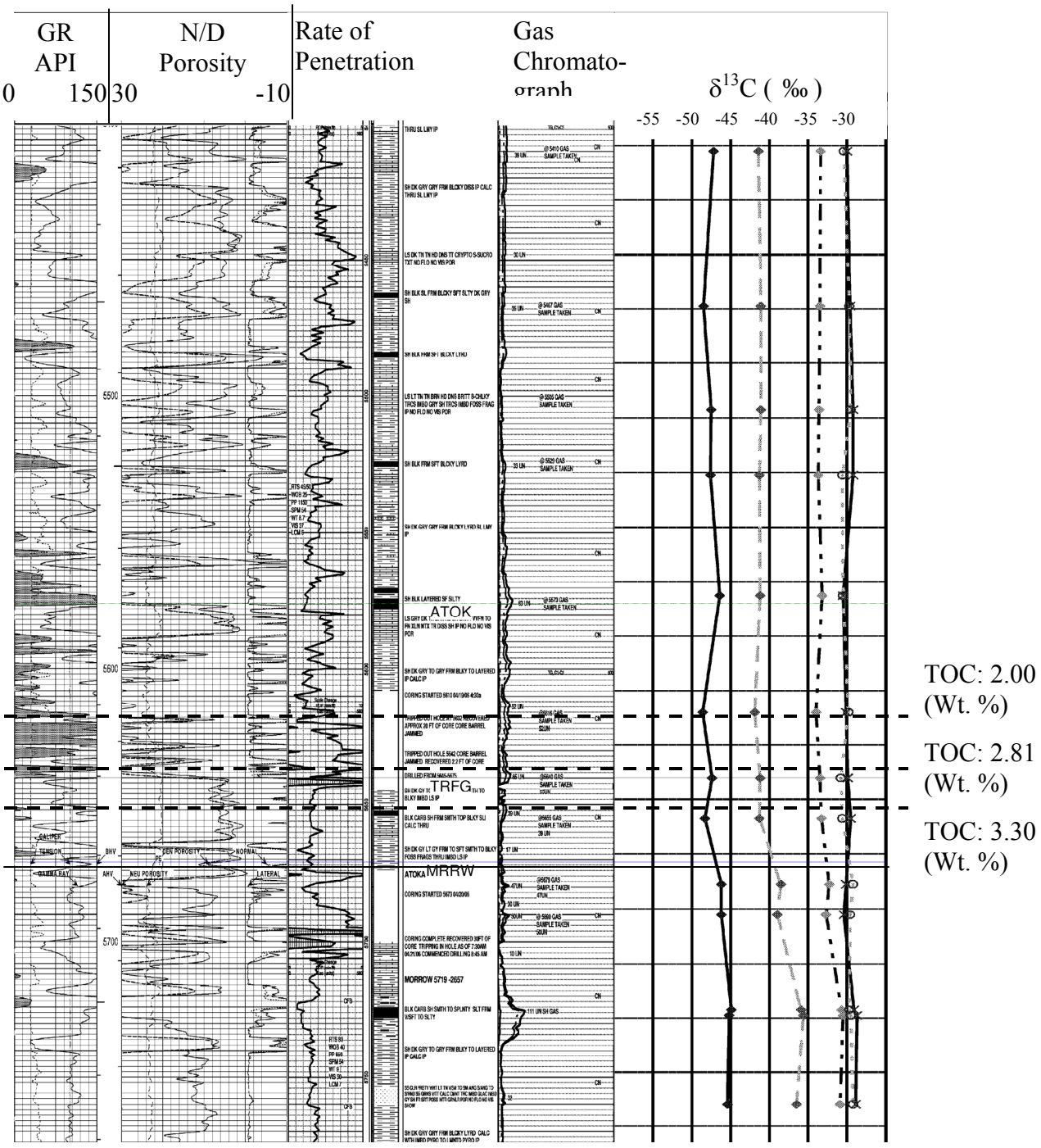

Figure 27. Well log of the Sullins 34 #1 well with neutron density log on left, mud log center and isotopic compositions on right. Atoka TOC sampling intervals indicated by horizontal dashed line.

Measured Depth (ft)	Sub Sea-level Depth (ft)	Gas Units	Formation	Well Name	Methane (‰, δ^{13}C V-PDB)	Ethane (‰, δ^{13}C V-PDB)	Propane (‰, δ^{13}C V-PDB)	i-Butane (‰, δ^{13}C V-PDB)	n-Butane (‰, δ^{13}C V-PDB)
4799	1753	13	MRMN	APSLEY 1 #1	-46.80	-37.97	-32.58	-32.40	-30.28
4914	1868	141	CHRK	APSLEY 1 #1	-45.30	-37.80	-31.80	-31.20	-30.20
4960	1914	45	CHRK	APSLEY 1 #1	-46.20	-37.50	-31.50	-30.90	-28.80
5085	2039	50	ATOK	APSLEY 1 #1	-46.00	-36.90	-31.50	-30.00	-29.40
5133	2087	33	ATOK	APSLEY 1 #1	-46.10	-36.70	-31.00	-30.50	-29.40
5200	2154	59	ATOK	APSLEY 1 #1	-46.20	-36.60	-30.60	-30.70	-29.20
5240	2194	30	TRFG	APSLEY 1 #1	-45.99	-36.10	-30.40	-30.60	-28.90
5290	2244	18	MRRW	APSLEY 1 #1	-46.37	-34.60	-29.20	-27.30	-27.70
5320	2274	20	MRRW	APSLEY 1 #1	-46.23	-34.50	-29.50	-29.00	-28.10
5358	2312	68	MRRW	APSLEY 1 #1	-45.60	-33.70	-28.10	-28.60	-26.00
5456	2410	-	CSTR	APSLEY 1 #1	-45.50	-33.50	-27.40	-28.20	-26.80
4085	1043	115	HBNR	JOYCE 14 #1	-47.31	-39.76	-36.31	-35.27	-33.57
4860	1818	25	MRMN	JOYCE 14 #1	-47.20	-39.90	-33.50	-	-31.10
5330	2288	650	CHRK	JOYCE 14 #1	-47.28	-39.88	-33.21	-32.20	-30.74
5400	2358	165	ATOK	JOYCE 14 #1	-47.12	-39.55	-32.93	-31.80	-30.35
5435	2393	95	ATOK	JOYCE 14 #1	-46.70	-39.40	-33.10	-31.50	-30.40
5460	2418	315	ATOK	JOYCE 14 #1	-46.89	-39.30	-33.00	-31.70	-30.30
5520	2478	85	MRRW	JOYCE 14 #1	-46.18	-38.20	-32.70	-31.50	-29.50
5524	2482	400	MRRW	JOYCE 14 #1	-45.89	-36.60	-30.00	-30.80	-29.10
5410	2362	35	CHRK	SULLINS 34 #1	-47.20	-41.40	-33.40	-30.00	-30.40
5467	2419	31.5	CHRK	SULLINS 34 #1	-48.50	-41.10	-33.50	-29.60	-29.70
5505	2457	18.6	CHRK	SULLINS 34 #1	-47.50	-41.10	-33.60	-29.20	-29.50
5529	2481	32	CHRK	SULLINS 34 #1	-47.60	-41.30	-33.70	-29.20	-30.60
5573	2525	65	ATOK	SULLINS 34 #1	-46.40	-41.20	-33.20	-30.50	-30.50
5616	2568	52	ATOK	SULLINS 34 #1	-48.60	-41.90	-34.00	-30.10	-29.80
5640	2592	65	ATOK	SULLINS 34 #1	-47.40	-41.20	-33.50	-29.90	-30.80
5655	2607	38	TRFG	SULLINS 34 #1	-48.30	-41.30	-33.30	-29.50	-30.60
5679	2631	47	TRFG	SULLINS 34 #1	-46.20	-38.50	-32.30	-30.10	-29.20
5690	2642	50.5	MRRW	SULLINS 34 #1	-46.20	-39.00	-32.70	-30.40	-29.60
5725	2677	65	MRRW	SULLINS 34 #1	-44.90	-35.90	-30.70	-29.10	-29.70
5727	2679	130	MRRW	SULLINS 34 #1	-45.20	-35.60	-30.50	-28.70	-29.50
5760	2712	28	MRRW	SULLINS 34 #1	-45.40	-36.50	-30.90	-28.90	-29.20

Table 3. Isotopic data from the Apsley 1 #1, Joyce 14 #1, and Sullins 34 #1 wells.

Measured Depth (ft)	Sub Sea-level Depth (ft)	Gas Units	Formation	Well Name	Methane (‰, δ^{13}C V-PDB)	Ethane (‰, δ^{13}C V-PDB)	Propane (‰, δ^{13}C V-PDB)	i-Butane (‰, δ^{13}C V-PDB)	n-Butane (‰, δ^{13}C V-PDB)
4576	1285	10	KSSC	ELKHART FOREST 14 #1	-49.20	-41.30	-33.40	-32.70	-30.70
4597	1306	15	MRMN	ELKHART FOREST 14 #1	-48.00	-40.20	-32.20	-31.00	-29.80
5063	1772	53	CHRK	ELKHART FOREST 14 #1	-48.70	-40.70	-32.60	-31.40	-30.00
5081	1790	38	CHRK	ELKHART FOREST 14 #1	-49.10	-41.40	-33.30	-31.50	-30.30
5090	1799	53	CHRK	ELKHART FOREST 14 #1	-49.80	-41.50	-33.40	-31.90	-30.40
5158	1867	372	CHRK	ELKHART FOREST 14 #1	-51.40	-42.20	-33.70	-32.00	-30.40
5212	1921	68	CHRK	ELKHART FOREST 14 #1	-50.40	-41.90	-33.40	-32.00	-30.30
5227	1936	98	CHRK	ELKHART FOREST 14 #1	-49.60	-41.80	-33.30	-31.80	-30.40
5279	1988	81	ATOK	ELKHART FOREST 14 #1	-49.50	-42.00	-33.40	-31.60	-30.40
5292	2001	75	ATOK	ELKHART FOREST 14 #1	-49.66	-42.00	-33.40	-31.90	-30.20
5301	2010	110	ATOK	ELKHART FOREST 14 #1	-50.56	-42.10	-33.20	-32.20	-29.70
5368	2077	116	TRFG	ELKHART FOREST 14 #1	-48.70	-41.00	-31.50	-32.20	-29.50
5908	2617	20	STLS	ELKHART FOREST 14 #1	-45.80	-37.30	-30.40	-31.20	-28.70
5955	2664	25	STLS	ELKHART FOREST 14 #1	-45.10	-36.90	-30.80	-30.90	-28.90
6084	2793	16	STLS	ELKHART FOREST 14 #1	-42.70	-36.50	-30.90	-31.00	-29.20
5490	2287	18	MRMN	HAMILTON 15 #1	-51.20	-43.20	-36.30	-35.00	-33.90
5539	2336	70	CHRK	HAMILTON 15 #1	-51.10	-42.30	-35.20	-32.10	-31.60
5672	2469	135	CHRK	HAMILTON 15 #1	-51.30	-42.60	-34.80	-	-31.70
5904	2701	200	ATOK	HAMILTON 15 #1	-51.10	-42.80	-34.40	-27.60	-29.80
5930	2727	35	ATOK	HAMILTON 15 #1	-50.36	-42.65	-33.29	-32.94	-30.87
5988	2785	45	ATOK	HAMILTON 15 #1	-50.75	-43.25	-34.01	-34.01	-31.04
5998	2795	130	TRFG	HAMILTON 15 #1	-51.20	-43.20	-34.94	-34.06	-33.20
6060	2857	145	TRFG	HAMILTON 15 #1	-50.80	-43.00	-33.70	-31.50	-31.40
6080	2877	65	MRRW	HAMILTON 15 #1	-49.60	-42.06	-33.68	-32.63	-31.83
6147	2944	140	MRRW	HAMILTON 15 #1	-49.41	-40.42	-33.47	-31.94	-30.78
6160	2957	800	MRRW	HAMILTON 15 #1	-50.40	-40.30	-33.10	-29.20	-31.00
6200	2997	20	MRRW	HAMILTON 15 #1	-48.00	-41.75	-35.13	-33.41	-32.55

Table 4. Isotopic data from the Elkhart Forest 14 #1 and Hamilton 15 #1 wells.

Measured Depth (ft)	Sub Sea-level Depth (ft)	Gas Units	Formation	Well Name	Methane (‰, δ^{13}C V-PDB)	Ethane (‰, δ^{13}C V-PDB)	Propane (‰, δ^{13}C V-PDB)	i-Butane (‰, δ^{13}C V-PDB)	n-Butane (‰, δ^{13}C V-PDB)
4146	1216	65	VRGL	NORMAN 22 #1	-47.30	-39.93	-34.22	-32.72	-31.37
4194	1264	75	VRGL	NORMAN 22 #1	-47.00	-39.80	-33.90	-31.80	-31.00
4274	1344	85	HBNR	NORMAN 22 #1	-42.60	-39.98	-30.76	-30.10	-29.70
5094	2164	65	KSSC	NORMAN 22 #1	-48.70	-40.70	-31.50	-30.70	-29.80
5150	2220	50	MRMN	NORMAN 22 #1	-50.88	-40.43	-32.00	-31.00	-30.40
5544	2614	200	CHRK	NORMAN 22 #1	-51.45	-40.60	-32.60	-31.00	-30.20
5684	2754	220	CHRK	NORMAN 22 #1	-50.48	-41.20	-32.80	-31.40	-30.30
5766	2836	230	ATOK	NORMAN 22 #1	-50.58	-41.00	-32.80	-31.40	-30.70
5805	2875	430	TRFG	NORMAN 22 #1	-50.10	-41.00	-32.90	-31.20	-30.30
5929	2999	190	MRRW	NORMAN 22 #1	-51.02	-41.30	-33.30	-31.20	-30.60
6084	3154	85	MRRW	NORMAN 22 #1	-49.10	-40.70	-32.50	-30.70	-30.10
6570	3640	12	STLS	NORMAN 22 #1	-48.70	-39.90	-31.80	-30.00	-29.80
4368	1408	-	HBNR	TOTO 15 #3	-47.08	-38.60	-33.20	-34.80	-32.80
5181	2221	-	MRMN	TOTO 15 #3	-49.00	-40.80	-34.10	-33.20	-32.10
5787	2827	-	CHRK	TOTO 15 #3	-53.30	-43.50	-34.70	-33.10	-31.97
5839	2879	-	CHRK	TOTO 15 #3	-51.50	-41.70	-34.00	-32.50	-31.80
5946	2986	-	CHRK	TOTO 15 #3	-55.60	-43.80	-34.20	-32.10	-31.10
6015	3055	-	ATOK	TOTO 15 #3	-53.40	-43.70	-34.20	-32.00	-30.80
6030	3070	-	ATOK	TOTO 15 #3	-52.70	-43.90	-34.00	-31.70	-30.50
6050	3090	-	ATOK	TOTO 15 #3	-51.20	-43.50	-33.90	-31.70	-30.69
6132	3172	-	TRFG	TOTO 15 #3	-51.50	-43.50	-33.80	-31.50	-30.50
6235	3275	-	MRRW	TOTO 15 #3	-47.30	-39.70	-32.30	-32.00	-30.70
6000	2693	16	ATOK	DEBRA 32 #1	-49.30	-40.70	-34.10	-29.40	-31.10
6050	2743	12	MRRW	DEBRA 32 #1	-48.70	-39.60	-32.70	-27.40	-30.30
6100	2793	10	MRRW	DEBRA 32 #1	-47.80	-39.10	-32.90	-28.70	-29.80
6149	2842	40	MRRW	DEBRA 32 #1	-47.10	-40.30	-33.00	-30.30	-31.80

Table 5. Isotopic data from the Norman 22 #1, Toto 15 #3 and Debra 32 #1 wells.

Measured Depth (ft)	Well Name	C_1 Conc. (mole %)	C_2 Conc. (mole %)	C_3 Conc. (mole %)	i-C_4 Conc. (mole %)	n-C_4 Conc. (mole %)	i-C_5 Conc. (mole %)	n-C_5 Conc. (mole %)	C_{6+} Conc. (mole %)
4799	APSLEY 1 #1	87.85	3.44	4.04	0.48	1.60	0.47	0.57	1.55
4914	APSLEY 1 #1	61.77	10.90	13.09	2.15	6.11	1.50	1.90	2.58
4960	APSLEY 1 #1	74.56	8.01	8.57	1.08	3.48	0.80	1.00	2.51
5085	APSLEY 1 #1	72.92	7.72	8.51	1.33	4.43	1.15	1.55	2.40
5133	APSLEY 1 #1	92.54	4.21	1.44	0.43	0.68	0.10	0.15	0.43
5200	APSLEY 1 #1	76.26	9.22	8.42	0.81	2.79	0.59	0.68	1.22
5240	APSLEY 1 #1	75.00	8.26	8.86	1.00	3.35	0.85	1.02	1.67
5290	APSLEY 1 #1	83.98	4.46	3.97	2.71	1.89	0.51	0.66	1.82
5320	APSLEY 1 #1	87.37	3.38	4.25	0.49	1.63	0.49	0.59	1.82
5358	APSLEY 1 #1	76.70	8.53	7.34	1.25	2.94	0.78	0.90	1.56
5456	APSLEY 1 #1	90.50	4.49	3.35	0.18	0.54	0.13	0.14	0.66
4085	JOYCE 14 #1	84.97	8.23	4.33	0.45	1.30	0.23	0.20	0.29
4860	JOYCE 14 #1	93.98	3.10	1.34	0.15	0.26	0.19	0.26	0.71
5330	JOYCE 14 #1	79.53	11.33	6.50	0.51	1.65	0.13	0.22	0.14
5400	JOYCE 14 #1	77.81	11.67	7.26	0.55	2.03	0.17	0.28	0.23
5435	JOYCE 14 #1	81.47	10.02	6.40	0.45	0.94	0.15	0.25	0.31
5460	JOYCE 14 #1	79.23	10.76	7.20	0.38	1.74	0.18	0.24	0.27
5520	JOYCE 14 #1	89.11	5.96	3.23	0.17	0.77	0.14	0.15	0.46
5524	JOYCE 14 #1	84.89	6.58	5.36	0.66	1.60	0.31	0.32	0.27
5410	SULLINS 34 #1	50.22	5.14	3.96	0.08	1.11	0.63	2.03	36.83
5467	SULLINS 34 #1	68.69	8.20	6.12	0.10	1.31	0.35	1.03	14.21
5505	SULLINS 34 #1	71.98	8.04	5.39	0.17	1.64	0.33	1.06	11.39
5529	SULLINS 34 #1	75.88	9.25	6.12	0.18	1.55	0.25	0.66	6.12
5573	SULLINS 34 #1	76.06	10.79	7.90	0.31	1.85	0.24	0.46	2.39
5616	SULLINS 34 #1	72.82	10.42	9.25	0.38	2.52	0.34	0.65	3.60
5640	SULLINS 34 #1	67.81	10.70	10.26	0.48	3.13	0.45	0.96	6.21
5655	SULLINS 34 #1	75.21	8.46	8.19	0.33	2.57	0.36	0.80	4.07
5679	SULLINS 34 #1	85.72	7.15	3.67	0.16	1.17	0.14	0.38	1.60
5690	SULLINS 34 #1	77.94	8.75	7.17	0.33	2.18	0.29	0.68	2.66
5725	SULLINS 34 #1	89.51	5.58	3.10	0.09	0.62	0.10	0.18	0.83
5727	SULLINS 34 #1	86.39	7.15	4.49	0.14	0.81	0.11	0.19	0.71
5760	SULLINS 34 #1	87.98	6.16	3.09	0.15	0.94	0.13	0.27	1.28

Table 6. Gas composition data from the Apsley 1 #1, Joyce 14 #1, and Sullins 34 #1 wells.

Measured Depth (ft)	Well Name	C_1 Conc. (mole %)	C_2 Conc. (mole %)	C_3 Conc. (mole %)	i-C_4 Conc. (mole %)	n-C_4 Conc. (mole %)	i-C_5 Conc. (mole %)	n-C_5 Conc. (mole %)	C_{6+} Conc. (mole %)
4576	ELKHART FOREST 14 #1	79.61	7.11	6.06	0.93	3.45	0.87	1.25	0.73
4597	ELKHART FOREST 14 #1	77.04	7.24	6.90	1.11	4.11	1.22	1.45	0.94
5063	ELKHART FOREST 14 #1	69.58	13.60	10.02	0.86	3.98	0.57	0.87	0.51
5081	ELKHART FOREST 14 #1	72.45	11.11	9.17	0.87	4.18	0.67	0.99	0.57
5090	ELKHART FOREST 14 #1	74.25	12.09	8.28	0.65	3.26	0.42	0.65	0.41
5158	ELKHART FOREST 14 #1	77.73	11.65	6.62	0.45	2.43	0.34	0.46	0.32
5212	ELKHART FOREST 14 #1	76.08	11.03	7.30	0.60	3.21	0.49	0.76	0.53
5227	ELKHART FOREST 14 #1	75.56	12.09	7.23	0.55	3.01	0.44	0.66	0.45
5279	ELKHART FOREST 14 #1	73.00	12.38	8.42	0.65	3.61	0.52	0.83	0.58
5292	ELKHART FOREST 14 #1	72.07	12.83	8.69	0.69	3.73	0.54	0.87	0.59
5301	ELKHART FOREST 14 #1	74.73	11.99	7.80	0.57	3.24	0.46	0.72	0.48
5368	ELKHART FOREST 14 #1	89.43	6.03	2.88	0.18	0.86	0.14	0.25	0.23
5908	ELKHART FOREST 14 #1	92.21	4.17	1.74	0.27	1.02	0.04	0.43	0.13
5955	ELKHART FOREST 14 #1	90.45	5.09	2.22	0.35	1.22	0.07	0.49	0.12
6084	ELKHART FOREST 14 #1	92.39	3.88	1.80	0.30	0.97	0.05	0.44	0.16
5490	HAMILTON 15 #1	93.54	1.87	3.86	0.11	0.16	0.13	0.33	0.00
5539	HAMILTON 15 #1	78.37	9.26	8.11	0.52	2.18	0.41	0.50	0.65
5672	HAMILTON 15 #1	83.27	8.39	6.38	0.26	1.19	0.15	0.20	0.17
5904	HAMILTON 15 #1	75.35	9.98	10.12	0.55	2.71	0.36	0.51	0.41
5930	HAMILTON 15 #1	75.26	8.70	10.36	0.50	3.12	0.56	0.75	0.75
5988	HAMILTON 15 #1	74.69	10.42	10.73	0.43	2.54	0.31	0.47	0.41
5998	HAMILTON 15 #1	73.48	10.69	10.68	0.63	2.80	0.39	0.56	0.77
6060	HAMILTON 15 #1	72.06	10.96	11.47	0.61	3.20	0.40	0.64	0.65
6080	HAMILTON 15 #1	81.47	7.99	7.72	0.32	1.68	0.20	0.34	0.28
6147	HAMILTON 15 #1	85.10	6.85	5.89	0.24	1.31	0.17	0.26	0.19
6160	HAMILTON 15 #1	87.86	5.82	4.25	0.27	1.10	0.19	0.25	0.27
6200	HAMILTON 15 #1	85.38	6.32	6.38	0.11	1.35	0.09	0.34	0.02

Table 7. Gas composition data from the Elkhart Forest 14 #1 and Hamilton 15 #1 wells.

Measured Depth (ft)	Well Name	C_1 Conc. (mole %)	C_2 Conc. (mole %)	C_3 Conc. (mole %)	i-C_4 Conc. (mole %)	n-C_4 Conc. (mole %)	i-C_5 Conc. (mole %)	n-C_5 Conc. (mole %)	C_{6+} Conc. (mole %)
4146	NORMAN 22 #1	88.29	5.37	3.41	0.42	1.28	0.43	0.24	0.57
4194	NORMAN 22 #1	86.31	5.44	4.61	0.51	1.50	0.55	0.30	0.78
4274	NORMAN 22 #1	90.60	4.80	2.74	0.21	0.66	0.17	0.10	0.73
5094	NORMAN 22 #1	81.30	7.74	5.97	0.70	1.95	0.51	0.45	1.39
5150	NORMAN 22 #1	86.73	5.59	4.35	0.40	1.08	0.28	0.23	1.34
5544	NORMAN 22 #1	82.34	8.62	6.71	0.38	1.33	0.15	0.17	0.29
5684	NORMAN 22 #1	86.73	5.59	4.35	0.40	1.08	0.28	0.23	1.34
5766	NORMAN 22 #1	81.17	7.90	7.45	0.50	1.98	0.27	0.29	0.44
5805	NORMAN 22 #1	81.13	8.12	7.33	0.48	1.93	0.26	0.28	0.48
5929	NORMAN 22 #1	81.71	7.95	7.08	0.46	1.87	0.25	0.26	0.43
6084	NORMAN 22 #1	83.78	6.59	6.02	0.43	1.77	0.28	0.29	0.85
6570	NORMAN 22 #1	89.05	3.97	3.26	0.19	1.22	0.43	0.59	1.29
4368	TOTO 15 #3	86.07	7.19	4.18	0.42	1.16	0.37	0.26	0.35
5181	TOTO 15 #3	83.12	6.42	5.85	0.68	1.96	0.66	0.57	0.73
5787	TOTO 15 #3	79.31	8.03	8.21	0.66	2.54	0.45	0.47	0.34
5839	TOTO 15 #3	74.71	8.45	10.13	0.92	3.70	0.73	0.79	0.58
5946	TOTO 15 #3	77.58	8.53	9.19	0.65	2.87	0.44	0.46	0.28
6015	TOTO 15 #3	77.58	8.64	9.35	0.62	2.73	0.41	0.43	0.25
6030	TOTO 15 #3	78.32	8.74	8.94	0.55	2.50	0.35	0.37	0.23
6050	TOTO 15 #3	77.54	8.64	8.93	0.63	2.83	0.47	0.52	0.45
6132	TOTO 15 #3	72.82	9.97	11.18	0.76	3.71	0.55	0.66	0.34
6235	TOTO 15 #3	73.54	9.23	9.87	1.02	4.09	0.73	0.97	0.53
6000	DEBRA 32 #1	80.51	8.69	7.86	0.19	2.05	0.22	0.27	0.19
6050	DEBRA 32 #1	85.93	6.49	5.41	0.07	1.42	0.24	0.31	0.14
6100	DEBRA 32 #1	86.10	6.57	5.83	0.07	1.10	0.11	0.17	0.03
6149	DEBRA 32 #1	84.32	7.69	4.99	0.33	1.74	0.23	0.44	0.26

Table 8. Gas composition data from the Norman 22 #1, Toto 15 #3 and Debra 32 #1 wells.

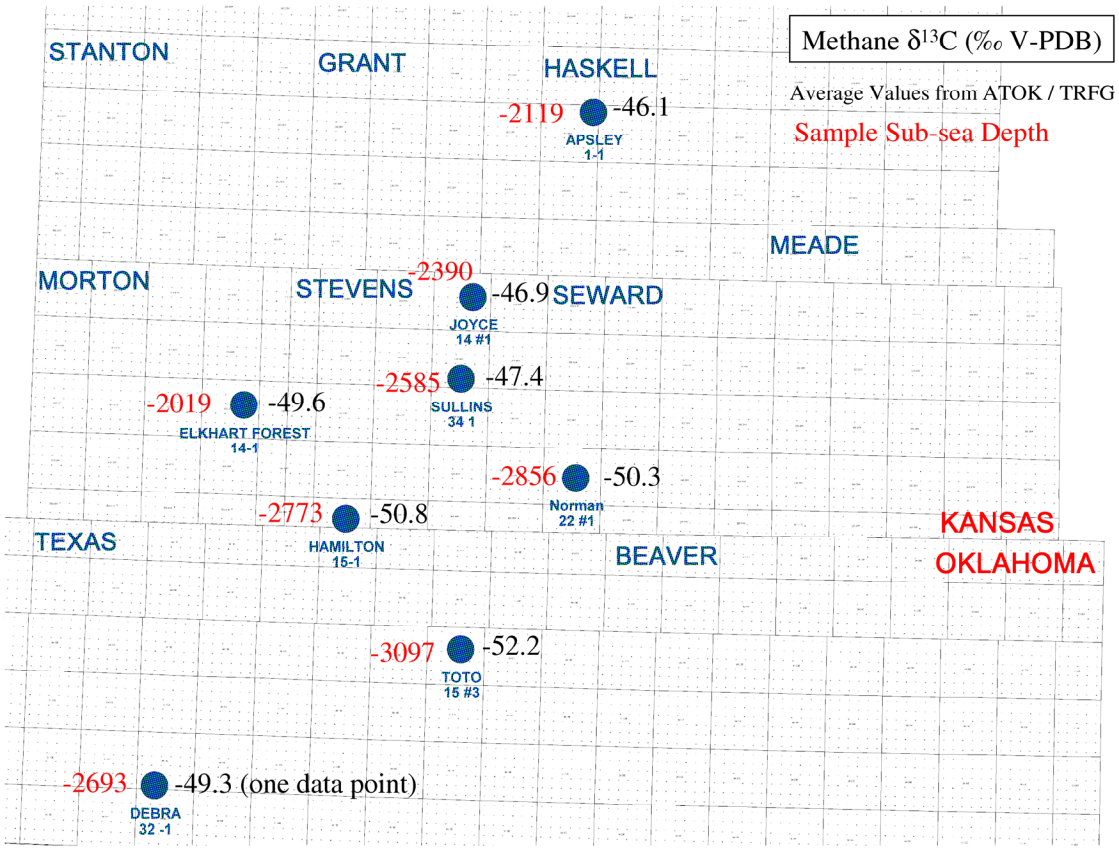

Figure 28. Map of study area with sub sea-level depth (red) and average isotopic methane values (black) from sample wells (blue circles).

Four samples from the Apsley 1 #1 well within the Atoka Group have an average methane isotopic composition of -46.07 ‰. The average depth of the Atoka Group from the Apsley 1 #1 well is 5,165 ft (Table 9). Three data points collected from the Joyce 14 #1 well within the Atoka Group have a average value of -46.90 ‰ methane.

Well Name	Mean Methane (‰, δ^{13}C V-PDB)	Mean Ethane (‰, δ^{13}C V-PDB)	Mean Propane (‰, δ^{13}C V-PDB)	Mean i-Butane (‰, δ^{13}C V-PDB)	Mean n-Butane (‰, δ^{13}C V-PDB)	Total Depth (ft)	Sub Sea-Level Depth (ft)
APSLEY 1 #1	-46.07	-36.58	-30.88	-30.45	-29.23	5165	2119
JOYCE 14 #1	-46.90	-39.42	-33.01	-31.67	-30.35	5432	2390
SULLINS 34 #1	-47.38	-40.82	-33.26	-30.02	-30.18	5633	2585
ELKHART FOREST 14 #1	-49.60	-41.78	-32.88	-31.98	-29.95	5310	2019
HAMILTON 15 #1	-50.84	-42.98	-34.07	-32.02	-31.26	5976	2773
NORMAN 22 #1	-50.34	-41.00	-32.85	-31.30	-30.50	5786	2856
TOTO 15 #3	-52.20	-43.65	-33.98	-31.73	-30.62	6057	3097
DEBRA 32 #1	-49.30	-40.70	-34.10	-29.40	-31.10	6000	2693

Table 9. Average isotopic composition data from the Atoka Group.

The average depth of the Atoka Group from the Joyce 14 #1 well is 5432 ft. Five data points collected from the Sullins 34 #1 well within the Atoka Group have a average value of -47.38 ‰ methane. The average sub-sea level depth of the Atoka Group from the Sullins 34 #1 well is 5,633 ft. Four data points collected from the Elkhart Forest 14 #1 well within the Atoka Group have a average value of -49.60 ‰ methane. The average sub-sea level depth of the Atoka Group from the Elkhart Forest 14 #1 well is 5310 ft. Two data points collected from the Norman 22 #1 well within the Atoka Group have a average value of -50.34 ‰ methane. The average sub-sea level depth of the Atoka Group from the Norman 22 #1 well is 5786 ft. Five data points collected from the Hamilton 15 #1 well within the Atoka Group have a average value of -50.84 ‰ methane. The average sub-sea level depth of the Atoka Group from the Hamilton 15 #1 well is 5,976 ft. Four data points collected from the Toto 15 #3 within the Atoka Group have a average value of -52.2 ‰ methane. The average sub-sea level depth of the Atoka Group from the Toto 15 #3 well is 6,057 ft. One data point collected from the Debra 32 #1 within the Atoka Group has a value of -49.3 ‰ methane. The sub-sea level depth of the Atoka Group from the Debra 32 #1 well is 6,000ft.

The Atoka Group shows a negative correlation between $\delta^{13}C_{methane}$ and subsurface depth for all values (Figure 28). In other words the methane isotopic compositions decrease (i.e. become more negative) with increasing depth (with the exception of the Elkhart Forest 14 #1). Excluding the Elkhart Forest 14 #1 well there is a strong correlation between depth and $\delta^{13}C_{methane}$ between wells within the Atoka Group (r^2 = 0.78, p = 2.62 x 10^{-8}). Including the Elkhart Forest 14 #1 well the correlation is not as strong (r^2 = 0.54, p = 1.28 x 10^{-5}).

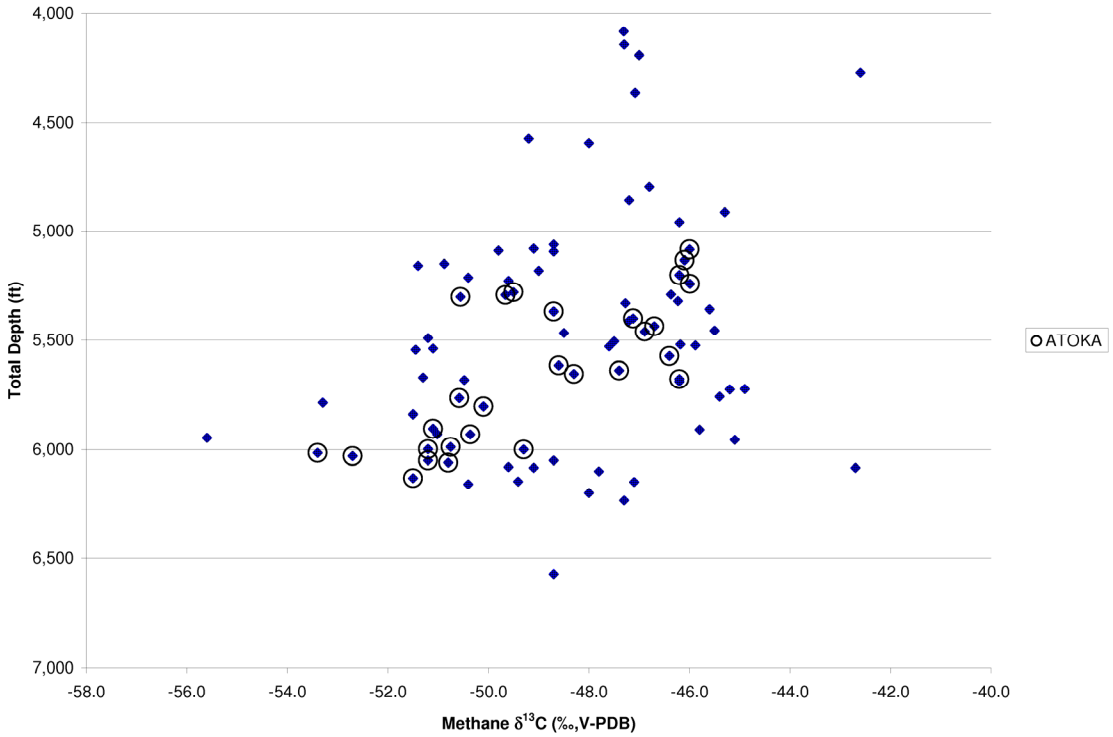

Figure 29. Total depth vs. isotopic methane for all data (blue diamonds) and Atoka Group (Circles). ($r = 0.75$, $p = 4.5 \times 10^{-6}$)

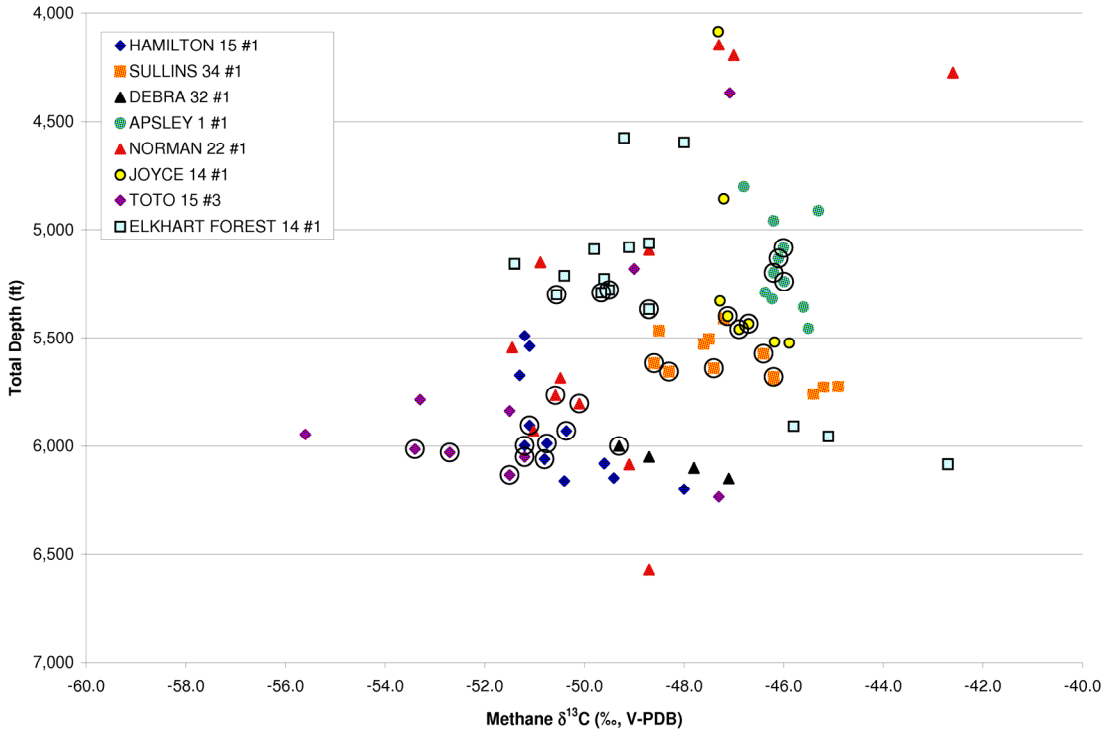

Figure 30. Total depth vs. isotopic methane for all data by well and Atoka Group (Circles). Colors correspond to wells. ($r = 0.75$, $p = 4.5 \times 10^{-6}$)

Measured vitrinite values within the Atoka Group (Table 1) from the Debra 32 #1, Norman 22 #1, and Sullins 34 #1 have average % Ro values of 0.83, 1.01, and 1.17, respectively. Although limited these data suggest an increase in thermal maturity to the North similar to the trend from the gas isotope data, which further supports the differential overburden removal model.

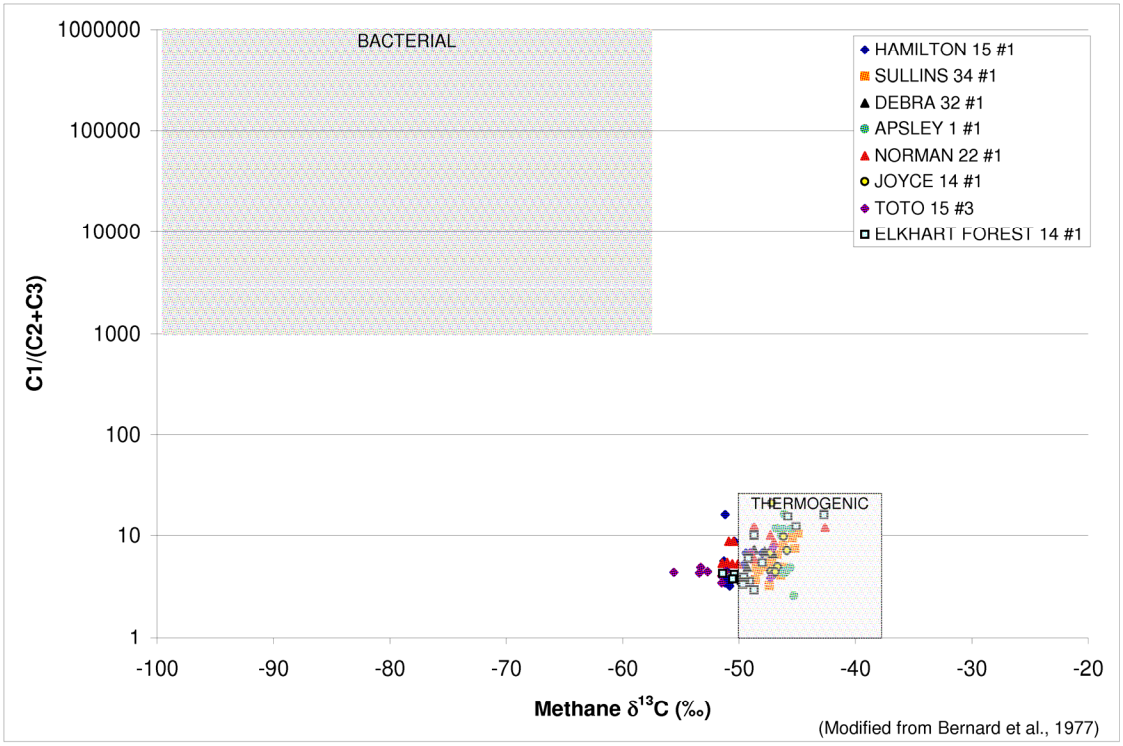

Figure 31. Plot of isotopic methane vs. gas wetness. Modified from Bernard et al. (1977).

The concentrations of the C_1-C_3 saturate hydrocarbons can be used to determine the source of the gas, by calculating a gas wetness value (Bernard, 1977). Bacterial gas has a larger methane component and will therefore demonstrate values ranging from 100 to 10,000 on the C_1 / (C_2+C_3) axis on a diagram similar to Figure 30 (Schoell, 1978). Thermogenic gas, on the other hand, is derived from the cracking (breaking of C-C

bonds) of kerogen or oil, due to increases in temperature, which overcome kinetic barriers to reaction (Whiticar, 1994).

It is important to differentiate between bacterial and thermogenic gas in petroleum exploration for various reasons. The presence of bacterial gas in a basin is not associated with the presence of an effective petroleum system (Faber, 1992). This is a result of how each gas type is formed. Bacterial gas is formed from anaerobic bacterial decomposition of OM at relatively shallow depths. Thermogenic gas is formed at relatively deep depths from either thermal cracking of sedimentary OM (primary) or thermal cracking of oil (secondary). Therefore, bacterial gas does not suggest the occurrence of liquid hydrocarbons in association with the gas and typically consists of exclusively methane. Furthermore, thermogenic gas is associated with the formation of oil or wet gas and contains relatively larger proportions of ethane, propane and butanes. While bacterial gas can be economic it is typically produced under unusual geologic conditions such as rapid sedimentation rates and/or the formation of early traps (Rice, 1993).

All Gas collected from in this study is thermogenic in origin (Figure 30, 31). Since all the data from this study plotted close to the thermogenic zone it has been formed from increased temperatures rather than bacterial decomposition.

As an alternative to the Bernard plot, Schoell (1978) used $\delta^{13}C_{methane}$ and gas wetness values to discriminate gas sources. When the data from this study are plotted on such a diagram (Figure 31), the results indicate that the samples are in the wet gas to oil range (Figure 31). These data appear to be broken out by well, which is likely the result of compositional differences with changes in location and degree of maturity or burial.

The majority of the data points lie in the wet gas region indicating that the sampled gas is coming from a thermally mature interval.

The isotopic composition of co-existing methane, ethane, and propane can be used to calculate an equivalent vitrinite reflectance value for the potential source rock (Faber, 1987; Berner and Faber, 1988).

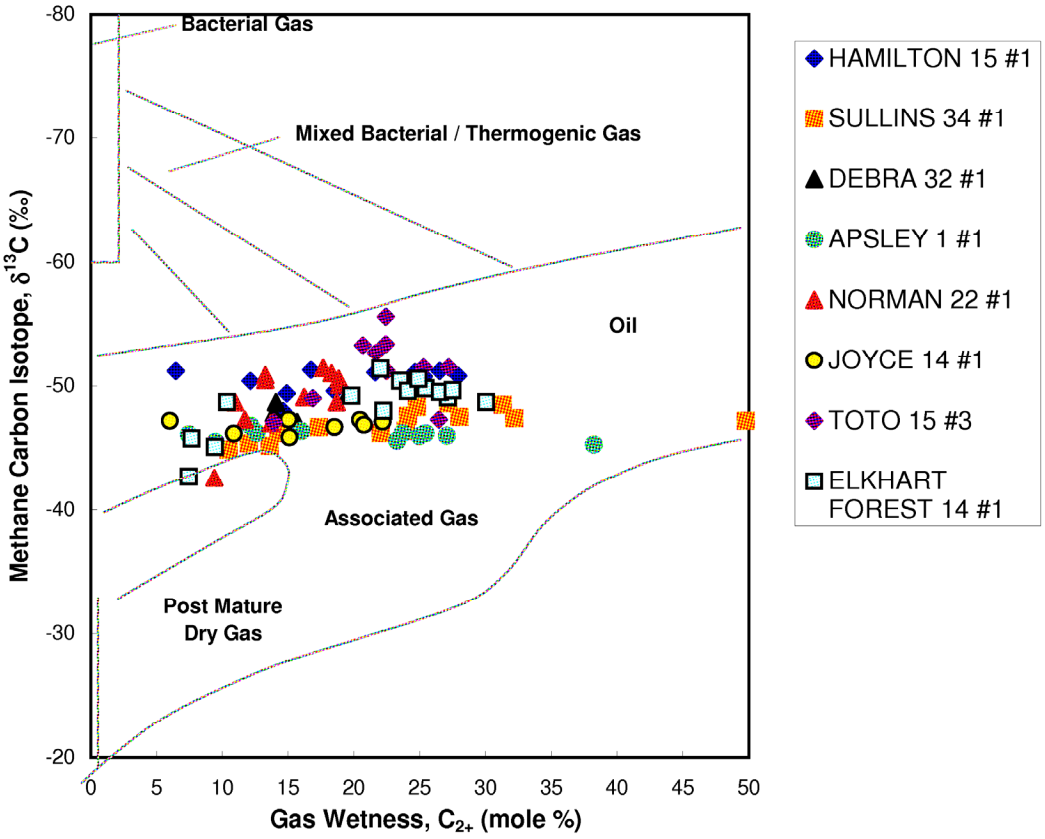

Figure 32. Plot of isotopic methane vs. gas wetness. Modified from Schoell (1978).

The calculated vitrinite reflectance measurements based on the isotopic composition of gases in the Hugoton Embayment range from 1.0 to 1.4 (% eRo) (Figure 32). More mature values were collected from the Apsley 1 # 1 well and less mature values were collected from the Toto 15 #3 well (Figure 32). Isotopic values collected

from the Atoka Group alone show a similar trend and stratification of values by well location (Figure 33).

The composition of $\delta^{13}C_{ethane}$, $\delta^{13}C_{propane,}$ and $\delta^{13}C_{butanes}$ show an overall increasing isotopic composition with depth by well and regionally show an increase in composition from South to North (Figure 34, 35). Each value falls within three standard deviations of the average.

The composition of $\delta^{13}C_{methane}$ shows a similar trend to the isotopic compositions of ethane, propane, and butanes. However, as in the Apsley 1 #1 well, there are isotopic shifts seen in the ethane, propane and butanes that are not seen in methane isotopic compositional shifts with depth (Figure 43).

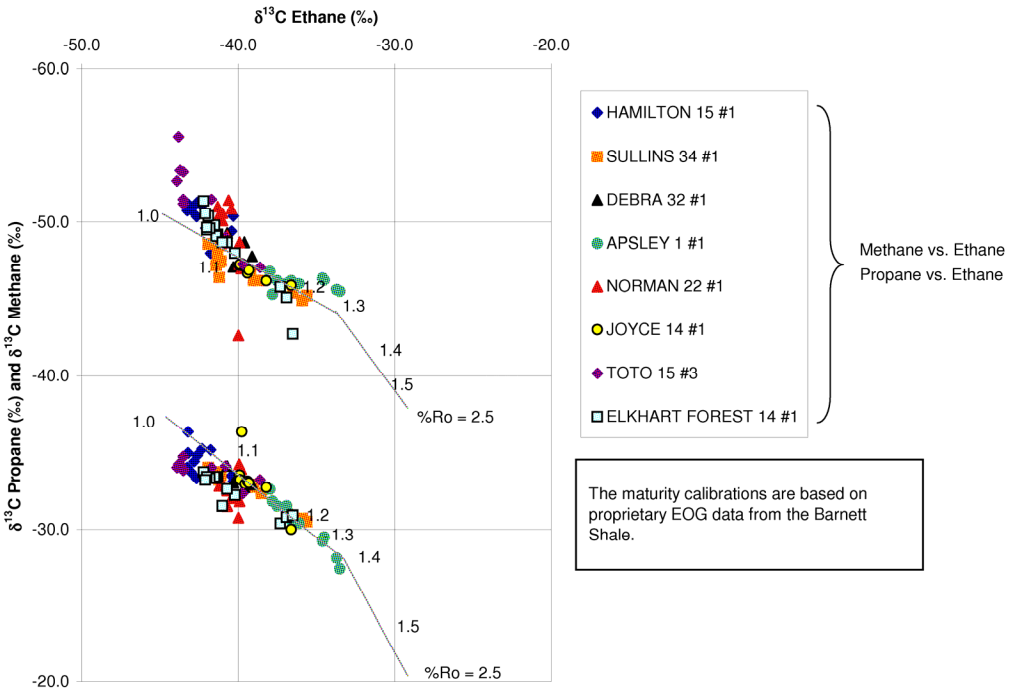

Figure 33. Estimated vitrinite reflectance values calculate from isotopic values of methane, ethane, and propane. Calibration line was determined from various basins and proprietary data from the Barnett Shale.

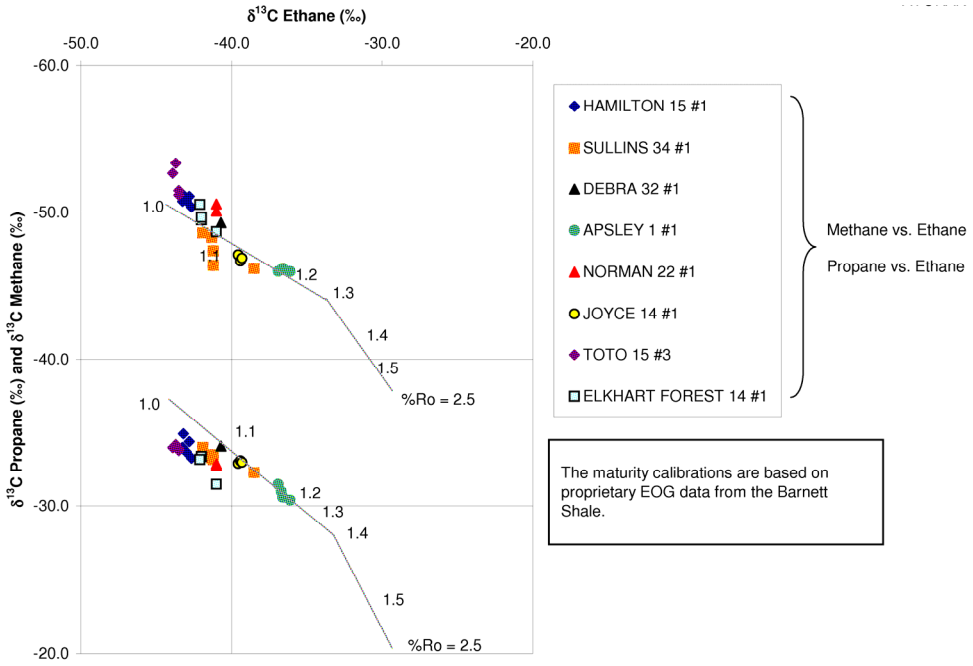

Figure 34. Estimated vitrinite reflectance values calculate from isotopic values of methane, ethane, and propane from the Atoka Group of SW Kansas. Calibration line was determined from various basins and proprietary data from the Barnett Shale.
the average except for one $\delta^{13}C_{n\text{-butane}}$ composition, which was collected in the Morrow.

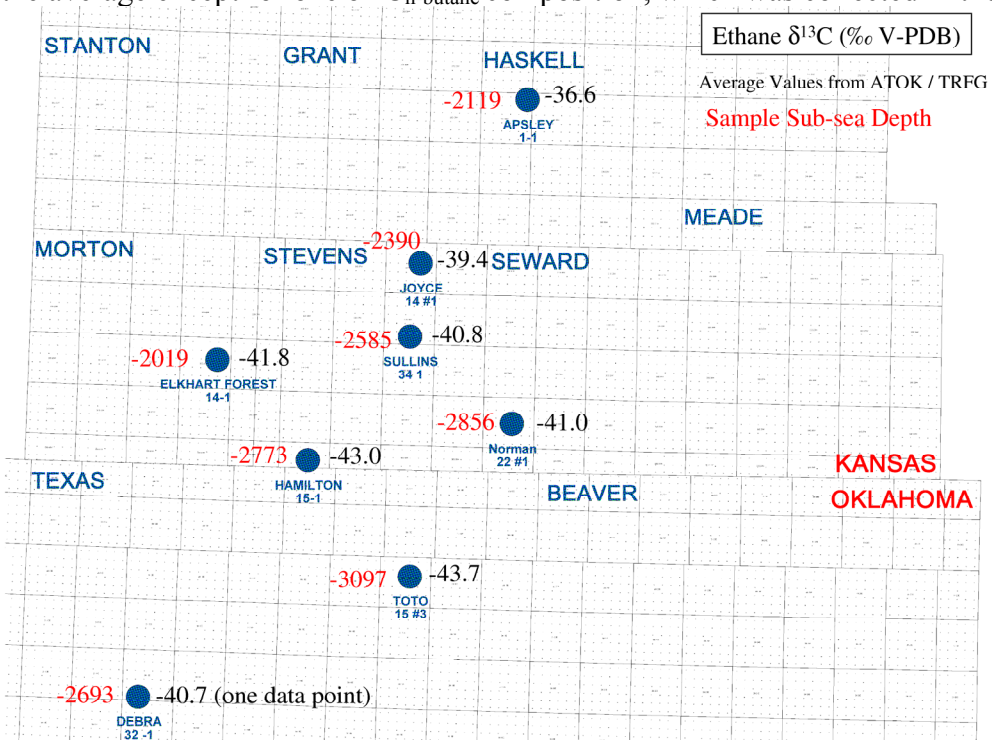

Figure 35. Map of study area with sub sea-level depth (red) and average isotopic ethane values (black) from sample wells (blue circles).

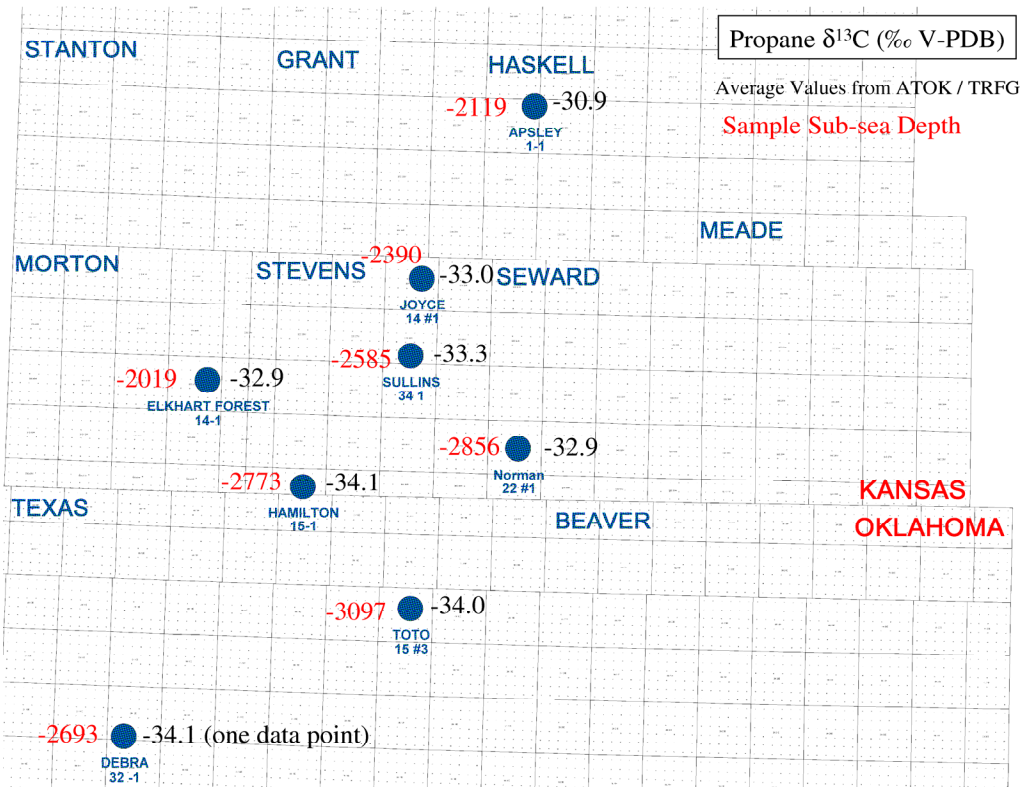

Figure 36. Map of study area with sub sea-level depth (red) and average isotopic propane values (black) from sample wells (blue circles).

The Toto 15 #3 well (Figure 37) shows a positive isotopic shift (less negative) between the base of the Atoka Group and the top of the Morrow Group. These data suggest a variation in the processes controlling the formation of gas between the two groups. Above the Atoka, methane values show an isotopically decreasing kick. However, this shift can be seen only slightly in the ethane trend and is not noticeable in the propane compositions. Butane data shows a relatively constant trend with a sight isotopic increase between Atoka and Morrow group sample intervals.

$\delta^{13}C_{methane}$ and $\delta^{13}C_{ethane}$ isotopic compositions from the Hamilton 15 #1 illustrate a relatively constant trend between 2,287 ft (sub sea-level depth) and the top of the Atoka Group (2,704 ft). Propane and n-butane values between 2,287 ft and the top of the Atoka Group show a relatively sharp isotopic increase followed by a gradual isotopic increase

from 2,336 ft to 2,704 ft. In the Atoka Group $\delta^{13}C_{methane}$, $\delta^{13}C_{ethane}$, and $\delta^{13}C_{n\text{-}butane}$ compositions show an initial isotopic increase followed by a slight decrease in weight through the Thirteen Finger limestone (TRFG). $\delta^{13}C_{methane}$ collected from the Morrow Group shows a jagged pattern that appears to isotopically increase with depth. $\delta^{13}C_{methane}$, $\delta^{13}C_{ethane}$, and $\delta^{13}C_{propane}$ compositions in the Morrow show an isotopic increase with depth except for an isotopic decrease recorded from the 2,997 ft data point. The Hamilton 15 #1 well demonstrates an isotopic shift in the Atoka group relative to the Cherokee and Morrow groups above and below. There is also an indication that the Thirteen Finger limestone has a separate isotopic character than the Atoka marl and Novi carbonate above (Figure 38).

Methane, ethane, propane, and butane data from the Norman 22 #1 show similar isotopic trends with depth (Figure 39). Data from the Norman 22 #1 shows an initial decrease in isotopic weight in the Morrow at 2,999 ft followed by an increase with depth as recorded by the following two sample points.

$\delta^{13}C_{methane}$, $\delta^{13}C_{ethane}$, and $\delta^{13}C_{propane}$ compositions from the Elkhart Forest 14 #1 well illustrate an isotopically decreasing trend between 1,772 ft (sub sea-level) and 1,876 ft within the Cherokee Group (Figure 40). Between 1,876 ft and 1,936 ft $\delta^{13}C_{methane}$ compositions isotopically decrease until to the top of the Atoka Group (1949 ft). In the Atoka, $\delta^{13}C_{methane}$ values initially plateau but decrease isotopically as the values reach the base of the Atoka Marl / top of the Thirteen finger limestone. $\delta^{13}C_{methane}$ values increase isotopically for the remainder of well. Ethane and $\delta^{13}C_{i\text{-}butane}$ slightly mimic the methane trend with depth. $\delta^{13}C_{propane}$ and $\delta^{13}C_{n\text{-}butane}$ show an isotopic decrease from the Cherokee

to the Atoka Group followed by an increase in the Atoka through the remainder of the well.

$\delta^{13}C_{methane}$ compositions from the Sullins 34 #1 well illustrate the Atoka Group interval as isotopically lighter than the Cherokee and Morrow Groups above and below (Figure 41). $\delta^{13}C_{ethane}$ and $\delta^{13}C_{propane}$ values show a relatively constant pattern followed by an isotopic increase in the Morrow Group. These data suggest that the Morrow isotopic signature varies from the Atoka and could be indicative separate gas formation processes.

$\delta^{13}C_{methane}$, $\delta^{13}C_{ethane}$, $\delta^{13}C_{propane}$, and $\delta^{13}C_{butane}$ compositions from the Joyce 14 #1 well show a slight isotopic increase into the Atoka group followed by an abrupt increase in isotopic weight into the Morrow Group (Figure 42). This shift is most noticeable in ethane and propane isotopic values.

$\delta^{13}C_{methane}$ values from the Apsley 1 #1 well have little variability but appear to increase with depth in the Morrow (Figure 43). Ethane, propane and $\delta^{13}C_{butane}$ values all show an isotopic increase with depth especially between the Atoka and Morrow Groups.

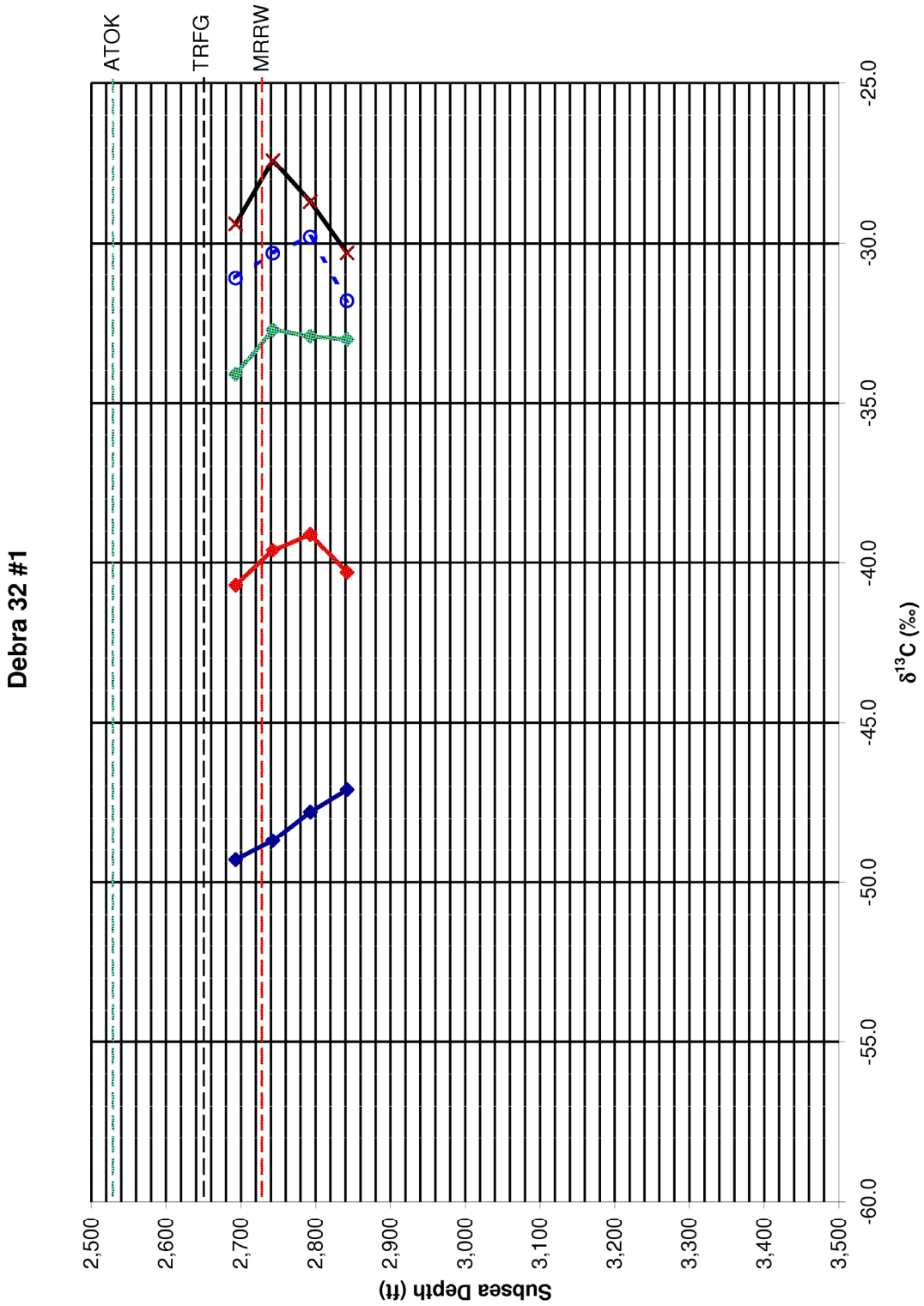

Figure 37. Debra 32 #1 sub sea-level depth vs. $\delta^{13}C$ (‰ , V-PDB). Blue line = methane, red line = ethane, green line = propane, black line = i-butane, and blue dashed line = n-butane. ATOK = Top of Atoka Group, TRFG = Top of Thirteen Finger limestone, MRRW = Top of Morrow Group.

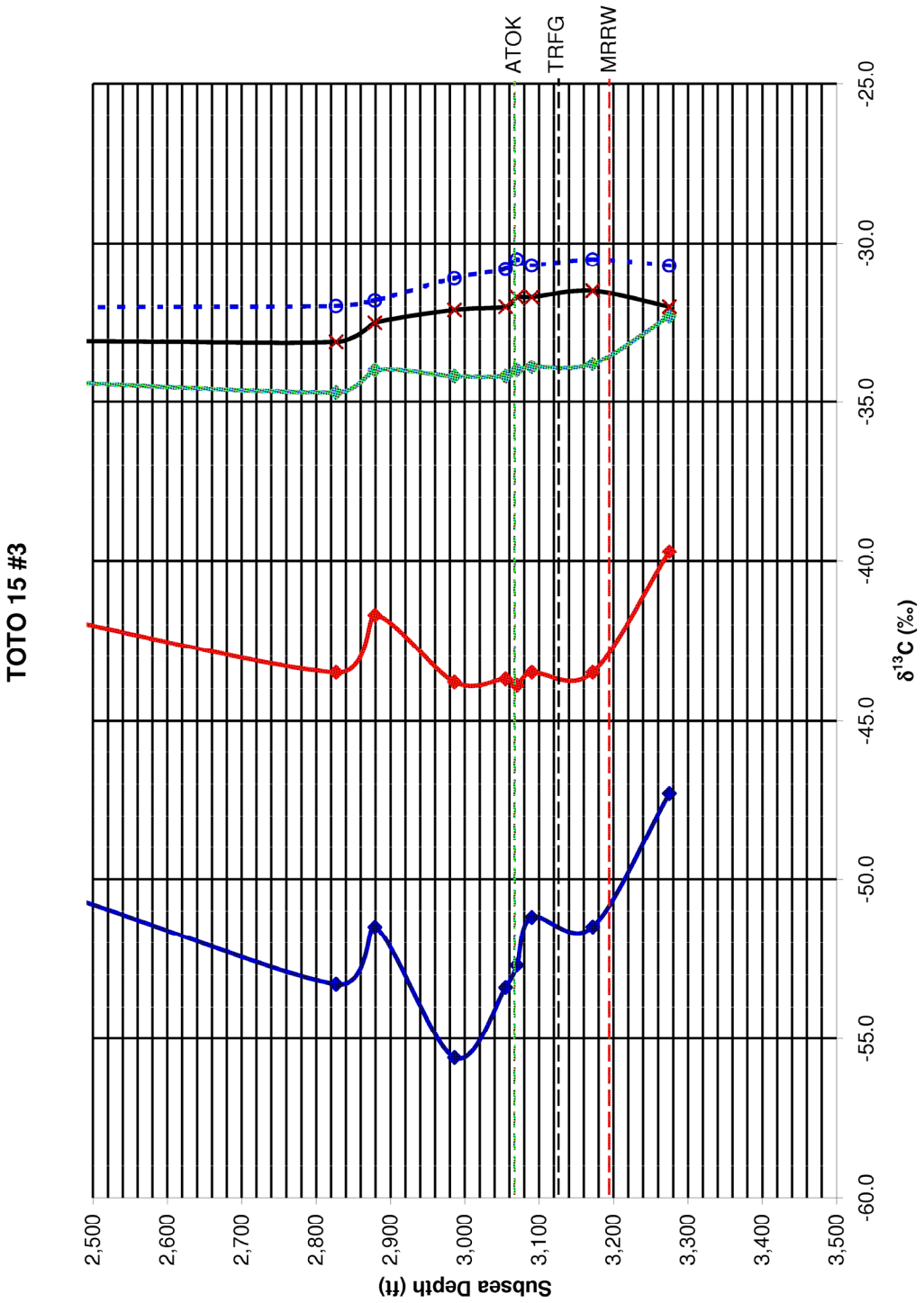

Figure 38. Toto 15 #3 sub sea-level depth vs. $\delta^{13}C$ (‰ , V-PDB). Blue line = methane, red line = ethane, green line = propane, black line = i-butane, and blue dashed line = n-butane. ATOK = Top of Atoka Group, TRFG = Top of Thirteen Finger limestone, MRRW = Top of Morrow Group.

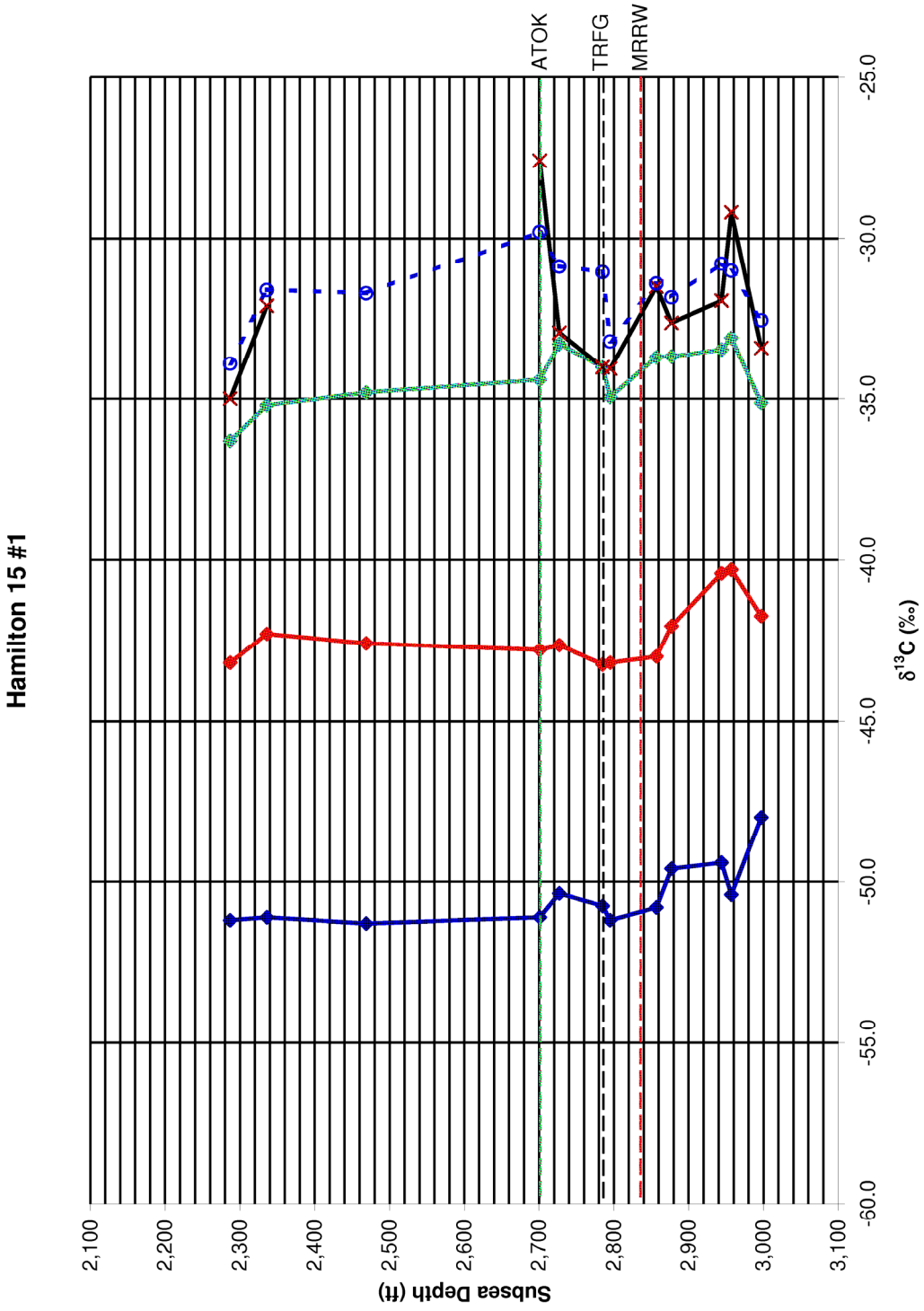

Figure 39. Hamilton 15 #1 sub sea-level depth vs. $\delta^{13}C$ (‰ , V-PDB). Blue line = methane, red line = ethane, green line = propane, black line = i-butane, and blue dashed line = n-butane. ATOK = Top of Atoka Group, TRFG = Top of Thirteen Finger limestone, MRRW = Top of Morrow Group.

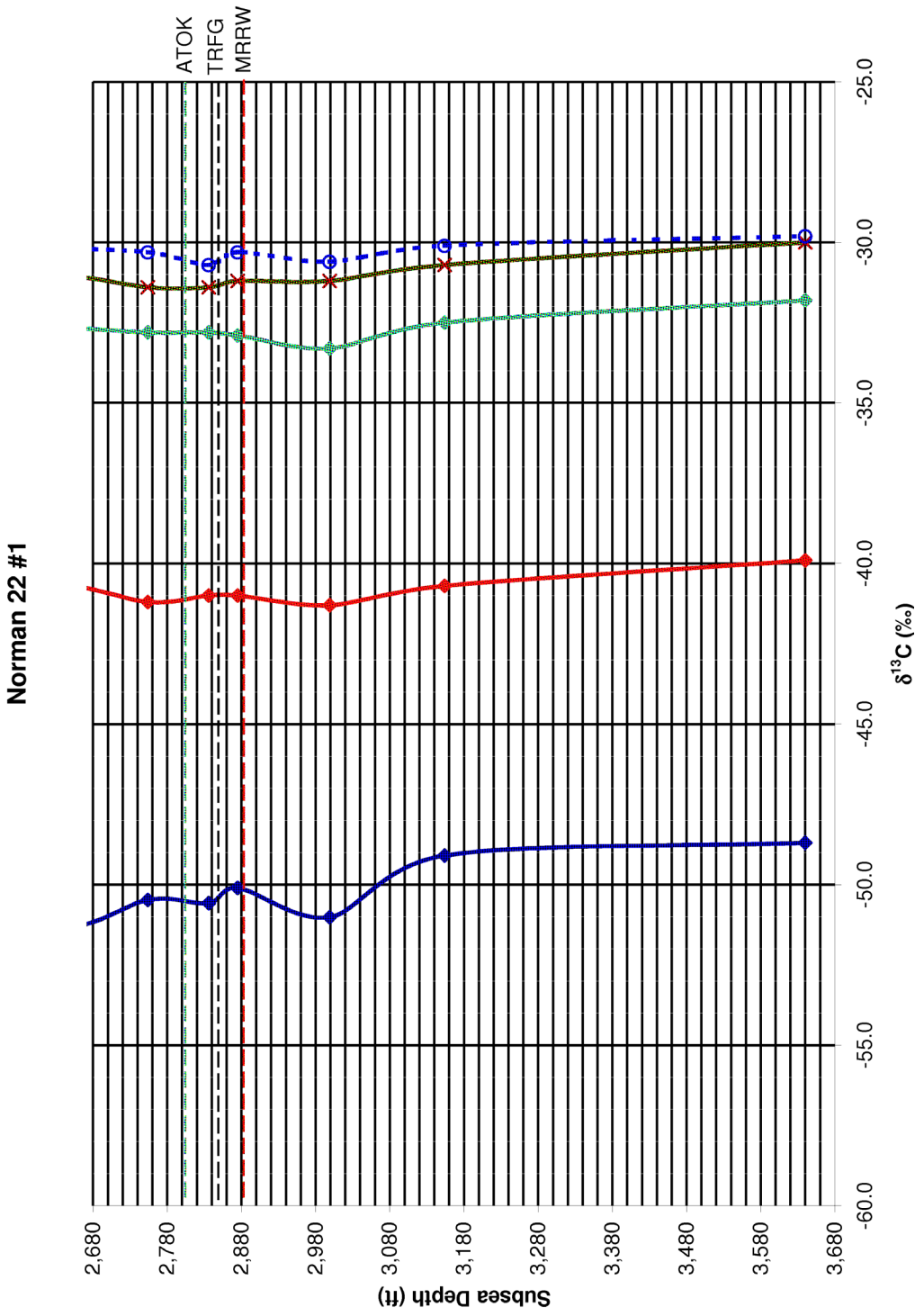

Figure 40. Norman 22 #1 sub sea-level depth vs. $\delta^{13}C$ (‰ , V-PDB). Blue line = methane, red line = ethane, green line = propane, black line = i-butane, and blue dashed line = n-butane. ATOK = Top of Atoka Group, TRFG = Top of Thirteen Finger limestone, MRRW = Top of Morrow Group.

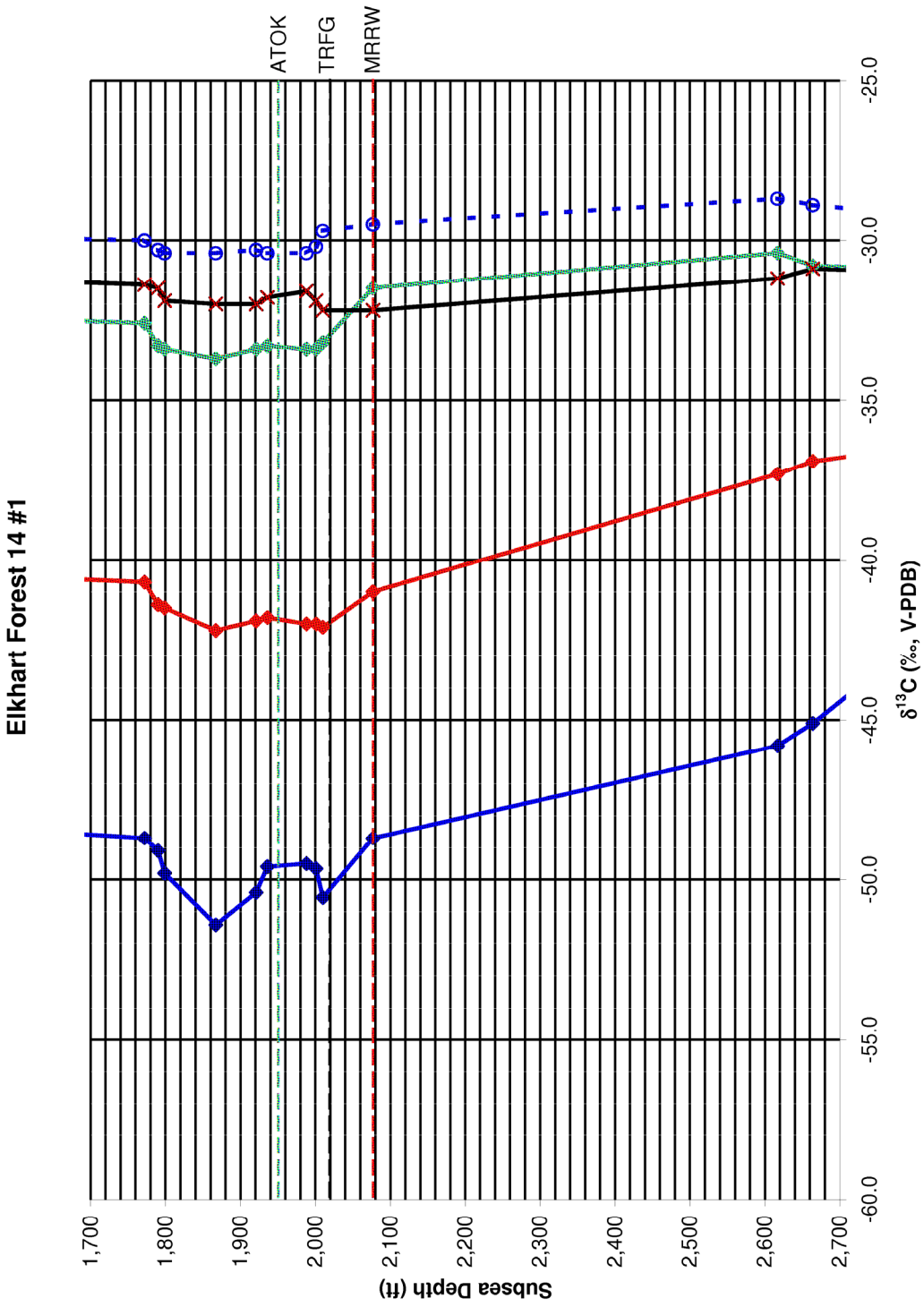

Figure 41. Elkhart Forest 14 #1 sub sea-level depth vs. $\delta^{13}C$ (‰ , V-PDB). Blue line = methane, red line = ethane, green line = propane, black line = i-butane, and blue dashed line = n-butane. ATOK = Top of Atoka Group, TRFG = Top of Thirteen Finger limestone, MRRW = Top of Morrow Group.

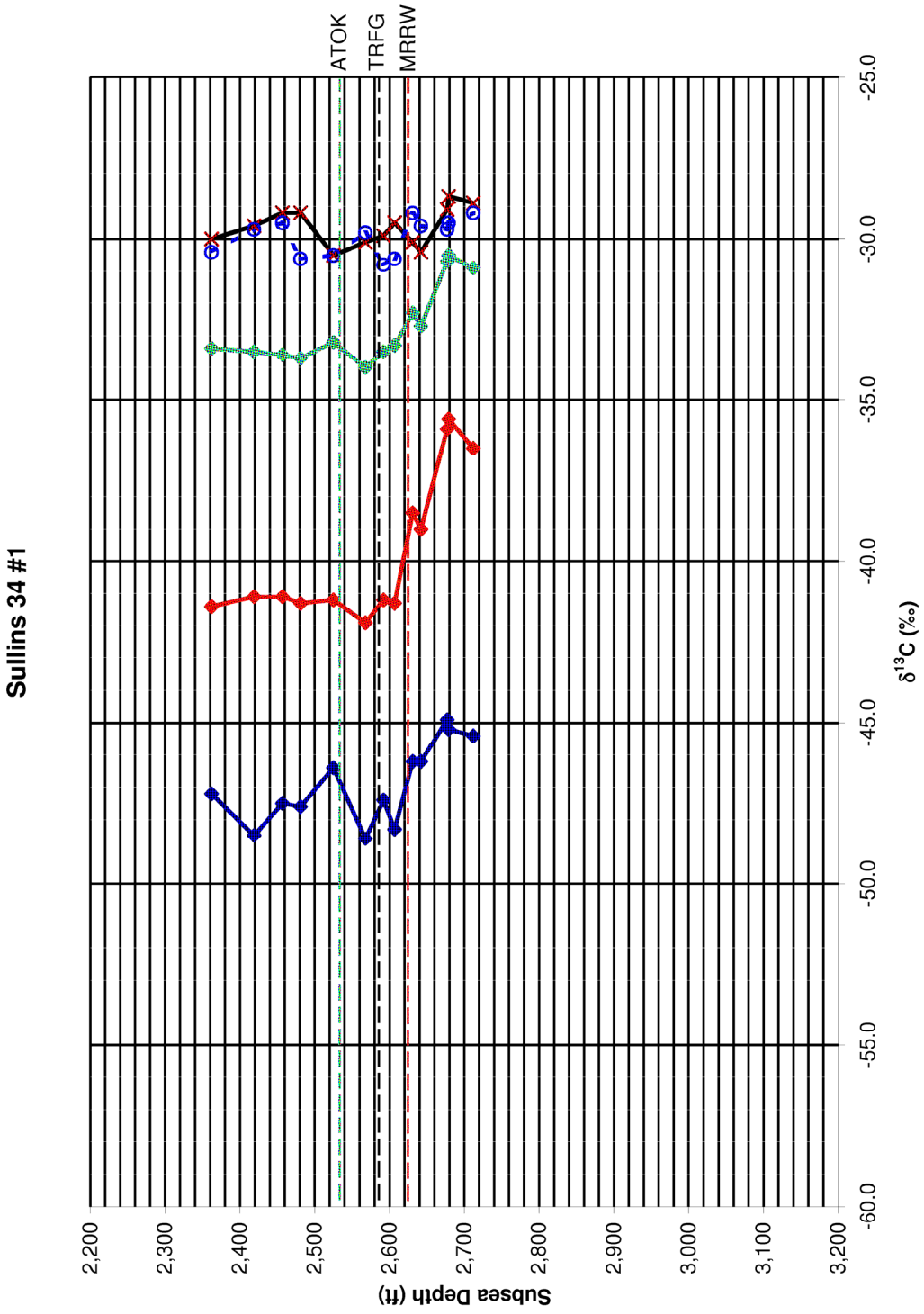

Figure 42. Sullins 34 #1 sub sea-level depth vs. $\delta^{13}C$ (‰ , V-PDB). Blue line = methane, red line = ethane, green line = propane, black line = i-butane, and blue dashed line = n-butane. ATOK = Top of Atoka Group, TRFG = Top of Thirteen Finger limestone, MRRW = Top of Morrow Group.

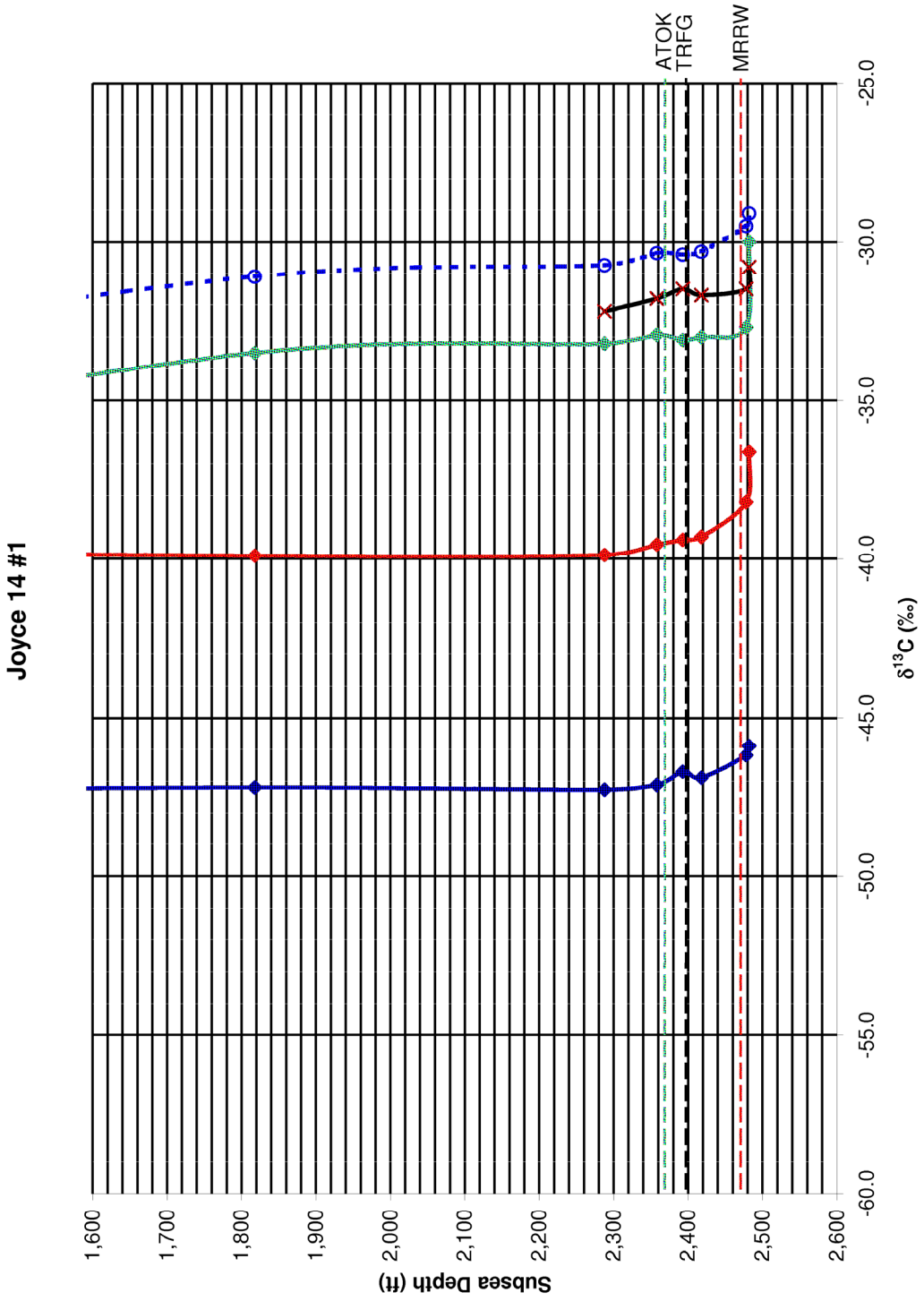

Figure 43. Joyce 14 #1 sub sea-level depth vs. $\delta^{13}C$ (‰ , V-PDB). Blue line = methane, red line = ethane, green line = propane, black line = i-butane, and blue dashed line = n-butane. ATOK = Top of Atoka Group, TRFG = Top of Thirteen Finger limestone, MRRW = Top of Morrow Group.

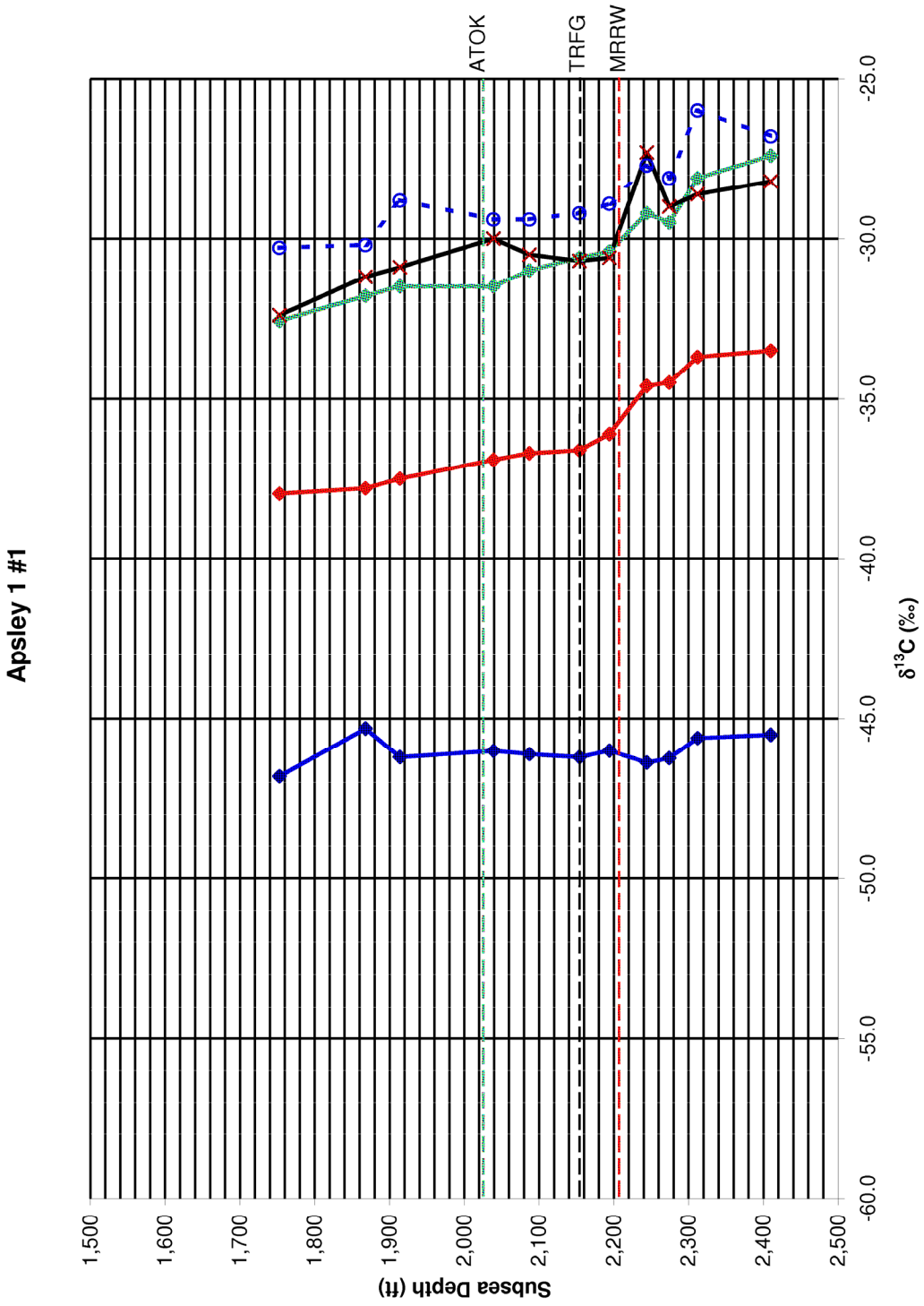

Figure 44. Apsley 1 #1 sub sea-level depth vs. $\delta^{13}C$ (‰ , V-PDB). Blue line = methane, red line = ethane, green line = propane, black line = i-butane, and blue dashed line = n-butane. ATOK = Top of Atoka Group, TRFG = Top of Thirteen Finger limestone, MRRW = Top of Morrow Group.

Chapter V

Discussion

Lithology does not appear to be a significant control on measured TOC values. In the Hamilton 15 #1 well higher TOC values are associated with clay or shale intervals while in the Sullins 34 #1 higher TOC values are associated with calcareous intervals. The Norman 22 #1 did not show much variation between TOC and rock type (Table 2).

The isotopic composition of C_1-C_4 gases vary with depth and lithology in each well. For example, in the Debra 32 #1 well (Figure 36) $\delta^{13}C_{methane}$, $\delta^{13}C_{ethane}$, and $\delta^{13}C_{n\text{-}butane}$, all increase with depth from the Atoka Group into the Morrow. However, $\delta^{13}C$ values for propane and i-butane increase with depth in the Atoka group, but are relatively enriched in the Morrow Group. Within the Morrow Group, $\delta^{13}C_{propane}$ and $\delta^{13}C_{i\text{-}butane}$ decrease with depth. These data suggest a difference in isotopic distribution between the Atoka and Morrow Groups, which is not evident in the methane data alone. These data suggest a difference in gas isotopic composition between the Atoka and Morrow Groups.

The between well $\delta^{13}C_{CH4}$ trend is contradictory to observations made in previous studies previous studies. For example, Schoell (1983) showed that light (less positive) methane isotopic compositions are generally associated with relatively immature sources

as compared to heavier methane isotopic compositions (Figure 13). Thus, this data suggests that the source is becoming less mature with increased depth. However, when the data are considered on a well-by-well basis, the opposite trend is observed; that is, the $\delta^{13}C_{methane}$ values increase with increasing dept, as observed by Schoell (1983). Such a trend is consistent with increasing temperatures, and thus, organic matter maturity, with depth. There is an opposite relationship (Figure 29), which supports Schoells' model.

The observed trend of increased thermal maturity (i.e. higher $\delta^{13}C_{methane}$ values) northward is likely the result of variation in relative regional differences in overburden removal. This is supported by an opposite (positive correlation between $\delta^{13}C_{methane}$ and total depth) relationship between isotopic composition and burial depth when viewed on a well-by-well basis (Figure 29). In other words, if overburden was consistent regionally there should be an increase in isotopic composition locally (each well) and regionally (between wells) but there is decrease on the regional scale.

There are two processes that could account for the northward trend of increased $\delta^{13}C_{methane}$ values with decreased well depth. Present day sub sea-level depth trends are not necessarily the same as in the past. Differential amounts of overburden removal could explain the seemingly inverted trend of increasing (isotopic equivalent) maturity with increasing depth. Mixing is a less likely scenario because of the strong regional trend in isotopic maturation values.

Chapter VI

Conclusion

There is a stratigraphic distribution of isotopic composition between wells within the Atoka Group of southwest Kansas with the exception of the Elkhart Forest 14 #1 well. The stratigraphic relationship shows an increase in isotopic weight with sequentially deeper stratigraphic units. Isotopic compositional distinctions with depth are indicated by variations in isotopic weight between gas collected from the Atoka and the Morrow Groups. Isotopic composition from the Morrow Group is on average heavier than the isotopic values from the Atoka. This suggests that the formation of gas from each interval were generated from separate processes.

Atoka Gas production in southwest Kansas likely is sourced from organic-rich Atoka marls rather than what has sourced Morrowan reservoirs because of the variation in isotopic composition from Atoka source rocks. The gas generated from the Atoka is thermogenic as indicated by how data from this study plotted on Schoell and Bernard diagrams, which show traces of liquid hydrocarbons associated with gas. Petrographic analyses and well logs suggest that the Atoka group is characterized by cyclic intervals of mud/shale, limestone, and traces of sand. Therefore, the Atoka

Group cannot be treated as a uniform package of organic-rich source rock. The primary location for hydrocarbon accumulations is most likely in porous and permeable in the Atoka Novi carbonate or in Cherokee reservoirs where oil and gas has migrated.

Future work needed to further classify the Atoka Group would be to continue isotopic sampling regionally, collection of hydrogen isotope samples, collection of CO_2 samples, and a description of core in Haskell County. Since the Elkhart Forest 14 #1 has shown a northeast to southwest increasing trend in isotopic compositions, further sampling of data points proximal to this location would be useful. Core data and more petrographic analyses would help to develop a more defined depositional model.

References

Abelson, 1963. P.H. Abelson, Organic geochemistry and the formation of petroleum. 6th World Petroleum Congress Proceedings, Sec 1 (1963), pp. 397–407.

Anderson T. F. and M.A. Arthur. 1983. Stable isotopes of oxygen and their application to sedimentologic and paleoenvironmental problems. Pp. 1-151. *In:* M. A. Arthur, T. F. Anderson, J. Veizer, and L. S. Land (eds.). Stable isotopes in sedimentary geology. Society of Economic Paleontologists and Mineralologists. Short Course. No. 10. Dallas.

Bebout, D.G., W.A. White, T.F. Hentz, and M.K. Grasmick, (eds.), 1993 Atlas of major mid-continent gas reservoirs. Texas Bureau of Economic Geology, Austin, TX; (for) Gas Research Institute, 85 p.

Berner, U., 1989, Entwicklung und Anwendung empirischer Modelle fur die Kohlenstoffisotopenvariationen in Mischungen thermogener Erdgase: Ph.D. thesis, Technische Universitat Clausthal.

Berner, U., and E. Faber, 1988, Maturity related mixing model for methane, ethane and propane, based on carbon isotopes: Org. Geochem., v. 13, p. 67-72.

Beeunas, M. A., and M. A. McCaffrey, 2004, Proprietary OilTracers Client Report.

Beeunas, M. A., D. K. Baskin, and M. Schoell, 1999, Application of gas geochemistry for reservoir continuity assessment and identification of fault seal breakdown, South Marsh Island 61, Gulf of Mexico - Abstract, AAPG Hedberg Research Conference "Natural Gas Formation and Occurrence" June 6-10, 1999, Durango, Colorado.

Beeunas, M. A., D. K. Baskin, J. L. Jurgens, A. R. Dincau, and M. Schoell, 1996, Application of Gas Geochemistry for Reservoir Continuity Assessment, Gulf of Mexico : AAPG/EAGE Research Symposium, "Compartmentalized Reservoirs: Their Detection, Characterization and Management (Abstract).

Bissada, K.K., 1982, Geochemical constraints on petroleum generation and migration – a review. Proceedings ASCOPE'81, p. 69-87.

Bowen, D.W., and P. Weimer, 2003, Regional sequence stratigrapic setting and reservoir geology of Morrow incised-valley sandstones (lower Pennsylvanian), eastern Colorado and western Kansas, AAPG Bulletin, v. 87, p. 781-815.

Bowen, D.W., P. Weimer, and A.J. Scott, 1993, The relative success of siliciclastic sequence stratigraphic concepts in exploration: examples from incised valley fill and turbidite systems reservoirs, in P. Weimer and H. Posamentier, eds., Siliciclastic sequence stratigraphy: AAPG Memoir 58, p. 15-42.

Bralower, T. J., and H. R. Thierstein, 1984, Low productivity and slow deep-water circulation in Mid-Cretaceous oceans, Geology Boulder, v. 12 i. 10 p. 614 – 618.

Brewer, J. A., R. Good, J. E. Oliver, L. D. Brown, and S. Kaufman,1983, COCORP profiling across the southern Oklahoma aulacogen:overthrusting of the Wichita Mountains and compression within the Anadarko basin: Geology, v. 11, p. 109–114.

Brown, W. G., 1984, Washita Valley fault system: a new look at anold fault, in J. G. Borger III, ed., Technical proceedings of the AAPG Mid-Continent Section 1981 regional meeting: Oklahoma City, Oklahoma Geological Society, p. 68–80.

Brownlow, A. H. 1996. Geochemistry. 2nd ed. Prentice Hall. New Jersey.

Burgess, W. J., 1976, Geological evolution of the mid-continent andGulf Coast areas—a plate tectonics view: Transactions, Gulf Coast Association of Geological Societies, v. 26, p. 132–143.

Burke, K., and J. F. Dewey, 1973, Plume generated triple junctions: key indicators in applying plate tectonics to old rocks: Journal of Geology, v. 81, p. 406–433.

Chung, H.M., Gormly, J.R., Squires, R.M., 1988. Origin of gaseous hydrocarbons in subsurface environments: theoretical considerations of carbon isotope distribution. Chemical Geology 71, 97–103.

Coleman, D. D., C.-L. Liu, K. C. Hackley, and S. R. Pelphrey, 1995, Isotopic Identification of L Denison, R. E., 1976, Evolution of the Anadarko basin (abs.): AAPG Bulletin, v. 60, p. 325.

Demaison G. I. and Moore G. T., 1980, Anoxic marine environments and oil source bed genesis. American Association of Petroleum Geologists Bulletin. 64, 1179-1209.

Durand, B., 1980, Kerogen, Insoluble Organic Matter from Sedimentary Rocks: Paris, Editions Technip, 519 p.

Evans, J. L., 1979, Major structural and stratigraphic features of the Anadarko basin, in N. J. Hyne, ed., Pennsylvanian sandstones of the mid-continent: Tulsa Geological Society Special Publication 1, p. 97–113.

Ellis, L. MGIL maximizes value of mud logging, 2004, Special Report: Drilling Technology, American Oil & Gas Reporter, April, 127-131.

Ellis, L., A. Brown, M. Schoell, and S. Uchytil, 2003, Mug gas isotope logging (MGIL) assists in oil and gas drilling operations: Oil & Gas Journal, v. 101, Issue 21, May 26, p. 32-41.

Ellis, L., A. Brown, M. Schoell, M. Haught 1999 Mudgas isotope logging while drilling: A new field technique for exploration and production: 19th International Meeeting on Org. Geochem., 6-10 September 1999, Istanbul, Turkey, Abstracts.

Espitalie, J.L. La Porte, M. Madec, F. Marquis, P. Le Plat, J. Paulet and A. Boutefeu, 1974. Methode rapide de caracterisation des roches meres de leur potential petrolier et de leur degre d'evolution. Revue l'Inst. Francais du Petrole 32 1 (1977), pp. 23–42.

Evans, C.R., M.A. Rogers, and N.J.L. Bailey, 1971. Evolution and alternation of petroleum in Western Canada: Chem. Geology, v. 8, no. 3, p. 147-170.

Faber, E., 1987, Zur isotopengeochemie gasformiger Kohlen wasserstoffe: Erdol Erdgas Kohle, v. 103, p. 210-218.

Faber, E., W. J. Stahl, and M. J. Whiticar, 1992, Distinction of bacterial and thermogenic hydrocarbon gases, in R. Vially, ed., Bacterial Gas, Paris, Editions Technip, p. 63-74.

Faber, E., 1987, Zur isotopengeochemie gasformiger Kohlen wasserstoffe: Erdol Erdgas Kohle, v. 103, p. 210-218.

Feinstein, S., 1981, Subsidence and thermal history of southern Oklahoma aulacogen: implications for petroleum exploration: AAPG Bulletin, v. 65, p. 2521–2533.andfill Methane: Environmental Geosciences, v. 2, p. 95-103.

Galimov, E.M., 1973, Carbon Isotopes in Oil–Gas Geology. , Nedra, Moscow.

Gilbert, M. C., 1983, Timing and chemistry of igneous events associated with the southern Oklahoma aulacogen: Tectonophysics, v. 94, p. 439–455.

Haworth, J., M. Sellens, and A. Whittaker, 1985, Interpretation of hydrocarbon shows using light (C1-C5) hydrocarbon gases from mud-log data: AAPG Bulletin, v. 69, p.1305-1310.

Hoffman, P. F., J. F. Dewey, and K. Burke, 1974, Aulacogens and their genetic relation to geosynclines, with a Proterozoic example from Great Slave Lake, N.W.T., in R. H. Dott, Jr., and R. H. Shaver, eds., Modern and ancient geosynclinal sedimentation: SEPM Special Publication 19, p. 38–55.

Hood, A., C.C.M. Gutjahr, and R.L. Heacock, 1975, Organic metamorphism and the generation of petroleum: AAPG Bull., v. 59, p 986-996.

Horsfield B. and J. Rullkötter, 1994, Diagenesis, catagenesis, and metagenesis of organic matter. In: Magoon, L.B., and Dow, eds., 1994, The petroleum system – from source to trap: AAPG Memoir 60.

Hunt, J.M. Hunt, 1996, Petroleum Geochemistry and Geology. 2nd Edition., W.H. Freeman and Company, New York (1996).

Jewett, J.M.; O'Connor, H.G.; and Zeller, D.E., 1968, Pennsylvanian System, *in*, Zeller, D.E., (ed.); The stratigraphic succession in Kansas: Kansas Geological Survey, Bulletin, no. 189, pp. 21-43

Johnson, K. S., 1989, Geologic evolution of the Anadarko basin, in K. S. Johnson, ed., Anadarko basin symposium, 1988: Oklahoma Geological Survey Circular 90, p. 3–12.

Johnson, K. S., and B. J. Cardott, 1992, Geologic framework and hydrocarbon source rocks of Oklahoma, in K. S. Johnson and B. J. Cardott, eds., Source rocks in the southern mid-continent,1990 symposium: Oklahoma Geological Survey Circular 93,p. 21–37.

Krauskopf, K. B. and D. K. Bird. 2003. Introduction to geochemistry. 3rd ed. McGraw Hill. New York.

Kvenvolden, K.A. and R.M. Squires, 1967. Carbon isotopic composition of crude oils from Ellenburger group (Lower Ordovician), Permian Basin west Texas and eastern New Mexico. American Association of Petroleum Geologists Bulletin 5 (1967), pp. 1293–1303.

Gerlach, P. 1999. Kansas Oil and Gas Exploration; 10 Year History and Future Strategies KGS, Open-file Report 1999-55.

Larskaya, Ye. S., and D. V. Zhabrev, 1964. Effects of stratal temperatures and pressures on the composition of dispersed organic matter (from the example of the Mesozoic-Cenozoic deposits of the western Ciscaspian region). Dokl. Akad. Nauk SSSR, 157 (4), 135-139.

Lewan, M.D., Winters, J.C., McDonald, J.H., 1979. Generation of oil-like pyrolyzates from organic rich shales. Science 203, 897–899.

Leythaeuser, D., and H.S. Poelchau, 1991, Expulsion of petroleum from type III kerogen source rocks in gaseous solution: modeling of solubility fraction. England, W.A. and Fleet, A.J. (eds), Petroleum Migration. Geological Society (London) Special Publication 59, p. 33-46.

Magoon, L.B., and Dow, eds., 1994, The petroleum system – from source to trap: AAPG Memoir 60.

McConnell, D. A., 1986, Pennsylvanian foreland deformation of Wichita uplift, southwest Oklahoma (abs.): v. 70, p. 618.

McConnell, D. A., 1989, Determination of offset across the northern margin of the Wichita uplift, southwest Oklahoma: Geological Society of America Bulletin, v. 101, p. 1317–1332.

Merriam, D. F., 1963, The geologic history of Kansas: Kansas Geol. Survey Bull. 162, 317 p.

Muehlberger, W. R., Denison, R. E., and Lidiak, E. G., 1967, Basement rocks in continental interior of United States: Am. Assoc. Petroleum Geologists Bull., v. 51, no. 12, p. 2351-2380.

Rascoe, B., Jr., and K. S. Johnson, 1988, Anadarko basin and Hugoton embayment, in L. L. Sloss, ed., Sedimentary cover—North American craton: U.S.: the geology of North America: Boulder, Colorado, Geological Society of America, v. D-2, p. 318–326.

Rice, D. D., 1993, Biogenic gas: controls, habitats, and resource potential, in D. G. Howell, ed., The Future of Energy Gases - U.S. Geological Survey Professional Paper 1570, Washington, United States Government Printing Office, p. 583-606.

Rice, D.D., and G.E., Claypool, 1981, Generation, accumulation, and resource potential of biogenic gas. American Association of Petroleum Geologists Bulletin, v. 65, p. 5-25.

Schoell, M., 1983, Genetic characterization of natural gases: AAPG Bulletin, v. 67, p. 2225-2238.

Schoell, M., 1988. Multiple origins of methane in the earth: Chemical Geology, v. 71, p. 1-10.

Silverman, S.R. 1965. Migration and segregation of oil and gas. In: A. Young and G.E. Galley, Editors, AAPG Memoir 4, American Association of Petroleum Geologists, Tulsa (1965), pp. 54–65.

Silverman S.R. and S. Epstein, 1958. Carbon isotopic composition of petroleums and other sedimentary organic materials. American Association of Petroleum Geologists Bulletin 42 (1958), pp. 998–1012.

Smith, J.E., J.G. Erdman, and D.A. Morris, 1971, Migration, accumulation and retention of petroleum in the earth: 8th World Petroleum Cong. Proc., v. 2, p. 13-26.

Stahl, W.J., 1977. Carbon and nitrogen isotopes in hydrocarbon research and exploration. Chemical. Geology 20 (1977), pp. 121–149.

Tissot, B. Durand, J. Espitalie and A. Combaz , 1974. Influence of nature and diagenesis of organic matter in formation of petroleum. American Association of Petroleum Geologists Bulletin 58 (1974), pp. 499–506.

Tissot, B. P., and D. H. Welte, 1984, Petroleum formation and occurrence: New York, Springer-Verlag, 699 p.

Van Krevelen, D.W., 1961. Coal: Typology-Chemistry-Physics-Constitution., Elsevier Science, Amsterdam (1961).

Waples, D.W., 1985. Geochemistry in petroleum exploration. Reidel Publ. Co, Dordrecht & IHRDC, Boston. 232 pp.

Weimer, R.J., 1992, Developments in sequence stratigraphy: foreland and cratonic basins, AAPG Bulletin, v. 76, n. 7, p. 965-982.

Welte, D.H., Hagemann, H.W., Hollerbach, A., Leythauser, D., Stahl, W., 1975. Correlation between petroleum and source rock. Proceedings 9th World Petroleum Congress. Applied Science Publishers II, London, pp. 179–191.

Whiticar, M. J., 1994, Correlation of natural gases with their sources, in L. B. Magoon, and W. G. Dow, eds., The Petroleum System, From Source to Trap, AAPG, p. 261-283.

Whittaker, A., 1991, Mud Logging Handbook: Englewood Cliffs, New Jersey, Prentice Hall, 531 p.

Whittaker, A., 1992, Mudlogging: Gas Extraction and Monitoring: Part 3. Wellsite Methods. In: Development Geology Reference Manual. AAPG Special Volumes, v. ME 10 p. 106-10.

VITA

Timothy M. Samson

Candidate for the Degree of

Master of Science

Thesis: ASSESSMENT OF THE ATOKA GROUP OF SOUTHWEST KANSAS AS A POTENTIAL PETROLEUM SYSTMEM

Major Field: Geology

Biographical:

Personal Data: Born in Boston July 4th, 1982. Son of Joseph E. Samson and Susan K. Samson. Brother of Andrew J. Samson.

Education:
Dover-Sherborn Regional High School (1997 – 2001). Dover, MA.
Worchester Polytechnic Institute (2001 – 2002). Worchester, MA.
Dickinson College (2002 – 2005). Carlisle, PA.
Oklahoma State University (2005 – May, 2007) Master's Degree Stillwater, OK.

Experience: Internship with EOG Resources Inc. during the summer of 2006.

Professional Memberships: AAPG, Phi Kappa Phi

Name: Timothy M. Samson Date of Degree: May, 2007

Institution: Oklahoma State University Location: OKC or Stillwater, Oklahoma

Title of Study: ASSESMENT OF THE ATOKA GROUP OF SOUTHWEST KANSAS AS A POTENTIAL PETROLEUM SYSTEM

Pages in Study: 83 Candidate for the Degree of Master of Science

Major Field: Geology

Abstract:

The purpose of this thesis is to determine if the Atokan Series of Southwest Kansas represents a petroleum system. This thesis is focused on determining the source rock characteristics of the Atoka using stable carbon isotope, gas composition, Rock-Eval, and total organic carbon (TOC) analyses.

Rock-Eval data indicate that the Atoka contains Type II and III kerogens that are oil prone. Atoka TOC values are greater than the minimum TOC content of 0.5 % required for hydrocarbon source rock classification. d13CCH4 values and vitrinite reflectance data indicate that Atoka rocks increase in maturity from south to north while depth of the Atoka decreases. This trend may reflect the preferential removal of overburden in the north following the Cretaceous. Within a given well, maturity increases with increasing depth. Overall, Atoka rocks have the potential to source overlying reservoirs, with a trend to the north of increasing gas-oil ratios.

ADVISER'S APPROVAL: Dr. Anna M. Cruse